Aus dem Max von Pettenkofer-Institut
für Hygiene und Medizinische Mikrobiologie,
Lehrstuhl Virologie

# Novel approaches to identify and characterise dominant negative mutants of essential MCMV genes

Dissertation zum Erwerb des Doktorgrades
der Naturwissenschaften der Medizinischen Fakultät
der Ludwig-Maximilians-Universität München

**Madlen Pogoda**

München, 2013

**Gedruckt mit Genehmigung der Medizinischen Fakultät**

**der Ludwig-Maximilians-Universität München**

| | |
|---|---|
| Erstgutachter: | Prof. Dr. rer. nat. K.-Klaus Conzelmann |
| Zweitgutachter: | Prof. Dr. rer. nat. Reinhard Zeidler |
| | |
| Dekan: | Prof. Dr. med. Dr. h.c. Maximilian Reiser, FACR, FRCR |
| | |
| Tag der mündlichen Prüfung: | 16.10.2013 |

# Eidesstattliche Versicherung

Hiermit erkläre ich an Eides statt, dass ich die vorliegende Arbeit selbständig verfasst, mich außer der angegebenen keiner weiteren Hilfsmittel bedient und alle Erkenntnisse, die aus dem Schrifttum ganz oder annähernd übernommen sind, als solche kenntliche gemacht und nach ihrer Herkunft unter Bezeichnung der Fundstelle einzeln nachgewiesen habe.

Ich erkläre des Weiteren, dass die hier vorgelegte Dissertation nicht in gleicher oder ähnlicher Form bei einer anderen Stelle zur Erlangung eines akademischen Grades eingereicht wurde.

München, 05.03.13                                                    **Madlen Pogoda**

# TABLE OF CONTENTS

# LIST OF FIGURES

# LIST OF TABLES

# SUMMARY

Knowledge of protein structure, sequence motifs or function is required for the construction of *trans*-dominant mutants. The information for the majority of herpesvirus proteins, however, is too limited to allow a knowledge-based construction of dominant negative (DN) proteins. A systematic screen of the essential murine cytomegalovirus (MCMV) protein pM53 revealed an accumulation of DN mutations within conserved region (CR) 2 and CR4. Whereas the strong inhibitory potential of the CR4 mutants allowed the characterisation of their phenotype, the DN effect of the mutations in CR2 was too weak to be analysed. Based on preliminary data obtained from pM53 proteins composed of the pM53 N-terminus fused to the C-terminal CRs of homologous herpesvirus proteins we hypothesised that chimeric pM53 proteins carrying one conserved, but non-complementing domain of the respective homologue will be inhibitory for MCMV replication. In addition to the domain shuffling approach, the CRs were also targeted by deletion. Thus, the present study describes the construction of pM53 mutants in which the single CRs were disrupted by targeted mutagenesis and the subsequent investigation of their inhibitory effect on MCMV replication using an established conditional expression system.

Indeed, the pM53 mutants with shuffled CR2 and CR4 as well as CR2 deletion were inhibitory for MCMV replication, whereas neither the shuffled nor the CR3 deletion mutant was. The phenotype induced by the strong CR2 DN mutant was analysed in detail. Overexpression of the CR2-deficient pM53 inhibited MCMV production by 10,000-fold, which was due to interference with capsid export from the nucleus and viral genome cleavage/packaging. In addition, the fate of the nuclear egress complex in the presence of DN pM53 overexpression was analysed. The CR2 mutants were able to bind to pM50, albeit to a lesser extent than the wild-type protein, and re-localised the wild-type nuclear egress complex in infected cells. Unlike the CR4 DN, the CR2 DN mutants did not affect the stability of pM50.

The second part of this study deals with the establishment of a high-throughput suitable screening system for the identification of inhibitory alleles of essential MCMV genes. In this screen, the site-specific recombination of an MCMV genome, cloned as bacterial artificial chromosome, and a rescue vector, which is mediated by the Flp recombinase, was transferred from the bacterial background to MCMV permissive host cells. Using a reference set of characterised pM53 mutants it was shown that the novel system is generally applicable to identify non-complementing as well as inhibitory mutants in a reduced time frame.

Last, the biological and biochemical properties of pM99, a protein suggested to be involved in the secondary envelopment process, were investigated to provide the basis for the application of the novel screening tools to test a comprehensive library of pM99 mutants.

# ZUSAMMENFASSUNG

Zur Konstruktion *trans*-dominanter Mutanten sind Informationen über die Struktur oder funktionelle Motive eines Proteins erforderlich. Für die Mehrheit der Herpesvirus-Proteine ist dieses Wissen jedoch zu begrenzt für eine gezielte Konstruktion dominant negativer (DN) Proteine. Eine systematische Untersuchung des essentiellen Proteins pM53 des murinen Zytomegalievirus (MCMV) ließ eine Ansammlung von DN Mutationen in den konservierten Regionen 2 (CR2) und 4 (CR4) erkennen. Die Mutationen in CR4 unterdrückten die Funktion des Wildtyp pM53, so dass ein Phänotyp charakterisiert werden konnte. Im Gegensatz dazu war der Effekt der CR2-Mutanten zu schwach um analysiert zu werden. Aufgrund bestehender Daten über pM53 Proteine, welche aus dem pM53 N-Terminus und den C-terminalen konservierten Regionen homologer Herpesvirusproteine aufgebaut sind, wurde spekuliert, dass chimäre pM53 Proteine mit einer konservierten, aber nicht komplementierenden Domäne eines Homologs inhibitorisch für die MCMV-Replikation sein würden. Zusätzlich zum Domain-Austausch wurden die konservierten Regionen deletiert. Basierend auf dieser Vermutung beschreibt die vorliegende Arbeit die Konstruktion von pM53 Mutanten, bei denen die einzelnen konservierten Regionen durch gezielte Mutagenese inaktiviert wurden, und die anschließende Analyse des inhibitorischen Effekts auf die MCMV-Replikation mittels eines konditionalen Expressionssystems.

Den Erwartungen entsprechend inhibierten die pM53 Mutanten mit ausgetauschter CR2 und CR4 sowie die CR2-Deletionsmutante die MCMV-Replikation, während dies für keine der CR3-Mutanten zutraf. Der durch die CR2 DN Mutante induzierte Phänotyp wurde genauer analysiert. Überexpression der CR2-Deletionsmutante blockierte den Kapsidexport aus dem Zellkern und verringerte zusätzlich die Generierung von Genomen mit spezifischer Größe, so dass die MCMV-Produktion um das 10.000-Fache reduziert war. Darüber hinaus wurde das Verhalten des sogenannten Kern-Austritt-Komplexes in Anwesenheit von DN pM53 untersucht. Die CR2-Mutanten interagierten mit geringerer Effizienz mit pM50 als Wildtyp pM53. Außerdem delokalisierten sie den Wildtyp Kern-Austritt-Komplex in infizierten Zellen. Im Gegensatz zu den CR4 DN Mutanten hatten die pM53 CR2 Mutanten keinen Einfluss auf die Stabilität von pM50.

Der zweite Teil dieser Studie beschreibt die Etablierung eines Hochdurchsatz-geeigneten Screeningsystems zur Identifikation inhibitorischer Allele essentieller MCMV Gene. Für diesen Screen wurde die durch die Flp-Rekombinase katalysierte sequenzspezifische Rekombination zwischen dem MCMV-Genom und einem Plasmidvektor von Bakterien in MCMV-permissive eukaryotische Zellen übertragen. Mittels einer Auswahl an bereits charakterisierten pM53 Mutanten konnte gezeigt werden, dass dieses neue System allgemein anwendbar ist um sowohl nicht-komplementierende als auch inhibitorische Mutanten mit reduziertem Zeitaufwand zu identifizieren.

Im letzten Teil wurden die biologischen und biochemischen Eigenschaften des Proteins pM99 untersucht, welches im sekundären Verhüllungsprozess involviert sein könnte. Diese Untersuchung bietet die Basis für die Anwendung des neuen Screeningsystems, um eine umfangreiche Bibliothek an pM99 Mutanten zu testen.

# 1 INTRODUCTION

## 1.1 Herpesviridae

Herpesviruses are large double stranded DNA viruses that infect vertebrates as well as non-vertebrates. Up to date, more than 90 herpesviruses have been identified including several human pathogens [63]. A feature shared by all herpesviruses is their capacity to establish life-long persistence in the infected host. Based on their host range, biology and genetics, the family of *herpesviridae* is classified into the three main groups of alpha-, beta- and gamma-*herpesvirinae*. Alpha-herpesviruses, such as the human pathogen herpes simplex virus (HSV), tend to replicate rapidly in cell culture accompanied by cytopathic effects and establish latency in neurons in sensory ganglia. An important non-human pathogen belonging to the alpha-*herpesvirinae* is pseudorabies virus (PrV), which infects swine and other farm animals. It has extensively been used as animal model to study aspects of alpha-herpesvirus biology [reviewed in 128].

Gamma-herpesviruses such as Epstein-Barr virus (EBV) replicate very slowly in tissue culture and establish latency in lymphoid tissues. Since exploration of EBV pathogenesis in humans is limited, infection of mice with murine herpesvirus 68 (MHV68) has been exploited as suitable model for gamma-herpesvirus biology [65, 119].

Human cytomegalovirus (HCMV) is a widespread pathogen belonging to the beta-*herpesvirinae*. Cytomegaloviruses (CMVs) are characterised by strict species specificity, tropism for hematopoietic tissue and secretory glands and a relatively slow replication cycle *in vitro*. In humans, after resolution of a primary acute infection that generally proceeds asymptomatically in immuno-competent patients, CMVs establish life-long persistence with alternate stages of virus reactivation and true latency, where no infectious virus can be detected [10, 81, 84, 114, 164]. However, perinatal infection as well as infection of immuno-compromised individuals such as AIDS patients or

transplantation recipients may result in severe and life-threatening illness including colitis, encephalitis, esophagitis, hepatitis, pneumonitis and retinitis. Intra-uterine infections of the foetus lead to embryopathies characterised by damages of the central nervous system causing hearing loss, seizures, mental retardation, or even abortion [reviewed in 84]. The strict species specificity of HCMV has hindered its study in animals. Since murine cytomegalovirus (MCMV) shares many features with HCMV, the mouse model has extensively been used for studying the pathogenesis of acute, latent and recurrent virus infection [99, 132].

### 1.1.1 Structure of the herpesvirus particles

A herpesvirus virion consists of three major structural elements: the capsid containing the linear double stranded viral DNA, the tegument layer and the envelope (Figure 1.1). The size of mature virions ranges between 120 and 260 nm due to the variable thickness of the tegument [137]. The icosahedral capsid, about 120 nm in diameter, is composed of 162 capsomers, which themselves are complexes of structural proteins. It is embedded in the tegument, a proteinaceous meshwork assumed to play a major role shortly after infection and during early gene expression. The tegument also contains both viral and host cell RNA that can be translated immediately after infection [20, 54]. A lipid bilayer originating from the host cell forms the viral envelope. Virus-encoded glycoproteins are incorporated in the envelope, allowing virus attachment to host cell receptors and mediating fusion with the membrane of the target cell.

Two more particle types are produced during a lytic herpesvirus infection besides mature virions: non-infectious enveloped particles (NIEPs), which are similar to mature virions but lack viral DNA, as well as so-called dense bodies (DBs), which lack both the capsid and the genome [64, 169]. A similar capsid-lacking structure, called L particles, was also described for HSV-1 [101].

Herpesviruses have the largest genomes among vertebrate viruses, ranging from 125 kb for varicella-zoster virus (VZV) to 230 kb for cytomegaloviruses [11, 131]. The core genes, which are highly conserved throughout the subfamilies, are located in the centre of the linear double stranded DNA genome. The products of these essential genes are involved in vital viral functions such as DNA replication, genome packaging or maturation of infectious viral particles. The core genes are flanked by genes shared within the subfamily. The genes located towards the ends of the genome define the

species specificity of the different viruses and are mainly involved in the cross talk with the host.
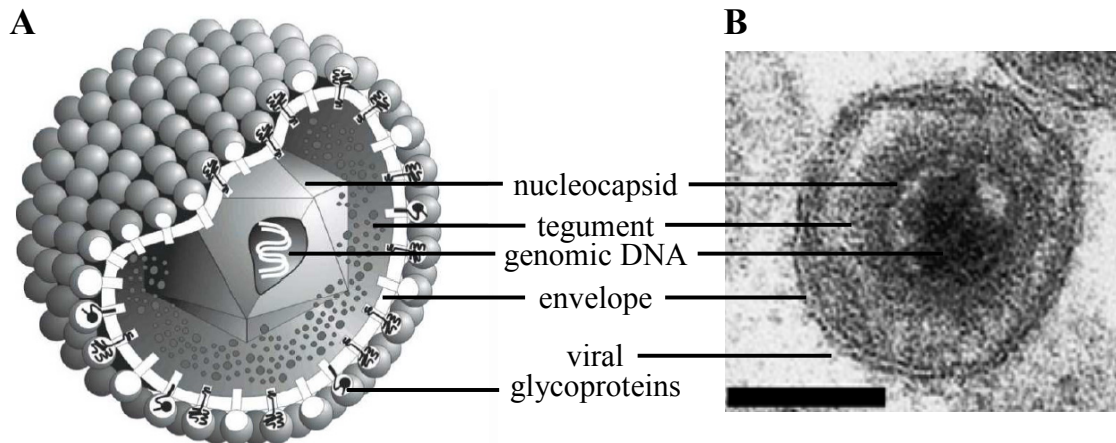


**Figure 1.1: Herpesvirus virion morphology**

**(A)** Schematic representation of a herpesvirus virion (© Marko Reschke, University of Marburg, 1994-1997). **(B)** Electron microscopy of an extracellular HCMV virion. Scale bar, 100 nm [109]. Major virion components are indicated. The icosahedral capsid enclosing the linear ds DNA is embedded in the tegument, a macromolecular meshwork containing viral proteins as well as viral and host cell mRNAs playing an important role directly after infection. The host cell-derived lipid envelope comprises viral glycoproteins that mediate attachment to the target cell.

### 1.1.2 Herpesvirus replication cycles

Host cell infection is initiated by virion attachment to cell surface receptors [167] and internalisation of the capsid together with tegument components. Depending on the cell type and its receptors, up-take occurs via fusion of the viral and cellular membrane or by endocytosis [reviewed in 35, 177]. The capsid is transported along microtubules [166] until it docks to a nuclear pore and delivers the linear genome into the nucleus. The genome circularises and either is silenced by the host cell, leading to latency, or the transcription of viral genes is forced, initiating the lytic replication cycle. Latently infected cells maintain viral genomes in a circular form and express only a minimal gene set to ensure persistence [51]. Infectious viral particles are not detected during latency.

The start of the lytic cycle is characterised by a strictly regulated consecutive viral transcription cascade, resulting in three classes of gene products [61]. Immediate-early (IE) proteins participate in the transcriptional activation of most of the other viral genes,

whereas early proteins are involved in the replication of the viral genome. Products of late genes are mainly structural components that are involved in capsid assembly and DNA encapsidation, maturation and egress.
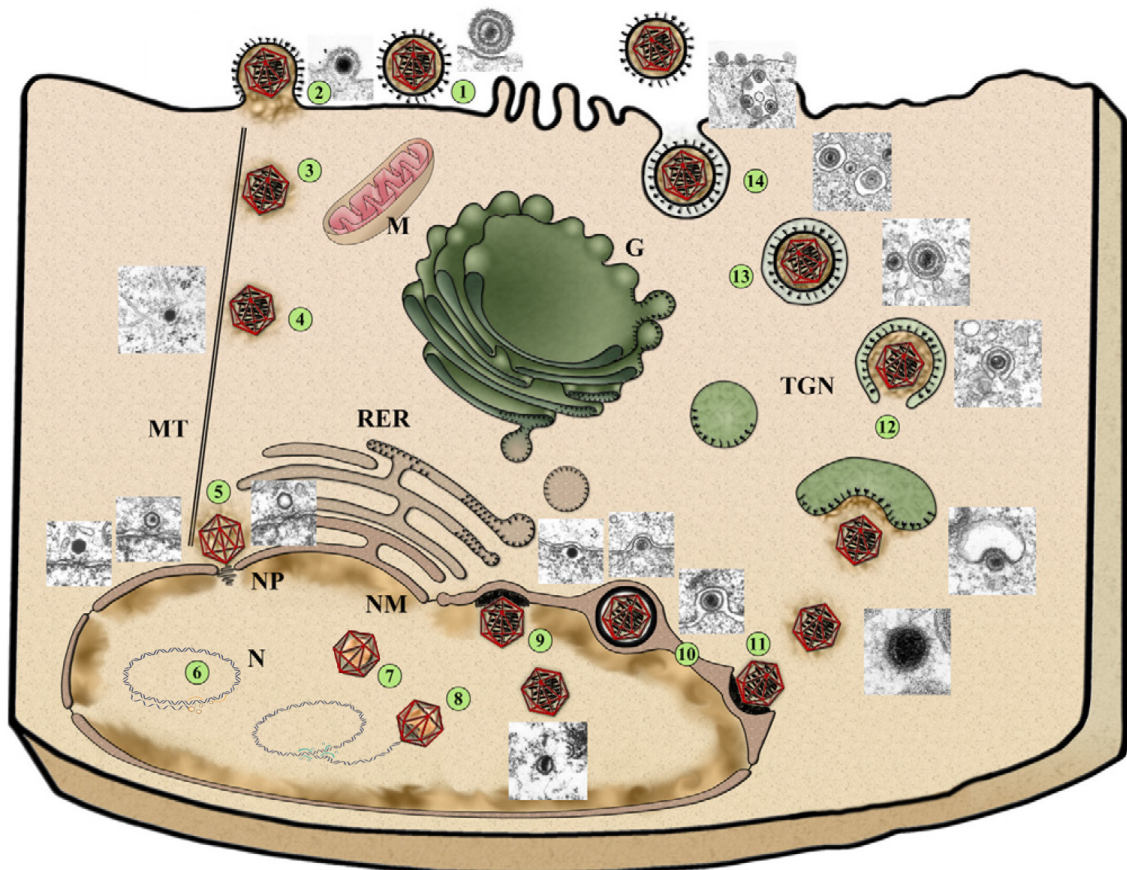


**Figure 1.2: Lytic replication cycle of herpesviruses**

Schematic representation of a lytic replication cycle, exemplified by electron micrographs for PrV. Virions attach (1) and penetrate (2) the target cell and are transported to the nucleus (3) via interaction with microtubules (4). The viral DNA is released into the nucleus upon docking to the nuclear pore (5), where transcription and replication of viral genes and genomes takes place (6). Concatemeric replicated DNA is cleaved into unit length genomes during packaging (8) into pre-assembled capsids (7). Mature capsids exit the nucleus by budding through the nuclear envelope (9-11). Cytosolic capsids are tegumented and bud into vesicles of the *trans*-Golgi network (12) containing viral glycoproteins (black spikes), resulting in enveloped particles within intracellular vesicles. Those are transported to the cell membrane (13), the membranes fuse (14) and mature, enveloped virions are released. G, Golgi apparatus; M, mitochondrion; MT, microtubule; N, nucleus; NM, nuclear membrane; NP, nuclear pore; RER, rough endoplasmic reticulum; TGN, *trans*-Golgi network. The picture was reproduced from [109] and modified.

Viral replication and capsid assembly occurs within the nucleus of infected cells, whereas maturation of the virions takes place in the cytoplasm. Production and release of infectious viral particles, whether in primary infection or recurrence from latency, is

invariably accompanied by destruction of the host cell. Lytic replication of herpesviruses disrupts the cytoskeleton, leading to cytopathic effects such as massive enlargement of the host cell (cytomegalia) or induces fusion of infected cells (syncytia). Replication of the viral genome produces concatemeric DNA that is cleaved into unit length genomes simultaneously to its encapsidation into pre-assembled capsids [104]. These mature, DNA-filled capsids are targeted to the nuclear rim and exit the nucleus by a complex course of envelopment and de-envelopment processes through the nuclear membrane (section 1.1.3). Final maturation occurs then in the cytoplasm, where the capsids are tegumented and acquire their secondary envelope by budding into vesicles of the *trans*-Golgi network (section 1.1.4) [149]. They are transported via the secretory pathway to the cell surface, where the membranes fuse und infectious virions are released into the extracellular space (Figure 1.2).

## 1.1.3 Role of the nuclear egress complex

The inner nuclear membrane (INM) of eukaryotic cells is lined by a complex fibrillar network, the nuclear lamina, which provides mechanical stability and anchors the nuclear core complexes embedded in the nuclear envelope. Since herpesvirus capsids exceed the size tolerated for transport through the nuclear pores (~39 nm) [122], they require an alternative exit mechanism. Capsid export through enlarged pores has been observed for HSV-1 and bovine herpesvirus [88, 174] and a recent study of PrV shows nuclear envelope breakdown as means of nuclear capsid exit [74]. Yet, the most prominent pathway requires budding through the nuclear envelope akin to the mechanism reported recently for large ribonucleoprotein granules during synaptic Wnt signalling [168]. First, mature capsids bud into the INM, forming capsid-containing vesicles in the perinuclear space [41]. By fusion of this primary envelope with the outer nuclear membrane (ONM), the nucleocapsids are liberated into the cytoplasm. This process is facilitated by a number of viral and host cell protein interactions (Figure 1.3).
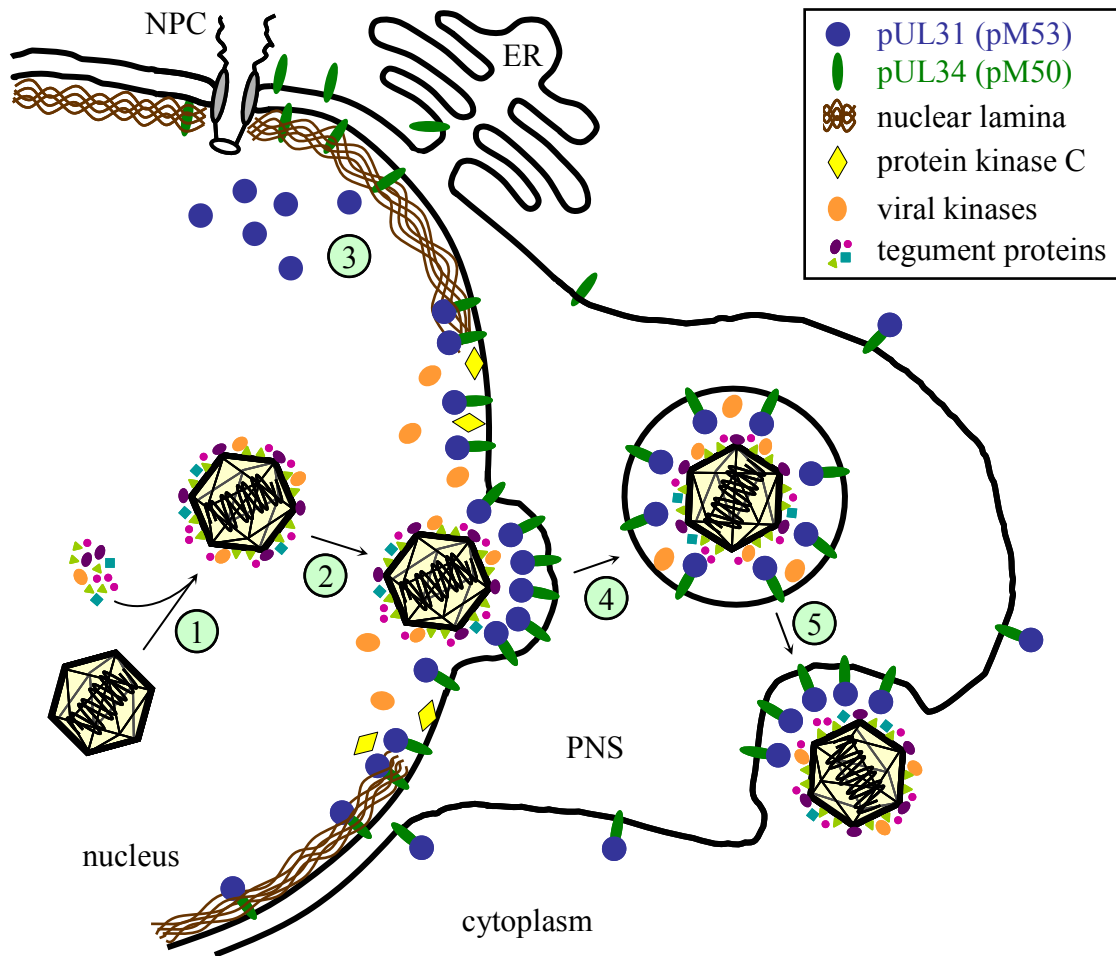
**Figure 1.3: Nuclear egress of herpesvirus capsids**

Schematic illustration of the nuclear egress of herpesviral capsids. DNA-filled nucleocapsids acquire a primary tegument (1) and are targeted to the nuclear rim (2). The respective members of the pUL31 and pUL34 families interact at the inner nuclear membrane (INM) (3), forming the nuclear egress complex by recruiting further viral and cellular proteins. This serves as docking station for the capsids, which bud into the INM (4). The thus acquired primary envelope fuses with the outer nuclear membrane, thereby releasing the capsids into the cytoplasm (5). ER, endoplasmic reticulum; NPC, nuclear pore complex; PNS, perinuclear space. The figure was produced by adapting schematic representation from [66, 108].

Studies in alpha-herpesviruses have shown that two viral proteins, pUL31 and pUL34, play a critical role in primary envelopment [49, 75, 140, 159]. Homologues of these proteins are found in all herpesviruses studied so far and are assigned to the pUL31 and pUL34 herpesviral protein families. The corresponding gene products in MCMV are called pM53 and pM50. Proteins of the pUL34 family are expressed in the early to late phase of infection. They are type II C-terminally anchored membrane proteins that primarily reside in the nuclear envelope. pUL31 family members are expressed late in infection. In the absence of other viral proteins, pM53 is distributed

throughout the nucleosol. It is targeted to the INM by interaction with pM50, a mechanism that is conserved among herpesviruses [22, 39, 46, 49, 50, 83, 95, 135, 151, 152, 159, 183]. pM50 and pM53 (and their homologues) form the nuclear egress complex (NEC) and serve as docking station for further cellular and viral proteins, such as protein kinase C and viral kinases. Those participate in the phosphorylation of nuclear lamins, which loosens the meshwork and allows contact between nucleocapsid and INM [15, 27, 73, 98, 111, 113, 115, 118, 123, 134, 136, 144]. Other lamina constituents such as emerin and the lamin B receptor are also displaced during infection [85, 86, 112, 154].

The mechanism by which the pUL31 and pUL34 homologues mediate capsid transition through the nuclear envelope is still not fully understood, but disruption of either partner usually leads to retention of viral capsids within the nucleus [22, 46, 49, 75, 95, 140, 185]. Insights into this mechanism were gained from studying the PrV proteins pUL31 and pUL34, which induce vesicle formation in the nuclei of transfected cells in the absence of other viral components [71], supporting their role in the capsid envelopment process at the INM. The reciprocal binding sites, which result in NEC targeting to the INM, are well characterised in pM53 and pM50, and are conserved throughout the pUL31 family [22, 49, 50, 89, 95, 148, 152]. Furthermore, recent studies of HSV-1 suggest a second essential interaction between the N-terminal domain of pUL34 and the C-terminus of pUL31, which results in membrane wrapping. This interaction is distinct from that required for INM targeting [14, 138, 139].

In addition to its role in primary envelopment, pUL31 family members are involved in an upstream step of capsid maturation and DNA cleavage/packaging, which is independent of the pUL34 binding [29, 52, 72, 82, 130]. Furthermore, a recent study in HSV-1 ascribes to pUL31 the function of targeting DNA-filled capsids from the nucleosol to the INM [184].

## 1.1.4 Role of the secondary envelopment complex

Viral particles loose their primary envelope upon entering the cytoplasm, where final tegumentation and addition of the secondary envelope at the *trans*-Golgi network (TGN) takes place. It is still not fully understood how tegumented capsids reach this so-called assembly complex and how viral glycoprotein assembly occurs, but is has been shown that the conserved viral homologues of the pUL11 and pUL16 protein families

are major players in these processes. Notably, while the pUL11 and pUL16 homologues are dispensable for viral replication in cell culture in alpha- and gamma-herpesviruses [5, 6, 31, 78, 96, 146], their homologues in beta-herpesviruses are essential [21, 45, 97, 125, 161].
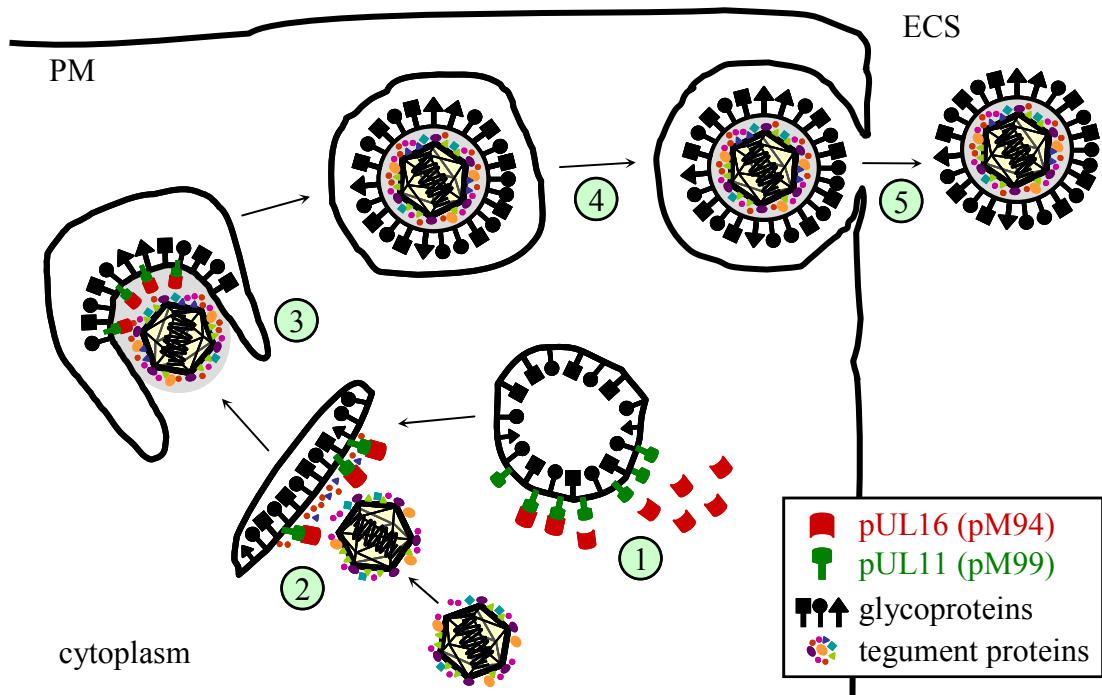


**Figure 1.4: Role of pM94/pM99 in secondary envelopment of herpesviruses**

Depicted is a model of the secondary envelopment. The pUL16/pUL11 complex is targeted to *trans*-Golgi derived vesicles containing viral tegument and glycoproteins (1). pUL16 docks tegumented capsids to these vesicles (2), which are enfolded, forming enveloped virions within cellular vesicles (3). The vesicles are transported to the cell surface (4) and virions are released upon fusion of the vesicle to the plasma membrane (5). ECS, extracellular space; PM, plasma membrane. Adapted from [108].

The pUL11 homologue of HCMV, pUL99 (pp28), is a small (190 amino acids) myristoylated and palmitoylated phospho-protein [67], which is expressed in the late phase of infection [70, 76] and accumulates at the cytoplasmic interface of Golgi-derived membranes [60, 149]. It has been shown to interact with the tegument protein pUL94 (the pUL16 homologue) in the absence of other viral proteins [90], forming the secondary envelopment complex (SEC), which is crucial for the functionality of both proteins [126]. This interaction was also confirmed for the MCMV proteins pM99 and pM94 [97] as well as for pUL11 and pUL16 [93, 178, 186]. In HCMV, disruption of either protein leads to retention of DNA-filled, tegumented capsids in the cytoplasm that

fail to acquire their final envelope, thereby completely blocking the production of infectious virions [125, 161]. Furthermore, pUL99 shows aberrant localisation in absence of its binding partner and vice versa, indicating that their interaction is a prerequisite for proper localisation to the assembly complex.

During infection, pUL94 and its homologues are found in the cytoplasm as well as the nucleus [91, 106, 121], suggesting that pUL94 targets the capsids to the assembly complex by interacting with TGN-associated pUL99 to permit secondary envelopment (Figure 1.4).

## 1.2 Reverse genetics in herpesviruses

Traditionally, irradiation or chemicals were used to increase the mutation rate during replication, and interesting phenotypes were subsequently investigated regarding the causative genetic change (forward genetics). However, comprehensive genetic analysis of herpesviruses by this approach was not feasible and the application of traditional methods of molecular cloning has long been limited due to the very size of their genomes. Primarily the establishment of genetic systems that permit targeted mutagenesis of the gene of interest in its genomic context facilitated the generation of virus mutants in order to analyse resulting phenotypic alterations (reverse genetics).

### 1.2.1 Site-directed mutagenesis

Functional analyses of isolated genes were enabled by cloning of viral fragments that could be modified *in vitro* and re-introduced into the viral genome. In principle, the cellular recombination machinery is exploited to replace the target sequence by the modified viral gene together with a marker gene (Figure 1.5A). Yet, the recombination frequency is low and the majority of produced viruses do not carry the desired mutation. Selection procedures are required to isolate mutated viruses, which can be tedious for mutants with growth deficits [reviewed in 143].

Further advance was gained with the cloning of the HSV-1 genome as set of overlapping cosmid fragments [176]. Assembly of the fragments by homologous recombination in permissive cells reconstitutes the virus. This system has two advantages, the wild-type (wt) genome is not required and mutations can be introduced

in any of the cosmid fragments by standard techniques. However, since full assembly necessitates several recombination events, the risk for unwanted mutations is increased. Besides, null mutations of essential genes cannot be generated using this approach [reviewed in 143].
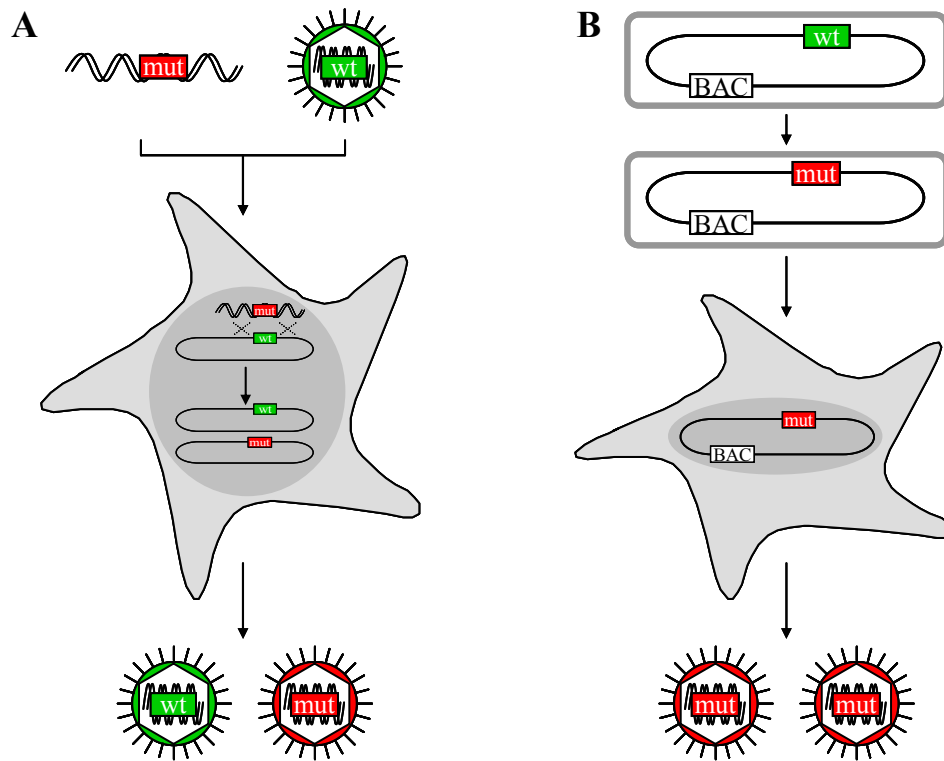


**Figure 1.5: Approaches of herpesvirus mutagenesis**

**(A)** Site-directed mutagenesis in eukaryotic cells. Infected cells are transfected with linear DNA fragments containing the mutation (red box). The mutated fragment replaces the wild-type (wt) sequence (green box) in some viral genomes by homologous recombination (crossed lines), resulting in a pool of wt and recombinant mutant (mut) viruses. **(B)** Mutagenesis based on bacterial artificial chromosomes (BACs). Recombinant BACs are generated using the *E. coli* recombination system. Mutant viruses are reconstituted by transfecting permissive cells with DNA derived from a verified BAC clone. Adapted from [143].

## 1.2.2 Mutagenesis of bacterial artificial chromosomes

The disadvantages of uncontrollable cellular recombination was overcome when full length herpesvirus genomes were cloned as infectious bacterial artificial chromosomes (BACs), which was pioneered for MCMV [107], and subsequently adapted to numerous herpesviruses such as HSV-1, PrV, HCMV, EBV and MHV68 [1, 17, 43, 147, 165]. Using BACs, herpesviral genomes can be readily modified using techniques developed

for bacterial genetics. Besides, the expression of viral functions is not required for the maintenance in *E. coli*, decreasing the risk of unwanted changes due to frequent sub-culturing of viral progeny. The modified DNA is transfected into permissive eukaryotic cells to reconstitute infectious virus, which results in pure, clonal viral populations, and even allows the production of attenuated mutants (Figure 1.5B). While the function of non-essential genes can be studied in the virus context using deletion and loss-of-function mutants, this approach is not applicable for essential genes. The study of null- or non-functional mutants of essential genes requires functional analysis by *trans*-complementation or the application of DN mutants [reviewed in 55].

## 1.2.3 Complementation systems for defects of essential genes

Viruses with inactivating mutations in essential genes can be propagated only if the target gene is provided in addition. This can be realised by expressing the complementing feature separately from the virus genome (*trans*-complementation), for example by a modified helper cell line or helper viruses. *Trans*-complementation is commonly used for IE gene products, which are required in small amounts for viral replication and whose expression is not detrimental for the cell. Alternatively, the complementing element can be inserted into the viral genome at an ectopic position (*cis*-complementation), often accompanied with regulating features. Recently, a conditional replication system has been adapted to MCMV [142], in which the two elements required for conditional gene expression – regulated transcription unit as well as regulator – were integrated as one cassette into the viral BAC genome. Combining regulator and regulated cassette has two major advantages. Since the conditional expression unit is present in the MCMV genome, the effect of the mutants can be studied upon induction in any permissive cell type as well as *in vivo*. Additionally, the cassette is inserted at an apparently neutral locus, so that regulation of the gene of interest should not interfere with the viral gene expression programme. Thus, the gene of interest is regulated as independently as possible from the viral genetic programme. The *tet*-regulated system has successfully been applied to the conditional expression of both essential genes and dominant negative (DN) alleles in the virus context [97, 130, 141].

## 1.3 Dominant negative mutants

Essential genes are not easily studied using traditional approaches because mutant viruses are difficult to reconstitute. However, functional inactivation of such proteins by co-expression of dominant negative (DN) mutants makes them amenable to comprehensive genetic analysis [58].

### 1.3.1 Inhibitory principle of DN proteins

DN alleles are able to induce the null phenotype in the presence of the wt gene product and permit functional analysis of essential genes. Prerequisites for effective DN mutants are that their wt counterparts are multi-functional proteins of essential genes that preferentially act in complexes. The DN mutant then out-competes the wt protein(s) when over-expressed, thus interrupting the physiological pathways and allowing the study of specific gene products as well as protein-protein interactions (Figure 1.6).

Well-known examples are transcription factors (TF). If the DNA-binding domain is intact, but the activation domain is non-functional, the mutant TF inhibits wt function by occupying the binding site, which prevents wt TF engagement, but does not activate transcription. Another example could be a protein that acts in a multimeric complex. The DN mutant still allows partial complex formation, but interferes with the execution of downstream functions. Thus, DN proteins may affect protein interactions as well as enzymatic functions.

A DN mutant can induce the same phenotype as the deletion of that gene. However, investigation of deletion mutants of essential genes requires propagation on a *trans*-complementing cell line. This is not necessary for DN mutants. Conditionally regulated DN mutants, integrated into the viral genome, circumvent this problem. Viruses are easily produced, and expression of the DN protein is induced on demand, enabling to study the function of the wt counterpart. Null-mutants only reveal the first dominant role of a protein. DN alleles, in contrast, have the potential to arrest viral pathways at different stages, thereby addressing multiple essential functions of a protein [reviewed in 117]. Therefore, DN mutants of important viral genes with specific and strong inhibitory activity are very valuable for both basic and applied research.
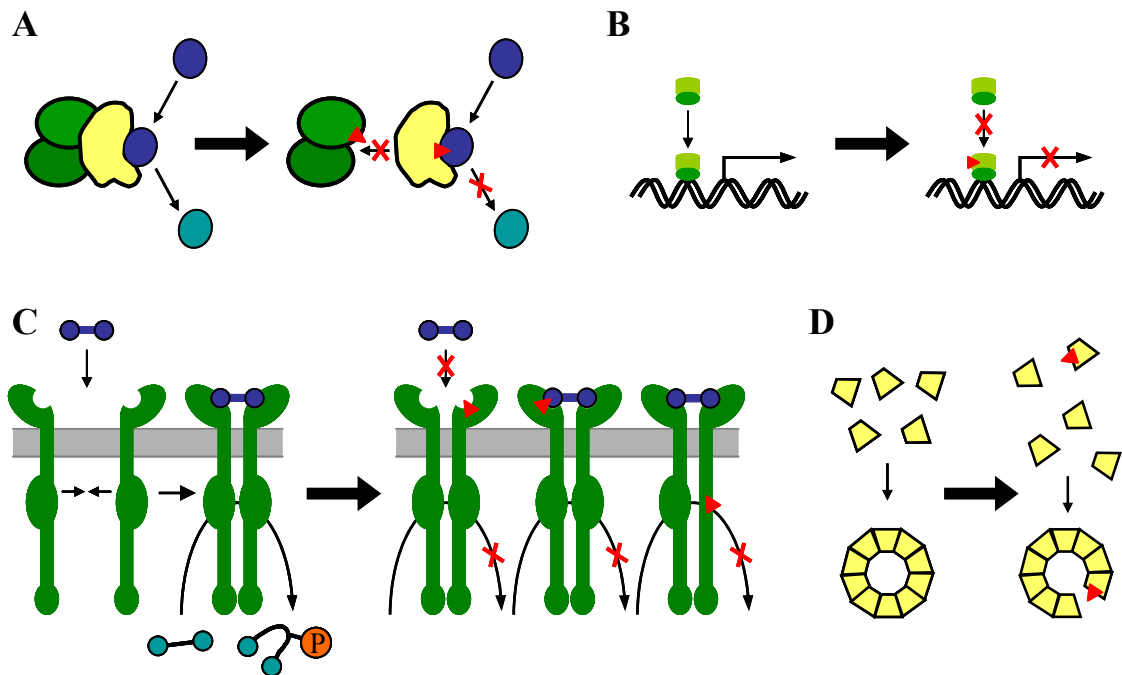
**Figure 1.6: Inhibitory principle of DN proteins**

**(A)** A mutation (red arrowhead) in the catalytic domain of an enzyme may allow substrate binding, but no conversion. Alternatively, a DN mutation does not permit binding of another subunit of a multimeric complex. **(B)** A DN transcription factor (TF) bound to DNA blocks the binding site for the wt TF, preventing gene expression. **(C)** Schematic illustration of a phosphorylation reaction which depends on substrate binding and homo-dimerisation of the membrane protein. A DN mutation may prevent substrate binding or result in irreversible substrate binding. Inactivation of the active site of one of the homo-dimers blocks phosphorylation of the target molecule. Grey bar, plasma membrane. **(D)** Incorporation of a conformationally altered subunit prevents assembly of a homotypic multimeric complex. Adapted from [117].

## 1.3.2 Identification of DN mutants

Isolation and characterisation of DN alleles became a standard procedure in genetics. Using in-depth functional knowledge and detailed experimental information regarding protein structure, such inhibitory mutants can be created by targeted introduction of crucial, but subtle mutations or by deleting a domain that represents an independent folding entity [reviewed in 58, and 117]. However, so far such data are limited for the majority of herpesvirus proteins, impeding a knowledge-based construction of DN mutants. Consequently, the entire coding sequence of a target gene needs to be subjected to a random mutagenesis to identify potential DN candidates [34, 97, 130, 141]. A standard method for random mutagenesis is the application of

transposons (Tn), mobile genetic elements that are randomly inserted into target DNA [36].
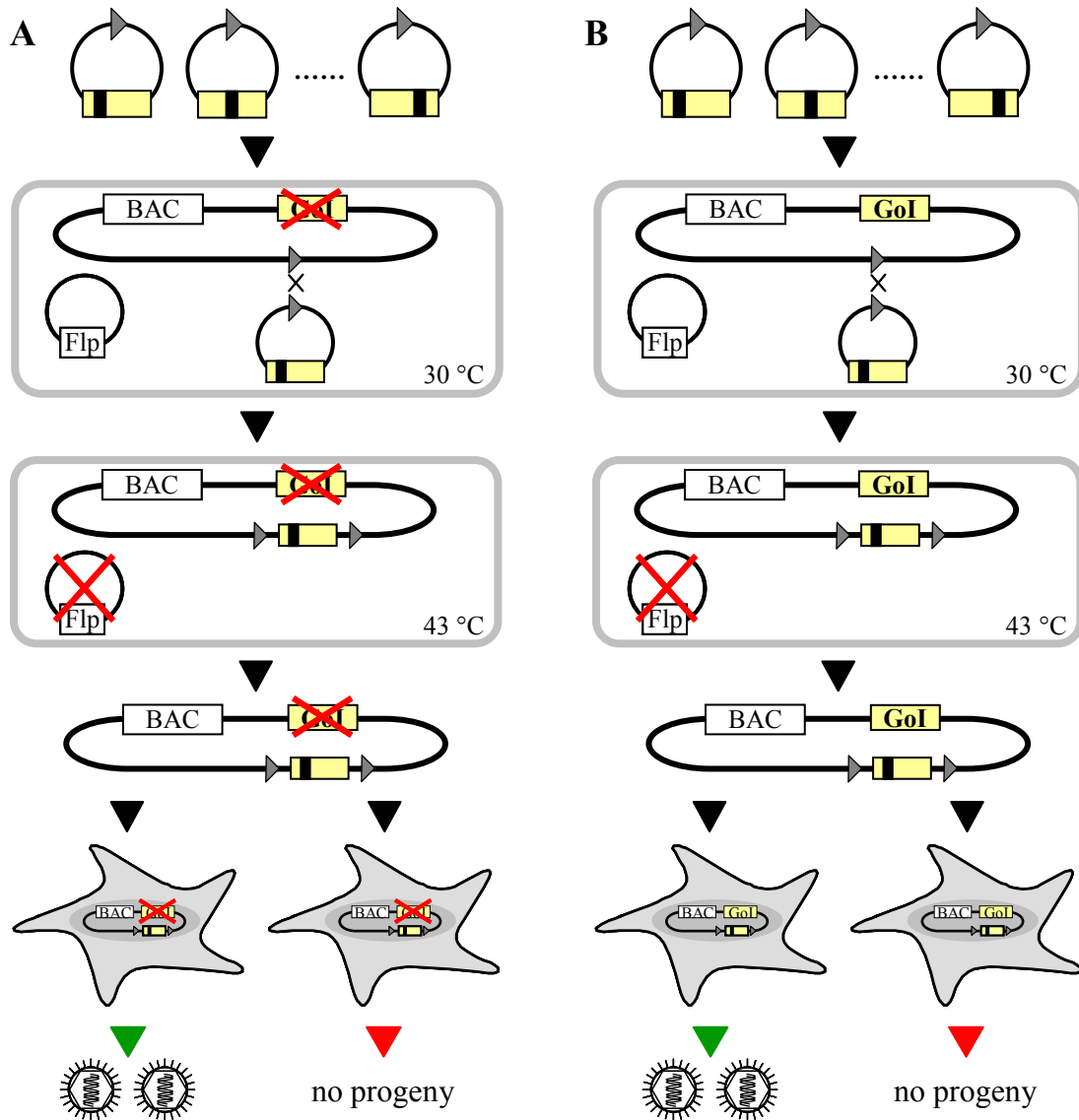


**Figure 1.7: Two-step screening approach for the identification of viral DN alleles**

**(A)** Illustration of the *cis*-complementation assay. Shuttle plasmids containing individual mutants of the gene of interest (GoI) generated by transposon mutagenesis (yellow box with black line) are inserted into an MCMV BAC lacking this gene by Flp-mediated recombination between FRT sites (grey arrowhead) at 30 °C. Flp recombinase is expressed from a temperature-sensitive plasmid, which is lost at 43 °C. Transfection of fibroblasts with BAC DNA results either in viral progeny or failure in reconstitution, which indicates essential sites. **(B)** Scheme of the inhibitory assay. Same principle as in (A), but using a wt MCMV BAC as acceptor for the shuttle plasmid. Failure in reconstitution indicates inhibitory regions. Figure was reproduced and modified from [97].

For comprehensive mutagenesis of a single viral gene, the open reading frame (ORF) is subcloned and the Tn mutagenesis performed on plasmid basis. The modified

plasmids are inserted individually into a BAC deficient for this gene and the targeting of essential and non-essential sites is identified by its ability to restore viral reconstitution. Loss-of-function mutants are then tested in a similar screen for their potential to inhibit the wt protein function by using a wt BAC as acceptor (Figure 1.7).

## 1.4 Aims

Inactivation of gene products by DN mutants is a valuable tool to assign functions to yet uncharacterised proteins, to map protein-protein interactions or to dissect physiological pathways. Detailed functional and structural knowledge about the target protein would allow the construction of inhibitory mutants by targeted mutagenesis. Yet, such data are limited for the majority of viral proteins, so that the target gene needs to be subjected to random mutagenesis to identify potential DN mutations. However, for herpesviruses the random mutagenesis requires a two-step screening approach which is time-consuming and labour-intensive. Thus, new approaches are called for which reduce screening efforts or enable faster screenings.

Analysis of numerous mutants derived from a random mutagenesis of the essential MCMV protein pM53 revealed an accumulation of inhibitory mutations in two of the four conserved regions (CRs) [95, 130] and that the homologous proteins could not complement each other [152], suggesting sub-family specific features. Based on these data we hypothesised that it should be possible to construct pM53 DN mutants by targeted mutagenesis of the CRs, which were either replaced by the homologous domain of another pUL31 family member (domain shuffling) or removed by deletion (domain deletion). The inhibitory potential of the resulting pM53 mutants was to be analysed in the viral context using conditional expression.

A further aim of this study was the establishment of an assay for the identification of inhibitory alleles of MCMV genes, which is suitable for high-throughput screening. The basis for this assay was the assumption that the Flp-mediated recombination of an MCMV BAC with a shuttle plasmid could occur in permissive host cells instead of *E. coli*. To circumvent the two-step screening, first an MCMV BAC lacking the essential gene to be tested could serve as acceptor genome which allows the identification of non-complementing mutations. The resulting non-functional mutants

were then to be discriminated from the DN mutants using a wt MCMV genome as acceptor that lacks an essential viral feature which cannot be *trans*-complemented.

Finally, the new assay system was to be applied to test a set of pM99 mutant. Its homologues have been shown to be involved in secondary envelopment of herpesviral capsids [6, 31, 161]. To confirm this role in MCMV, the biological and biochemical properties of pM99, including its essentiality, were to be studied first.

# 2 MATERIALS AND METHODS

## 2.1 Materials

### 2.1.1 Devices

| | |
|---|---|
| Typhoon 9400 | Amersham Bioscience, Freiburg, D |
| Tissue cell culture lamina flow | BDK, Sonnenbühl-Genkingen, D |
| Centrifuge Avanti™ J-20 XP | Beckman Coulter, Krefeld, D |
| Optima™ L-80 XP Ultracentrifuge | Beckman Coulter, Krefeld, D |
| PCR machine TGradient | Biometra, Göttingen, D |
| Photo documentation apparatus (Eagle Eye) | Bio-Rad, München, D |
| Mini-PROTEAN® 3 Cell | Bio-Rad, München, D |
| Trans-Blot™ SD Semi-Dry Electrophoretic Transfer cell | Bio-Rad, München, D |
| Axiovert 200M (confocal microscope) | Carl Zeiss, Jena, D |
| Axiovert 25 (phase contrast microscope) | Carl Zeiss, Jena, D |
| Econo-Submarine Electrophoresis System | C.B.S., Del Mar, CA, USA |
| pH meter 430 | Corning, Miami, FL, USA |
| Bio-Photometer | Eppendorf, Hamburg, D |
| Centrifuge 5417 R | Eppendorf, Hamburg, D |
| Thermomixer 5436 | Eppendorf, Hamburg, D |
| Branson Digital Sonifier® W-250D | Heinemann Ultraschall- und Labortechnik, Schwäbisch Gmünd, D |
| Incubator B5050E | Heraeus, Hanau, D |
| Incubator BB16CU | Heraeus, Hanau, D |
| Multifuge 3 S-R | Heraeus, Hanau, D |
| Water Bath F10 | Julabo, Seelbach, D |
| Amaxa® 4D-Nucleofector™ System with 96-well Shuttle™ Device | Lonza, Cologne, D |
| Crosslinker BLX-254 | MS Laborgeräte, Wiesloch, D |
| Developing machine Optimax TR | MS Laborgeräte, Wiesloch, D |
| Olympus IX17 (fluorescence microscope) | Olympus, Hamburg, D |
| NanoDrop™ ND-1000 Spectrophotometer | Peqlab, Erlangen, D |
| LightCycler® 2.0 | Roche, Mannheim, D |
| Bacterial shaker Certomat R BS-1 | Sartorius, Göttingen, D |
| CASY® cell counter | Schärfe System, Reutlingen, D |
| Hybridisation Oven 612 | UniEQuip, Martinsried, D |

## 2.1.2 Consumables

| | |
|---|---|
| Cell culture dishes (Ø 6 cm, Ø 10 cm) | Becton Dickinson, Heidelberg, D |
| Cell culture dishes (Ø 14,5 cm) | Sarstedt, Nümbrecht, D |
| Cell culture plates (6-, 12-, 48-, 96-well) | Becton Dickinson, Heidelberg, D |
| Cell scraper (25 cm, 39 cm) | Costar, Bodenheim, D |
| Combitips plus (5 mL, 10 mL) | eppendorf, Hamburg, D |
| CryoTube™ Vials | nunc, Langenselbold, D |
| Electroporation cuvettes | Bio-Rad, München, D |
| Falcon conical tubes (15 mL, 50 mL) | Becton Dickinson, Heidelberg, D |
| Gene Pulser® Cuvettes | Bio-Rad, München, D |
| Hybond™-N$^+$ Nylon membrane | GE Healthcare, Freiburg, D |
| Hybond™-P PVDF Transfer membrane | GE Healthcare, Freiburg, D |
| Hyperfilm™ ECL™ detection film | GE Healthcare, Freiburg, D |
| Pipettes (2 mL, 5 mL, 10 mL, 25 mL) | Sarstedt, Nümbrecht, D |
| Photometer cuvettes | Brand, Wertheim, D |
| Reaction tubes (0.5 mL, 1.5 mL, 2 mL) | eppendorf, Hamburg, D |
| Whatman blotting paper (0.7 mm) | Macherey-Nagel, Düren, D |
| LightCycler® Capillaries (20 µL) | Roche, Mannheim, D |

## 2.1.3 Reagents

If not listed below, reagents were purchased from Invitrogen (Karlsruhe, D), Merck (Darmstadt, D), Roth (Karlsruhe, D) or Sigma-Aldrich (Steinheim, D)

| | |
|---|---|
| ammonium sulfate (> 99.5%, p.a.) | Fluka Chemie, Buchs, CH |
| Bacto™ Agar | Becton Dickinson, Heidelberg, D |
| Bacto™ Tryptone | Becton Dickinson, Heidelberg, D |
| Bacto™ Yeast Extract | Becton Dickinson, Heidelberg, D |
| calf intestinal alkaline phosphatase (CIP) | NEB, Frankfurt/Main, D |
| Difco™ MacConkey Agar Base | Becton Dickinson, Heidelberg, D |
| DNA ladder (100 bp, 1 kb) | NEB, Frankfurt/Main, D |
| DNA polymerase I (Large Klenow fragment) | NEB, Frankfurt/Main, D |
| EDTA (p.a.) | VWR, Darmstadt, D |
| FCS | PAN-Biotech, Aidenbach, D |
| FuGene | Promega, Madison, USA |
| MOPS (≥ 99%) | Fluka Chemie, Buchs, CH |
| dNTP mix | NEB, Frankfurt/Main, D |
| Prestained Protein Marker | Fermentas, St. Leon-Rot, D |
| Protease Inhibitor Cocktail Tablets | Roche, Mannheim, D |
| restriction enzymes & buffers | NEB, Frankfurt/Main, D |
| sodium dodecyl sulfate (p.a.) | SERVA, Heidelberg, D |
| SuperFect® Transfection Reagent | Qiagen, Hilden, D |
| T4 DNA ligase | NEB, Frankfurt/Main, D |

## 2.1.4 Commercially available kits

| | |
|---|---|
| Amaxa® Cell Line 96-well Nucleofector® Kit SG | Lonza, Cologne, D |
| DIG Easy Hyb Granules | Roche, Mannheim, D |
| DIG Luminescent Detection Kit | Roche, Mannheim, D |
| DNeasy™ Blood and Tissue Kit | Qiagen, Hilden, D |
| ECL Plus™ Western Blotting Detection System | GE Healthcare, Freiburg, D |
| Expand High Fidelity PCR System | Roche, Mannheim, D |
| GFX™ *Micro* Plasmid Prep Kit | GE Healthcare, Freiburg, D |
| GFX™ PCR and DNA Gel Band Purification Kit | GE Healthcare, Freiburg, D |
| NucleoBond® PC100 Plasmid DNA Purification Kit | Macherey-Nagel, Düren, D |
| PCR DIG Probe Synthesis Kit | Roche, Mannheim, D |
| QIAquick Gel Extraction Kit | Qiagen, Hilden, D |
| Superscript™ RNase H – Reverse Transcriptase | Invitrogen, Karlsruhe, D |

## 2.1.5 Plasmids

**Table 2.1: Commercially available and published plasmids**

| Name | Comments |
|---|---|
| pCAGGS-Flpe | Gene Bridges GmbH, Heidelberg, D; expression plasmid for enhanced Flp recombinase (Flpe) [24] |
| pCP20 | [30]; encodes Flp recombinase, contains a temperature sensitive ori pSC101 |
| pEF5/FRT-V5-DEST | Invitrogen |
| pENTR11 | Invitrogen |
| pIRES2-AcGFP1 | Clontech Laboratories, Inc. |
| pLitmus28 | New England Biolabs |
| pL-M53 | [95] |
| pOriR6K-zeo | [22]; expression vector containing the R6K origin permitting plasmid replication only in PIR1 bacteria [77] and a gene conferring resistance to zeocin |
| pO6-ie-M50 | [22]; constitutive expression of pM50, original name pOriR6K-zeo-ie-M50 |

**Table 2.1: Commercially available and published plasmids, continued**

| Name | Comments |
|---|---|
| pO6-ie-M53 i46, i104, i115, i128, i146, i207, i212, i220, i313, s168 | [95]; constitutive expression of pM53 and indicated pM53 mutants, original name of first plasmid pOriR6K-zeo-ie-M53 |
| pO6-ie-M666 | [152]; encodes a pM53 mutant with CR2-4 exchanged for CR2-4 of MHV68 pORF69 |
| pOriR6K-zeo-MPPP | [152]; encodes a pM53 mutant with CR2-4 exchanged for CR2-4 of PrV pUL31 |
| pO6T-M53s309 | [130]; encodes the truncated mutant pM53 s309 |
| pO6-ie-FlagM53 | [95]; constitutive expression of Flag-tagged pM53 |
| pO6-SVTe | [142]; vector containing the "empty" dox-inducible expression cassette |
| pO6-SVT-M53 | [130]; dox-inducible expression of pM53 |
| pO6-SVT-Flag-ΔN-s309 | [130]; contains an M53 mutant which lacks the N-terminal Sak epitope that is recognised by the polyclonal anti-M53 antiserum |
| pO6T-C-M53 | [152]; constitutive expression of BlaC-tagged pM53, BlaN-tagged pM50 and the BlaN-tagged, pM53 binding deficient mutant pM50DM |
| pO6T-N-M50 | |
| pO6T-N-M50DM | |

**Table 2.2: Plasmids constructed during this study**

All pO6-derived plasmids (including the pDNS vectors) were propagated in *E. coli* PIR1, all other plasmids in *E. coli* DH10B. During plasmid construction, DNA fragments obtained by endonuclease digest were referred to according to their size, beginning with fragment A (fraA) for the biggest fragment. The primers referred to are listed in the Supplement, Table 6.3.

| Name (Resistance) | Comments |
|---|---|
| pDEST-pac (amp) | generated by inserting the amplicon PCR-MCMVpac (PCR on pSM3fr-Δ1-16-FRT using primer pair 34/35) into pEF5/FRT-V5-DEST after treatment with *Nde*I/*Rsr*II |
| pDEST-pac-M53, i115, i128, i146, i207, i220, i313, s309 | constitutive expression of pM53 mutants;<br>The indicated M53 genes were excised from the pO6-ie-derived vector and inserted into pENTR11 using *Kpn*I/*Not*I. All genes were transferred from the pENTR11 vector into pDEST-pac employing the LR reaction of the Gateway system. |

**Table 2.2: Plasmids constructed during this study, continued**

| Name (Resistance) | Comments |
|---|---|
| pDNS-M99F (kan) | constitutive expression of Flag-tagged pM99 under control of $P_{CMV}$; generated by insertion of pMA-T-M99F fraB (synthesised by GeneArt, Invitrogen) into pO6-A5-DNS-Che after *Nhe*I/*Sal*I treatment |
| pDNS-M99F-igfp (kan) | constitutive expression of Flag-tagged pM99 under control of $P_{CMV}$, IRES-coupled GFP expression; generated by ligation of pDNS-M99F fraA and pIRES2-AcGFP1 fraB after treatment with *Not*I/*Sal*I |
| pDNS-M99-igfp (kan) | constitutive expression of pM99 under control of $P_{CMV}$; generated by insertion of the *Nhe*I/*Sal*I treated amplicon PCR-M99 (PCR on pDNS-M99F using primer pair 27/28) and fraB of *Not*I/*Sal*I cleaved pIRES2-AcGFP1 into *Nhe*I/*Not*I opened pDNS-M99F |
| pDNS-PM99F-igfp (kan) | constitutive expression of Flag-tagged pM99 under control of $P_{M99}$; generated by insertion of the *Nhe*I/*Pac*I treated amplicon PCR-P(M99) (PCR on pSM3fr-Δ1-16-FRT using primer pair 36/37) into *Nhe*I/*Pac*I opened pDNS-M99F-igfp |
| pDNS-PM99-igfp (kan) | constitutive expression of pM99 under control of $P_{M99}$; generated by insertion of the *Nhe*I/*Sal*I treated amplicon PCR-M99 (PCR on pDNS-M99F using primer pair 27/28) and *Nhe*I/*Pac*I treated amplicon PCR-P(M99) (PCR on pSM3fr-Δ1-16-FRT using primer pair 36/37) into *Pac*I/*Sal*I opened pDNS-M99F-igfp |
| pDNS-PM99ΔGly2-igfp (kan) | constitutive expression of pM99 lacking the N-terminal Gly under control of $P_{M99}$; generated by insertion of the PCR-amplified M99 amplicon (PCR on pDNS-PM99-igfp using primer pair 29/28) into pDNS-PM99-igfp fraA by treatment with *Nhe*I/*Sal*I |
| pDNS-PM99ΔM94-igfp (kan) | constitutive expression of pM99 lacking aa 22-43 under control of $P_{M99}$; generated by insertion of *Pac*I-treated PCR-5'-ΔM94 (primer pair 36/30) and *Sal*I-treated PCR-3'-ΔM94 (primer pair 30/28) into pDNS-PM99-igfp opened with *Pac*I/*Sal*I (fraA), PCR on pDNS-PM99-igfp |
| pDNS-PM99ΔAC-igfp (kan) | constitutive expression of pM99 lacking aa 43-55 under control of $P_{M99}$; generated by insertion of *Pac*I-treated PCR-5'-ΔAC (primer pair 36/32) and *Sal*I-treated PCR-3'-ΔAC (primer pair 33/28) into pDNS-PM99-igfp opened with *Pac*I/*Sal*I (fraA), PCR on pDNS-PM99-igfp |
| pO6-A5-DNS-Che (kan) | constitutive expression vector; assembled from pIRES-Che-pA (provided by Sigrig Seelmeir) fraA and pDEST-pac fraB following *Nde*I/*Rsr*II cleavage; the resulting plasmid was cut with *Pac*I, blunted using T4 DNA polymerase, re-ligated, cleaved with *Afe*I/*Mlu*I and unified with pO6-A5-CMVgfp (provided by Simone Boos) fraA treated with the same enzymes |
| pO6-BlaC-M53Δ2 (zeo) | constitutive expression of BlaC-tagged pM53Δ2; generated by insertion of pO6-SVT-M53Δ2 fraB into pO6T-C-M53 by treatment with *Bsi*WI/*Psh*AI |

**Table 2.2: Plasmids constructed during this study, continued**

| Name (Resistance) | Comments |
|---|---|
| pO6-BlaC-M53Δ3 (zeo) | constitutive expression of BlaC-tagged pM53Δ3; generated by insertion of pO6-SVT-M53Δ3 fraB into pO6T-C-M53 by treatment with *Psh*AI/*Pst*I |
| pO6-BlaC-M53s309 (zeo) | constitutive expression of BlaC-tagged truncated mutant pM53s309; generated by insertion of pO6T-M53s309 fraB into pO6T-C-M53 by treatment with *Not*I/*Sac*II |
| pO6-ie-M53Δ2 (zeo) | constitutive expression of pM53Δ2; generated by insertion of *Asc*I/*Stu*I excised fraB of pO6-SVT-M53Δ2 into *Asc*I/*Hpa*I treated pOriR6K-zeo |
| pO6-ie-FlagM53s168 (zeo) | constitutive expression of Flag-tagged truncated mutant pM53s168; generated by insertion of pO6-ie-FlagM53s168 fraB into pO6-ie-FlagM53 by treatment with *Acc*65I/*Bsp*EI |
| pO6-ie-FlagΔNΔ2 (zeo) | constitutive expression of Flag-tagged pM53Δ2 lacking the epitope recognised by the α-M53 antiserum; generated by insertion of the PCR-amplified Flag-tag containing amplicon (primer pair 06/07 on pO6-SVT-Flag-ΔN-s309) into pO6-ie-M53Δ2 by treatment with *Kpn*I/*Sal*I |
| pO6-ie-FlagΔNΔ2A, FlagΔNΔ2B, FlagΔNΔ3, FlagΔNM6MM, FlagΔNMM6M, FlagΔNMMM6 (zeo) | constitutive expression of Flag-tagged pM53 mutants lacking the epitope recognised by the α-M53 antiserum; The M53 mutant genes were transferred from the conditional pO6-SVT-backbone by excision with *Asc*I/*Stu*I and insertion into the *Asc*I/*Hpa*I treated pOriR6K-zeo vector. The Sak epitope was deleted by inserting the PCR-amplified Flag-tag containing amplicon (primer pair 06/07 on pO6-SVT-Flag-ΔN-s309) by treatment with *Kpn*I/*Sal*I. |
| pO6-ie-M56 | constitutive expression of pM56; The M56 ORF was PCR-amplified in fragments from pSM3fr-16FRT17 using primer pairs 17/18 (PCR-M56-1, *Age*I/*Kpn*I), 19/20 (PCR-M56-2, *Age*I/*Hin*dIII), 21/22 (PCR-M56-3, *Bsi*WI/*Bam*HI) and 23/24 (PCR-M56-4, *Bsi*WI/*Nsi*I). Each amplicon was inserted into into pLitmus28 after cleavage with the indicated enzymes, giving rise to pL-M56-x. pL-M56-2 fraA was ligated with pL-M56-3 fraB after treatment with *Bsi*WI/*Sac*II, giving rise to pL-M56-23. Finally, *Bsp*EI/*Bsp*MI treated pL-M56-23 fraB and *Bsp*MI/*Nsi*I treated pL-M56-4 fraB were inserted into *Bsp*EI/*Nsi*I opened pL-M56-1, giving rise to pL-M56. pL-M56 fraB and pOriR6K-zeo-MPPP [152]were ligated after cleavage with *Kpn*I/*Nsi*I. |
| pO6-ie-M99Flag (zeo) | constitutive expression of Flag-tagged pM99; generated by insertion of PCR-M99Flag (PCR on pSM3fr-Δ1-16-FRT using primer pair 25/26) into pOriR6K-zeo after treatment with KpnI/NotI |

**Table 2.2: Plasmids constructed during this study, continued**

| Name (Resistance) | Comments |
|---|---|
| pO6-SVT-M53Δ2 (zeo) | dox-inducible expression of pM53Δ2; generated by insertion of AscI cleaved PCR-5'-2A (primer pair 09/10) and PstI cleaved PCR-3'-2B (primer pair 14/12) into pO6-SVT-M53 opened by AscI/PstI, PCR on pO6-SVT-M53 |
| pO6-SVT-M53Δ2A (zeo) | dox-inducible expression of pM53Δ2A; generated by insertion of *Asc*I cleaved PCR-5'-2A (primer pair 09/10) and *Pst*I cleaved PCR-3'-2A (primer pair 11/12) into pO6-SVT-M53 opened by *Asc*I/*Pst*I, PCR on pO6-SVT-M53 |
| pO6-SVT-M53Δ2B (zeo) | dox-inducible expression of pM53Δ2B; generated by insertion of *Asc*I cleaved PCR-5'-2B (primer pair 09/13) and *Pst*I cleaved PCR-3'-2B (primer pair 14/12) into pO6-SVT-M53 opened by *Asc*I/*Pst*I, PCR on pO6-SVT-M53 |
| pO6-SVT-M53Δ3 (zeo) | dox-inducible expression of pM53Δ3; generated by insertion of *Asc*I cleaved PCR-5'-3 (primer pair 09/15) and *Pst*I cleaved PCR-3'-3 (primer pair 16/12) into pO6-SVT-M53 opened by *Asc*I/*Pst*I, PCR on pO6-SVT-M53 |
| pO6-SVT-M6MM (zeo) | dox-inducible expression of pM6MM; The fraB of pMA-CR2_M6MM (synthesised by GeneArt, Invitrogen) was inserted into pL-M53 after treatment with *Bgl*II/*Sac*II, giving rise to pL-M6MM. The M6MM fragment (fraB) was excised using *Asc*I/*Stu*I and ligated into the *Asc*I/*Hpa*I treated pO6-SVTe. |
| pO6-SVT-MM6M (zeo) | dox-inducible expression of pMM6M; The fraB pMA-CR3_ORF69 (synthesised by GeneArt, Invitrogen) was ligated into pL-M53 after treatment with *Pml*I/*Pst*I, giving rise to pL-MM6M. The *Asc*I/*Pvu*II excised fraB of pL-MM6M was inserted into *Asc*I/*Hpa*I treated pO6-SVTe. |
| pO6-SVT-MMM6 (zeo) | dox-inducible expression of pMMM6; The PCR-amplified N-terminal two thirds of the M53 ORF (primer pair 03/04 on pO6-ie-M53) were inserted into pL-M53 after treatment with *Bgl*II/*Xho*I, giving rise to pL-MMM. pL-M666 was generated by inserting pO6-ie-M666 fraB into pL-M53 by treatment with *Sal*I/*Xba*I. The *Xho*I recognition site in pL-M666 was removed by cleavage with *Not*I/*Xba*I and re-ligation subsequent to blunting using the Klenow fragment of DNA polymerase I, giving rise to pL-M666ΔX. The CR4 of MHV68 ORF69 PCR-amplified (primer pair 05/08 on pL-M666ΔX), cleaved with *Pvu*II/*Xho*I and ligated with the *Stu*I/*Xho*I treated pL-MMM, giving rise to pL-MMM6. Finally, the *Asc*I/*Stu*I excised fraB of pL-MMM6 was inserted into *Asc*I/*Hpa*I treated pO6-SVTe. |

### 2.1.6 Bacterial artificial chromosomes

**Table 2.3: Published BACs and BACs available in the lab**

| Name | Comments |
|------|----------|
| pSM3fr-16FRT17 | [23]; wt MCMV genome with an FRT site inserted between genes *m16* and *m17*, BAC-derived virus has wt growth properties |
| pSM3fr-Δ1-16-FRT | [97]; MCMV with ORFs 1 to 16 deleted, BAC-derived virus has wt-like growth properties |
| pSM3fr-ΔM53 | [95]; MCMV with M53 deleted |
| pSM3fr-ΔM53-EM53K128A | [95]; MCMV with an M53 gene having a point mutation at position 128 of the M53 protein resulting in attenuated growth |
| pSM3fr-Δm157rekegfp | [145]; MCMV with *m157* replaced by the *egfp* gene |
| pSM3fr-Δ1-16-FRT-ΔM56 | MCMV genome lacking ORF M56; provided by Sigrid Seelmeir |
| pSM3fr-Δ1-16-FRT-ΔM104 | MCMV genome lacking ORF M104; provided by Sigrid Seelmeir |
| pSM3fr-Δ1-16-FRT-SCPiChe | mCherry expression coupled by an IRES element to SCP expression; provided by Sigrid Seelmeir |

**Table 2.4: BACs constructed during this study**

| Name (Resistance) | Comments |
|-------------------|----------|
| SVT-Δ2<br>SVT-Δ2A<br>SVT-Δ2B<br>SVT-Δ3<br>SVT-M6MM<br>SVT-MM6M<br>SVT-MMM6<br>(cam, zeo) | exemplified for SVT-Δ2: generated by ectopic insertion of pO6-SVT-M53Δ2 into pSM3fr-Δ1-16-FRT via the Flp/FRT system, dox-inducible expression of pM53Δ2 in addition to wt pM53; other listed BACs were constructed similarly |
| Δpac (cam, kan) | generated by homologous recombination to replace the packaging signal of pSM3fr-Δ1-16-FRT by a kan resistance cassette |
| ΔM99 (cam, amp) | generated by homologous recombination to replace the M99 ORF of pSM3fr-Δ1-16-FRT by an amp resistance cassette |

**Table 2.4: BACs constructed during this study, continued**

| Name (Resistance) | Comments |
|---|---|
| SCPiChe-ΔM99 (cam, amp) | generated by homologous recombination to replace M99 ORF of pSM3fr-Δ1-16-FRT-SCPiChe by an amp resistance cassette |
| ΔM99EPM99 (cam, amp, kan) | generated by ectopic insertion of pDNS-PM99-igfp into the ΔM99 BAC via the Flp/FRT system, constitutive pM99 expression under control of $P_{M99}$ |
| ΔM99EPM99F (cam, amp, kan) | generated by ectopic insertion of pDNS-PM99F-igfp into the ΔM99 BAC via the Flp/FRT system, constitutive pM99F expression under control of $P_{M99}$ |

### 2.1.7 Viruses

The viruses used in this study were derived from the BACs listed in Table 2.3 and Table 2.4. For virus reconstitution, BAC DNA was transfected into murine fibroblasts as described in section 2.7.1. Viruses were called as their respective BACs tagged with an "MCMV" prefix. Further viruses used were MCMV-SVT-M53 [MCMV-SVT-M53R in 130] and MCMV-SVT-gfpSCP [18, SCP-GFP-2 in 142].

### 2.1.8 Oligonucleotides

All oligonucleotides were synthesised by metabion GmbH (Martinsried, D). Oligonucleotides longer than 33 nt were HPLC purified. Standard primers for sequencing were provided by GATC Biotech (Konstanz, D). For sequences, refer to supplementary tables in section 1.1.

## 2.1.9 Antibodies

**Table 2.5: List of primary antibodies and antisera**

| Antibody/ antiserum | Description | Comments/Source |
|---|---|---|
| CROMA101 (α-pp89) | mouse monoclonal antibody | provided by S. Jonjic, University of Rijeka, Croatia |
| α-Flag M2 | mouse monoclonal antibody | Sigma-Aldrich |
| α-Flag M2 HRP | mouse monoclonal antibody | Sigma-Aldrich |
| α-GAPDH | rabbit monoclonal antibody | Cell Signaling |
| α-HA (3F10) | rat monoclonal antibody | Roche |
| α-M50 | rabbit polyclonal immune serum | [118] |
| α-M53 | rat polyclonal immune serum | [95] |
| α-M99[1] | rabbit polyclonal immune serum | Eurogentec GmbH, Cologne, D |
| α-MCP | rat polyclonal immune serum | [142] |

[1] #700: raised against the epitope spanning aa 98-112 (C+SAKNGAGVKKKVRAL)
 #701: raised against the epitope spanning aa 12-33 (DSLKDSSGRRVDLGT+C)
The terminal cysteines were introduced to couple the epitopes to the adjuvant.


Horseradish peroxidase (HRP) coupled secondary antibodies (directed against mouse, rabbit and rat) were purchased from Dianova (Hamburg, D). Alexa Fluor conjugated secondary antibodies (directed against mouse, rabbit and rat) were obtained from MoBiTec (Göttingen, D).

Primary antibodies were used in 1/1,000 dilution for Western blot analysis and 1/100 for immunofluorescence (IF). Secondary antibodies were diluted 1/8,000 for Western blots and 1/150 for IF.

## 2.2 Bacterial culture

Bacteria (Table 2.6) were grown either in suspension or on agar plates using Luria-Bertani (LB) medium (10 g/L Bacto tryptone, 5 g/L Bacto yeast extract, 5 g/L NaCl) or LB agar (15 g/L). The respective antibiotics (Table 2.7) were added for plasmid and/or BAC selection. *E. coli* DH10B and PIR1 were grown at 37 °C, whereas SW102 were grown at 32 °C. Cell density was determined by measuring the optical density of the bacterial suspension at 600 nm ($OD_{600}$).

For long-term availability of the bacteria bearing the DNA of interest, glycerol stocks were prepared by suspending 600 µL of bacterial culture in 400 µL of 50% glycerol to a final concentration of 20% (volume/volume) and stored at -80 °C.

**Table 2.6: Bacterial strains used during this study**

| *E. coli* strain | Genotype |
|---|---|
| DH10B | F⁻ *mcr*A Δ(*mrr*−*hsd*RMS−*mrc*BC) Φ80*lac*ZΔM15 Δ*lac*X74 *rec*A1 *end*A1 *ara*D139 Δ(*ara*, *leu*) 7697 *gal*U *gal*K *rps*L *nup*G λ⁻ (Invitrogen, Karlsruhe, D) |
| PIR1 | F⁻ Δ*lac*169 *rpo*S(Am) *rob*A1 *cre*C510 *hsd*R514 *end*A *rec*A1 *wid*A(Δ*mlu*I)::*pir*-116 (Invitrogen, Karlsruhe, D) |
| SW102 | DH10B [λ*c*1857 (*cro-bio*A)<>*Tet*] *gal*490 Δ*gal*K [181] |

**Table 2.7: Commonly used antibiotic concentrations**

| Antibiotic | Concentration |
|---|---|
| ampicillin (amp) | 50 µg/mL in solution, 100 µg/mL in LB agar plates |
| chloramphenicol (cam) | 25 µg/mL |
| kanamycin (kan) | 50 µg/mL |
| zeocin (zeo) | 30 µg/mL |

### 2.2.1 Generation of electro-competent bacteria

Unless stated otherwise, all steps were performed at 4 °C or on ice. To prepare electro-competent *E. coli* strains DH10B and PIR1, 400 mL of LB were inoculated with 1.5 mL of an overnight (o/n) culture and grown shaking at 37 °C to an $OD_{600} \sim 0.5$

(middle logarithmic phase). After reaching the desired cell density, the culture was chilled on ice for 30 min and centrifuged at $6,000 \times g$ for 10 min (Beckman Coulter™ Avanti™, JLA 16.250). To remove all salt residuals, the pellet was washed once with 200 mL pre-cooled $dH_2O$ and twice with 200 mL pre-cooled 5% glycerol using the same centrifugation parameters to collect the bacteria. Cells were then resuspended in 10 mL of pre-cooled 10% glycerol and centrifuged at 3,500 rpm/$2,600 \times g$ for 15 min (Heraeus Multifuge 3 S-R). Finally, the volume of the cell pellet was estimated and resuspended in an equal volume of 10% glycerol Aliquots of 50 µL bacterial suspension were immediately frozen in liquid nitrogen and stored at -80 °C until usage.

Electro-competent *E. coli* SW102 were always prepared freshly on the day of transformation. For this, 50 mL LB were inoculated with 500 µL of an o/n culture and grown at 32 °C/160 rpm to an $OD_{600}$ of 0.55 to 0.6. Aliquots of 4 mL were pelleted (eppendorf 5417 R, 5,000 rpm, 5 min) and washed twice with 1 mL ice-cold sterile, distilled water to remove any salt contaminants. Each aliquot of the electro-competent *E. coli* SW102 was resuspended in 80-120 µL ice-cold water and kept on ice until transformation.

### 2.2.2 Transformation of electro-competent bacteria

Bacteria to be transformed were thawed on ice, DNA was added to the cell suspension and the mixture was transferred to 2 mm electroporation cuvettes (Gene Pulser® Cuvette), which had been pre-cooled to -20 °C. Cells were electro-shocked at 2.5 kV (25 µF/200 Ω) using the GenePulser Xcell™ (Bio-Rad, München, D), immediately diluted in 1 mL LB, incubated by shaking under non-selective conditions (pCP20-containing *E. coli* DH10B 30 °C, *E. coli* SW102 32 °C, otherwise 37 °C) for one hour, plated in 100 µL-aliquots on LB agar plates containing the appropriate antibiotic(s), and incubated at the appropriate temperature until colonies formed (usually o/n).

### 2.2.3 Generation of chemically competent bacteria

Unless stated otherwise, all experimental steps were performed at 4 °C or on ice. 50 mL LB medium containing appropriate antibiotic(s) was inoculated with 1 mL of an o/n pre-culture and grown shaking at 37 °C. At $OD_{600} \sim 0.5$ (logarithmic growth phase)

cells were harvested, chilled on ice for 5 min, centrifuged at $2,600 \times g$ for 15 min (Heraeus Multifuge 3 S-R), and resuspended in 10 mL ice-cold buffer TfB I (100 mM $RbCl_2$, 50 mM $MnCl_2$, 30 mM KAc, 10 mM $CaCl_2$, pH 5.8). Cell suspension was incubated on ice for 50 min, centrifuged as above and resuspended in 1 mL ice-cold buffer TfB II (10 mM MOPS (pH 7.0), 10 mM $RbCl_2$, 75 mM $CaCl_2$, 15% glycerol). Aliquots of 100 µL were immediately frozen in liquid nitrogen and stored at -80 °C.

### 2.2.4 Transformation of chemically competent bacteria

Chemically competent cells were thawed on ice, 10 ng of the DNA to be transformed was added and the mixture incubated on ice for 30 min. After a heat shock at 42 °C for 45 seconds and incubation on ice for 2 min, 1 mL LB was added, and cells were incubated by shaking at 30 °C (pCP20-containing bacteria) or 37 °C for one hour. Cultures were plated in 100 µL aliquots on LB agar plates containing the appropriate antibiotic(s) and incubated at 30 °C or 37 °C o/n.

## 2.3 Isolation and purification of nucleic acid

### 2.3.1 Small scale isolation of plasmid DNA

Bacteria were cultivated o/n (o/n) on Luria-Bertani (LB) agar plates (10 g/L Bacto tryptone, 5 g/L Bacto yeast extract, 5 g/L NaCl, 15 g/L agar) containing the appropriate antibiotic(s) for selecting the plasmid of interest. For small scale plasmid (mini)-preparation, single clones were picked to inoculate 3 mL LB containing the respective antibiotic(s) and grown at 37 °C/160 rpm o/n. Plasmid DNA was isolated based on the alkaline lysis principle using the GFX™ *Micro* Plasmid Prep Kit (GE Healthcare) according to the manufacturer's instructions. As a variant of the protocol, DNA was recovered from the DNA binding column in 75 µL Tris-HCl (pH 8.0). Five µL of the purified DNA was subjected to restriction pattern analysis (section 2.4.3).

### 2.3.2 Large scale isolation of plasmid DNA

Plasmid DNA in high quantity was purified from 200 mL cultures that were either inoculated with a single colony from an LB agar plate or a scratch of a glycerol stock.

Plasmids were purified using the NucleoBond® PC100 Plasmid DNA Purification Kit (Macherey-Nagel) according to the manufacturer's instructions. Dried DNA was dissolved in 150 µL Tris-HCl (pH 8.0) at 4 °C o/n and stored at -20 °C.

### 2.3.3 Small scale isolation of BAC DNA

For small scale isolation of BAC DNA, 10 mL LB containing 25 µg/mL chloramphenicol were inoculated with a single colony of *E. coli* strain DH10B containing the respective BAC, incubated at 37 °C and 160 rpm o/n and bacteria were harvested by centrifugation at $2,600 \times g$ for 15 min (Heraeus Multifuge 3 S-R). Cells were resuspended in 300 µL of QIAGEN Resuspension buffer P1 (20 mM Tris-HCl, 10 mM EDTA, pH 8.0), lysed in 300 µL of buffer 2 (0.2 M NaOH, 1% SDS), and neutralised by addition of 300 µL of QIAGEN Neutralization Buffer P3 (3 M KAc, pH 4.8). Suspensions were incubated on ice for 10 min and centrifuged at 14,000 rpm (eppendorf 5417 R) for 5 min. Proteins were removed from the supernatants by extraction with an equal volume of phenol/chloroform. Following gentle rotation for at least 10 min and centrifugation at 14,000 rpm for 10 min (eppendorf 5417 R), BAC DNA was precipitated from the aqueous fraction by addition of 1 mL isopropanol and centrifugation at 14,000 rpm for 30 min (eppendorf 5417 R). DNA pellets were washed with 1 mL of 70% ethanol (room temperature), centrifuged for 10 min, and dried at 45 °C until pellets became opaque. DNA was dissolved in 50 µL Tris-HCl containing 100 µg/mL RNase H (pH 8.0) by gently shaking at 37 °C for 15 min and stored at 4 °C until use. The total volume of DNA solution was subjected to restriction pattern analysis (section 2.4.3).

### 2.3.4 Large scale isolation of BAC DNA

Large amounts of BAC DNA were obtained from 200 mL bacterial cultures using the NucleoBond® PC100 Plasmid DNA Purification Kit (Macherey-Nagel) according to the manufacturer's instructions. BAC DNA was eluted with elution buffer N5 pre-heated to 50 °C and applied in two steps. Dried DNA precipitates were recovered in 100 µL Tris-HCl (pH 8.0) at 4 °C o/n and stored at 4 °C. For handling solutions containing BAC DNA during or after the preparation, pipette tips were cut with a pair

of scissors to minimise shear forces during pipetting that might cause damage to the BAC molecules.

### 2.3.5 DNA isolation from cultured mammalian cells

To obtain DNA from mammalian cells, approximately $1 \times 10^6$ cells were harvested, washed once with PBS and DNA was isolated using the DNeasy™ Blood & Tissue Kit (Qiagen) according to the protocol "Purification of total DNA from Animal Blood or Cells (spin-column protocol)". Finally, DNA was eluted from the column in 100 µL ddH$_2$O applied in two successive aliquots.

### 2.3.6 RNA isolation from cultured cells

Approximately $1 \times 10^6$ mammalian cells were harvested and total cellular RNA was purified using the RNeasy® Mini Kit (Qiagen) according to the protocol "Animal Cells, Spin". RNA was eluted in 30 µL RNase-free water.

### 2.3.7 Determination of DNA concentration and purity

To determine the concentration and purity of the isolated nucleic acid, the optical density (OD) was measured at 260 nm and 280 nm using a NanoDrop® *ND-1000 Spectrophotometer* (peqlab Biotechnologie GmbH). The content was calculated as 1 unit of OD$_{260}$ equalling 50 µg/mL double stranded DNA or 40 µg/mL RNA, respectively. The ratio OD$_{260}$/OD$_{280}$ provided an estimation of the purity and should optimally range around 1.8 for a DNA and around 2.0 for an RNA solution.

## 2.4 Analysis and manipulation of nucleic acid

### 2.4.1 Reverse transcription of RNA

To generate cDNA, purified RNA (Section 2.3.6) was reverse transcribed using the Superscript™ RNase H – Reverse Transcriptase (Invitrogen). For this, 500 ng RNA was mixed with 5 µM Oligo (dT)$_{20}$ Primer (Invitrogen) and 1 mM dNTP mix in a final volume of 10 µL in RNase-free water. The reaction was incubated at 70 °C for 10 min

and cooled down on ice, before further components were added to the mixture: 4 μL First Strand Reaction buffer, 5 mM MgCl$_2$, 10 mM DTT, 40 U RNasin and 1200 U Superscript Transcriptase in a final volume of 20 μL in ddH$_2$O. The mixture was incubated at 50 °C for 60 min, followed by 5 min at 85 °C. Finally, the remaining RNA was removed by incubation with 5 U RNase H at 37 °C for 20 min.

## 2.4.2 Polymerase chain reaction (PCR)

### Amplification of DNA fragments for cloning

To ensure high specificity of the PCR product without the need of optimising the protocol for each template/primer pair, a touch down programme was used. The PCR started at an annealing temperature equal or above the expected annealing temperature of the primers and was decreased by one degree in each of the first 17 cycles. The primers then bind to the template at the highest temperature least-permissive for unspecific annealing. Thus, the first amplicons are those with highest primer specificity, which in most cases cover the region of interest. Due to the exponential nature of the PCR, these products will out-compete any unspecific fragments to which the primers may bind when the PCR proceeds to the cycles with lower annealing temperatures. Lower annealing temperatures, however, favour a higher yield and therefore improve the productivity of the PCR [44].

In general, 50 μL PCR reaction mix consisted of 10-50 ng template DNA, 300 nM of each forward and reverse primer, 200 μM dNTP mix, 1/10 volume of 10x Expand High Fidelity reaction buffer including MgCl$_2$ as well as 3 U of Expand High Fidelity PCR system Polymerase (Roche). When BAC DNA was used as template, proper aliquoting was ensured by vigorous vortexing for at least 30 seconds before pipetting it to the reaction mixture. The PCR mixes were prepared on ice. Primers are listed in the Supplement.

PCRs were performed in a Tgradient PCR machine (Whatman Biometra® GmbH). Presence and specificity of the amplicons was confirmed by subjecting 5 μL of the reaction mix to agarose gel electrophoresis (1% agarose, TAE; section 2.4.5). The remaining DNA was purified using the GFX™ PCR DNA and Gel Purification Kit (GE Healthcare) according to the manufacturer's instructions or by ethanol precipitation (section 2.4.7).

**Table 2.8: General Touch Down PCR programme**

| Step | | Temperature | Time | |
|---|---|---|---|---|
| 1 | Denaturation | 95 °C | 5 min | |
| 2 | Denaturation (Touch Down) | 95 °C | 30 s | |
| 3 | Annealing (Touch Down) | 62-45 °C | 30 s | per cycle -1 °C |
| 4 | Elongation (Touch Down) | 72 °C | 0.5-3 min[1] | 17x back to step 2 |
| 5 | Denaturation (amplification) | 95 °C | 30 s | |
| 6 | Annealing (amplification) | 45 °C | 30 s | |
| 7 | Elongation (amplification) | 72 °C | * | 20x back to step 5 |
| 8 | End-elongation | 72 °C | 5 min | |
| 9 | End | 4 °C | ∞ | |

[1] The elongation time was adjusted to the length of each amplicon by assuming DNA polymerase activity of approximately 1,000 bp per minute.

### Synthesis of Southern blot probes

To generate the probe used in the Southern blot analysis (section 2.4.12), PCR was performed on 50 ng of the pSM3fr-Δ1-16-FRT BAC as described above using the PCR DIG Probe Synthesis Kit (Roche) according to the manufacturer's instructions.

### Quantitative PCR

To quantify the viral genome load during infection, quantitative PCR (qPCR) with real-time detection (also called real-time PCR) was performed. For this, 5 µL (~ 200 ng) of *Pae*I digested sample DNA was added to 15 µL reaction mix consisting of 10 µL QuantiTect™ SYBR® Green PCR Master Mix (Qiagen), 1 µL DNase-free water and 0.5 µM of each primer and PCRed according to the protocol in Table 2.4 on a Light Cycler (Roche), followed by melting curve analysis to confirm specific amplification. Relative quantification was performed based on normalisation to the gene of the lamin B receptor (*lbr*) according to the equation

$$ratio = 2^{|ct(M54)-ct(lbr)|}$$

**Table 2.9: PCR programme for qPCR**

| Step | | Temperature | Time | |
|------|--------------|-------------|--------|-------------------|
| 1 | Denaturation | 95 °C | 10 min | |
| 2 | Denaturation | 95 °C | 10 s | |
| 3 | Annealing | 58 °C | 3 s | |
| 4 | Elongation | 72 °C | 10 s | 45x back to step 2 |

### 2.4.3 Restriction enzyme digest

For restriction pattern analysis of the DNA, 5 µL of the plasmid mini-preparation, corresponding to approximately 300-600 ng DNA, was suspended with 1/10 of the recommended 10x reaction buffer, 1 mg/mL BSA (if required), at least 10 U (1 µL) of the appropriate restriction enzyme and ddH$_2$O in a total volume of 20 µL and incubated for 1-2 hours at the recommended temperature. For preparative digestion of plasmid DNA for cloning, 1 µg of DNA was digested in a total volume of 40 µL for at least 3 hours using the same conditions as above.

Restriction pattern analysis of BAC DNA was performed in a total volume of 60 µL (without BSA) or 70 µL (if BSA was required). For that, the recommended 10x reaction buffer as well as 10-50 U (1 µL) of the appropriate restriction enzyme were added to the 50 µL BAC mini-preparations (section 2.4.3) and incubated at the appropriate temperature for at least 3 hours. For restriction pattern analysis of large scale BAC preparation, 2 µg of BAC DNA was digested in a total volume of 40 µL for at least 3 hours using the same conditions as above.

### 2.4.4 Buffer exchange

PCR products and digested DNA were prepared for further processing by buffer exchange using the GFX™ PCR DNA and Gel Band Purification Kit (GE Healthcare) according to the manufacturer's instructions. DNA was eluted in 20 µL Tris-HCl (pH 8.0).

## 2.4.5 Agarose gel electrophoresis

To analyse DNA fragments obtained by restriction enzyme digest, DNA was subjected to horizontal, non-denaturing agarose gel electrophoresis. Digested plasmid DNA as well as PCR products were separated on 1% agarose gels in TAE buffer (40 mM Tris-HCl, 20 mM acetic acid, 1 mM EDTA, pH 8.0) at a field strength of 10-15 V/cm, whereas BAC DNA fragments were separated on 0.8% agarose gels in TBE buffer (90 mM Tris, 90 mM boric acid, 2.5 mM EDTA, pH 8.0) at a field strength of 1.5-3 V/cm. DNA was visualised by addition of 1 µg/mL ethidium bromide to the gels and monitored using UV light in an Molecular Imager ChemiDoc XRS System (Bio-Rad Laboratories GmbH). Data were processed using the Quantity One 1-D Analysis Software.

## 2.4.6 Isolation of DNA fragments from agarose gels

Following preparative restriction enzyme digestion, DNA fragments to be used for cloning were separated by agarose gel electrophoresis. The desired bands were excised and the DNA was purified using the Qiaquick Gel Extraction Kit (QIAGEN) according to the manufacturer's instructions. To avoid damage to the DNA during excision, very weak high wave length UV light was applied to visualise the DNA bands (IL-350-L 366 nm, Bachofer GmbH).

## 2.4.7 Ethanol precipitation

To concentrate DNA, 1/10 volume of 3 M sodium acetate (pH 5.3) and three volumes ice-cold 100% ethanol were added to the DNA containing solution and incubated at -80 °C for 20 min. The mixture was centrifuged at 14,000 rpm and 4 °C for 30 min (eppendorf 5417 R). The precipitated DNA was washed with an equal volume of 70% ethanol and centrifuged again for 15 min. Ethanol was removed carefully; DNA pellets were air-dried at r/t and dissolved in 10 µL distilled water.

## 2.4.8 De-phosphorylation of DNA ends

To prevent re-circularisation of linearised vector DNA, the 5' phosphate groups of the free DNA ends were removed using calf intestinal alkaline phosphatase (CIP). 1 µg

linearised vector DNA was suspended in a total volume of 20 µL containing 1/10 volume of the recommended 10x reaction buffer and 0.5 U CIP and incubated at 37 °C for 60 min. The de-phosphorylated vector was purified by agarose gel extraction (section 2.4.6).

### 2.4.9 Blunting DNA ends

To allow ligation of DNA fragments with non-complementary ends, the DNA ends were blunted using either T4 DNA polymerase or the Klenow fragment of DNA polymerase I. Both enzymes possess polymerisation and 3'-5' exonuclease, but not 5'-3' exonuclease activity.

For the blunting reaction, 1 µg DNA was incubated in a total volume of 20 µL containing 1 U of the polymerase and 1/10 volume of any of the supplied 10x restriction enzyme buffers supplemented with 33 µM of each dNTP. The reaction was incubated at 12 °C (T4) or 25 °C (Klenow) for 15 min and inactivated by addition of 10 mM EDTA and heating at 75 °C for 20 min.

### 2.4.10 Ligation of DNA fragments

To join DNA fragments covalently, 100 ng vector DNA was mixed with 300 ng of (each) insert fragment, 100 U (1 µL) T4 DNA ligase and 1/10 volume of the 10x T4 ligase reaction buffer in a total volume of 20 µL. The reaction was incubated at 16 °C o/n. 1 µL of the ligation mix was used to transform electro-competent cells (section 2.2.2).

### 2.4.11 LR reaction (Gateway® system)

An LR reaction was performed to transfer a gene from a Gateway® entry plasmid to a destination vector. To this end, 50-150 ng of entry (pENTR11) and destination (pEF5/FRT-V5-DEST) vector were mixed with 2 µL LR Clonase™ II enzyme mix (Invitrogen) in TE buffer (pH 8.0) in a final volume of 10 µL and incubated at 25 °C for 60 min. The reaction was terminated by addition of 1 µL proteinase K solution (Invitrogen) and incubation at 37 °C for 10 min. Competent cells were transformed with 1 µL of this reaction.

## 2.4.12 Southern blot analysis

To assess viral cleavage/packaging, $1.5 \times 10^6$ M2-10B4 were infected at an MOI of 0.1, cells were harvested 48 hpi and total DNA was purified using the DNeasy™ Blood and Tissue Kit as described in section 2.3.5. Using 40 U *Apa*LI, 6 µg of the purified DNA was digested at 37 °C for 16 hours and separated by 0.8% agarose gel electrophoresis. Size markers were documented by photographing the gel next to a ruler before the gel was cut to minimal size for detection of the required bands. DNA was mobilised within the gel by incubation in 0.25 M HCl twice for 10 min followed by 45 min in denaturation buffer (1.5 M NaCl, 0.5 M NaOH) and final incubation in neutralisation buffer (1 M Tris, 1.5 M NaCl, pH 7.4) for 30 plus 10 min. The gel was rinsed briefly with water between the buffer changes.

The mobilised DNA was then transferred to a positively charged nylon membrane (Hybond™-N$^+$, GE Healthcare) by capillary force. For this, the gel was placed on two layers of blotting paper of the same width, which were soaked with 20x SSC (3 M NaCl, 0.3 M sodium citrate). The membrane in gel size was placed on top of the gel and overlaid with two blotting papers soaked in 20x SSC and two dry ones, all in gel size. A tower of paper towels was built on top of this, balanced and fixed by weight. Following o/n blotting, the construction was disassembled and the DNA cross-linked to the membrane using 0.125 J UV-light, while successful DNA transfer was confirmed by UV illumination of the gel. The membrane was then incubated in 20 mL hybridisation buffer (prepared from DIG Easy Hyb Granules, Roche, according to the manufacturer's instructions) at 60 °C for at least three hours in a hybridisation oven.

The probe was generated by a PCR on pSM3fr-Δ1-16-FRT using primers Apa2-for and Apa2-rev (Table 6.3) and the amplicon purified using the GFX PCR DNA and Gel Band Extraction Kit (GE Healthcare). 1.25 µg of probe DNA was heated to 95 °C for 10 min to separate the strands, added to the hybridisation buffer and hybridisation allowed at 60 °C o/n.

The following day, the membrane was washed twice for 5 min with washing buffer I (2% SSC, 1% SDS) at r/t and twice for 15 min with washing buffer II (0.5% SSC, 1% SDS) at 60 °C. Bound DIG labelled probe was visualized using the DIG Luminescent Detection Kit (Roche) and exposure to chemiluminescence films. For signal quantification, chemiluminescence emission was measured using a Typhoon scanner and the resulting image processed using the ImageQuant software (GE Healthcare).

### 2.4.13 DNA sequencing

The accuracy of the generated constructs was confirmed using the sequencing service of GATC Biotech (Konstanz, D). For this, 30 µL of DNA (70-100 ng/µL) together with 10 µM primer flanking the region of interest was sent for analysis on an ABI sequencer.

# 2.5 BAC mutagenesis

The MCMV genome became accessible for directed mutagenesis after stably introducing a BAC cassette encoding a selection marker (chloramphenicol) and the replication origin of the fertility factor (F-factor) [107]. Since the genome contains repetitive sequences, it is maintained in an *E. coli* strain with disrupted recABCD recombination system such as DH10B to prevent genomic rearrangements. Furthermore, control of the F-factor replicon allows only one BAC copy per cell, reducing risk of homologous recombination between different genomes [48].

Nevertheless, due to their large size and the high frequency of restriction sites, classical cloning strategies are not suitable for BACs.

### 2.5.1 Homologous recombination using linear DNA fragments

To construct recombinant MCMV BACs, linear DNA fragments were used to replace the sequences of interest, thereby introducing a selection marker (Figure 2.1). The linear fragment contains a selection marker, such as a gene encoding galactokinase or an antibiotic resistance, and at both ends approximately 50 bp homologous to the sequences flanking the region of interest.

The bacterial strain used for this, *E. coli* SW102, contains the temperature-inducible λ prophage recombineering system. Furthermore, the galactokinase gene has been deleted from the galactose operon has been modified. The galactokinase function can be added *in trans*, thereby restoring the ability to grow on galactose as carbon source [181].

generation of a linear
PCR fragment
containing homologies

homologous
recombination

mutated BAC
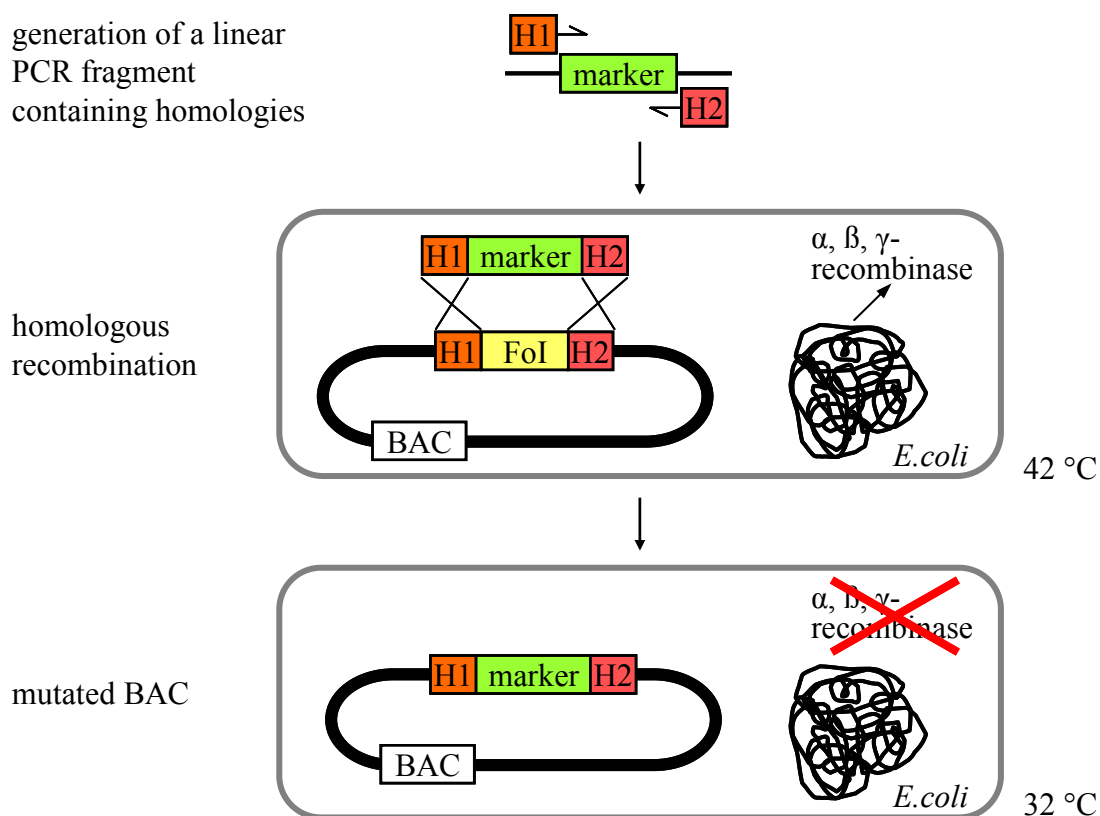


**Figure 2.1: Homologous recombination using a linear PCR fragment**

Recombinase expression is induced by a heat-shock at 42 °C in *E. coli* SW102 harbouring the target BAC followed by transformation of a linear PCR fragment that encodes a genetic marker and contains homologies (H1 and H2) to the regions flanking the feature of interest (FoI). After transformation, bacteria are grown at 32 °C to avoid further recombination and mutants are enriched in the presence of selection pressure for the marker.

The recombination fragment was PCR-amplified (section 2.4.2) using pGPS1.1-derived plasmids as template, the amplicon purified from the PCR mix (section 2.4.4), and the template DNA disintegrated by *Dpn*I digest for at least 2 hours. The remaining DNA was precipitated (section 2.4.7) and dissolved in 10 µL ddH$_2$O.

*E. coli* SW102 harbouring the BAC to be modified were grown at 32 °C to an OD$_{600}$ of 0.55-0.6. Half of the culture was transferred into a new flask and heat-shocked at 42 °C for exactly 15 min to induce recombinase expression. The remaining culture was left at 32 °C as control. After 15 min, both cultures were cooled in an ice/water bath slurry, washed twice with cold ddH$_2$O, and transformed (section 2.2.2) with 100 ng of the PCR amplicon prepared before.

## 2.5.2 Gene insertion by Flp recombinase

Insertion of viral genes into BACs to allow for *cis*-complementation was performed by Flp recombinase-mediated recombination between two FRT sites (Figure 2.2) [102]. One FRT site is located at a neutral position in the viral genome cloned as BAC, the second is found on a shuttle plasmid carrying the genetic elements to be inserted. The shuttle plasmid is derived from pOriR6K [22]. Replication of this plasmid requires the π-protein that is expressed by *E. coli* PIR1, but not by the DH10B strain [77]. Thus, the shuttle plasmid is lost in DH10B if it is not integrated into the BAC.
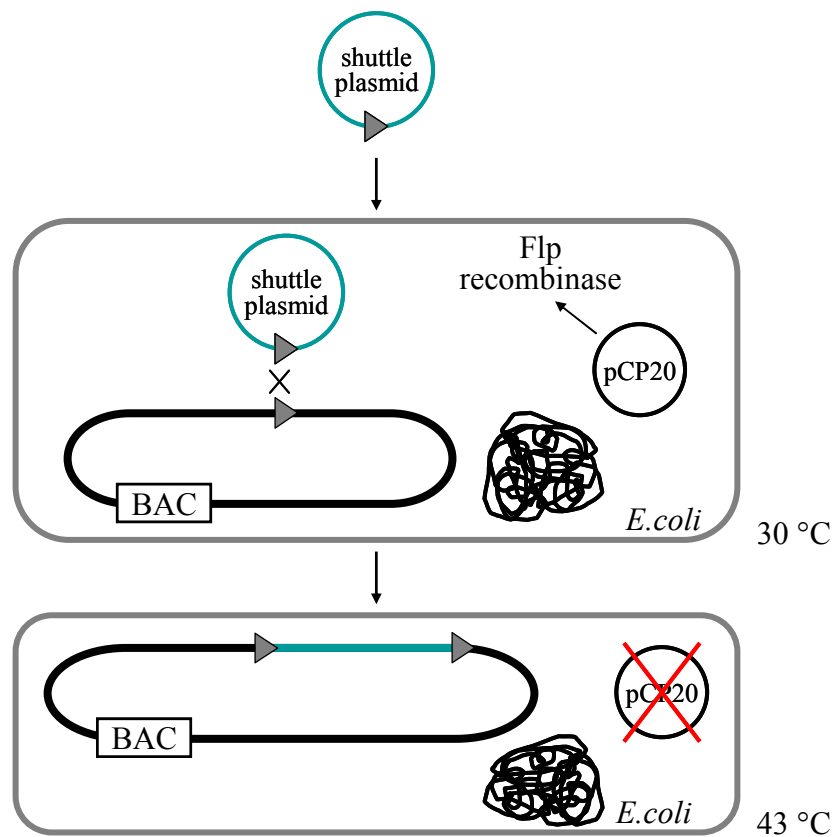


**Figure 2.2: Flp-mediated gene insertion**

*E. coli* DH10B are transformed with a shuttle plasmid containing an FRT site (grey arrowhead). A second FRT site is located in the BAC already contained in the bacteria. The shuttle plasmid is integrated into the BAC site-specifically upon expression of Flp recombinase from the pCP20 plasmid, which is lost subsequently due to its temperature sensitive origin of replication. Bacteria carrying recombinant BACs are selected using combined selection pressure.

In order to create recombinant viral DNA, electro-competent *E. coli* DH10B were transformed with an MCMV BAC and in a second step over-transformed (chemically) with the plasmid pCP20 encoding Flp recombinase. From transformants carrying BAC

and pCP20 electro-competent cells were prepared by propagation at 30 °C. Those bacteria were then transformed with 70-100 ng of the pOriR6K-derived shuttle plasmid.

Flp-mediated recombination was allowed by culturing the transformants at 30 °C for 60 min in LB medium without any antibiotics. Bacterial clones were selected for insertion of the pO6-derived constructs on agar plates containing cam (for the BAC) and zeo (for the shuttle plasmid), as bacteria with successful insertions were resistant to both antibiotics. The pCP200 plasmid was eliminated by incubating the transformants at the non-permissive temperature of 43 °C o/n. Colonies were picked for BAC mini-preparation to check for single copy insertions of the shuttle plasmid at the target site on the following day.

If all recombinant BACs carried multiple insertions, the incubation time under non-selective conditions was shortened to 30 or 15 min.

## 2.6 Cell Culture

### 2.6.1 Cultivation of mammalian cells

All eukaryotic cells were maintained in Heraeus incubators at 37 °C in 5% $CO_2$ and 95% humidity. Cells were split as listed in Table 2.10. To split adherent cells, medium was removed, cells were washed once with PBS and detached from the plates by incubation with a few drops of 0.25% trypsin/ EDTA for 1-2 min at r/t. The trypsin was inactivated by adding the respective fully supplemented medium, in which the cells were resuspended and aliquots were seeded on fresh cell culture plates.

Doxycycline (dox; Sigma-Aldrich) 10 mg/mL stock solution was prepared in PBS and stored at -80 °C. Small aliquots of 1 mg/mL were stored at -20 °C and only used once after thawing at a final concentration of 1 µg/mL. In continuous experiments, fresh dox was applied every three days due to its light sensitivity. Phosphonoacetic acid (PAA) stocks were stored at -20 °C and applied at a final concentration of 300 µg/mL.

**Table 2.10: Cell lines and growth conditions used during this study**

List of cell lines and culture medium, as prepared from commercially available media and additives. The last column indicates the ratio and intervals of splitting. ATCC, American Type Culture Collection; NEAA, non-essential amino acids.

| Cells | Source and Description | Basic medium Additives[1,2] | Split ratio Interval |
|---|---|---|---|
| 293 | ATCC CRL-1573 human embryonic kidney cells transformed with adenovirus 5 | DMEM 10% FCS, P/S, Q | 1:6 2-3 days |
| 293T | ATCC CRL-11268 human kidney carcinoma cells | DMEM 10% FCS, P/S, Q | 1:6 2-3 days |
| M2-10B4 | ATCC CRL-1972 bone marrow stroma cells from (C57BL/6J X C3H/HeJ) F1 mouse | RPMI 10% FCS, P/S | 1:6 2-3 days |
| MEF | embryonic fibroblasts of Balb/c mice; preparation as described in [157] | DMEM 10% FCS, P/S | 1:2 3-4 days |
| NIH/3T3 | ATCC CRL-1658 murine embryonic fibroblast cell line from NIH Swiss mouse | DMEM 5% FCS, P/S | 1:6 3-4 days |
| Flpe-NIH | murine fibroblasts (ATCC CRL-1658) stably transformed with pCAGGS-FLPe (Gene Bridges) to express Flp recombinase, generated by Jens B. Bosse | DMEM 5% FCS, P/S 3 µg/mL puromycin | 1:3 2-3 days |
| U-2 OS | ATCC HTB-96 human osteosarcoma cell line | DMEM 10% FCS, P/S, Q, NEAA | 1:10 3-4 days |

[1] P/S, 0.6% (w/v) penicillin, 1.3% (w/v) streptomycin; Q, 0.3 mg/mL glutamine

[2] FCS had been inactivated by incubation at 56 °C for 45 min prior initial use

## 2.6.2 Freezing and thawing of cells

To keep a stock of cells with low passage numbers, cells were frozen as permanent cultures in liquid nitrogen. Cells were grown to 80% confluence and harvested using trypsin. The cell pellet (1,200 rpm, 5 min, Heraeus Multifuge 3 S-R) was resuspended in the usual culture medium supplemented with 10% DMSO and 25% serum (1 mL as equivalent for one 10 cm dish). Aliquots of 1 mL were transferred to cryo-tubes (Nunc)

and kept in cryo-boxes at -80 °C for 24 hours, before being placed in liquid nitrogen. Isopropanol-insulated cryo-boxes allowed gentle freezing of the cells (1 °C per minute).

Frozen cell aliquots were removed from liquid nitrogen and thawed in a 37 °C water bath. To remove the DMSO, each aliquot was washed with 20 mL adequate medium, centrifuged (1,200 rpm, 5 min, Heraeus Multifuge 3 S-R) and seeded on one or two 10 cm cell culture dishes.

### 2.6.3 Transfection of eukaryotic cells using FuGene and PEI

To investigate proteins by immunofluorescence microscopy (section 2.8.6), U-2 OS cells were transfected with the respective expression vectors using FuGene Transfection Reagent. For this, 8 well 1 µ-Slides (ibidi GmbH) were coated with 10 µg/mL fibronectin from bovine plasma for one hour at 37 °C and washed three times with PBS, before $2 \times 10^4$ cells were seeded per well and allowed to attach for 6 hours. DNA was suspended in 50 µL Opti-MEM, FuGene was added to yield a DNA-to-reagent ratio of 1:1, the mixture was incubated at r/t for 30 min and added drop wise onto the cells.

To analyse proteins by immunoprecipitation (section 2.8.2), protein complementation assay (section 2.8.5) or Western blot (section 2.8.4), aliquots of $7.5 \times 10^5$ 293 or 293T cells were seeded in 6-well plates and allowed to attach for 5-6 hours. Required DNA (usually 3-4 µg) was suspended in 100 µL Opti-MEM, 15 µL polyethylenimine (PEI) were added, vigorously mixed, incubated at r/t for 40 min and added drop-wise into the culture media.

### 2.6.4 Nucleofection of eukaryotic cells

To perform nucleofection reactions, 0.5 µg BAC DNA was mixed with 0.5 µg plasmid DNA (preferably in a maximum volume of 4 µL) in a 96-well plate with conical bottom. Low-passage Flpe-expressing NIH/3T3 were harvested, pelleted at $90 \times g$ for 10 min (Heraeus Multifuge) and suspended in aliquots of $5 \times 10^5$ cells in 20 µL solution SG onto the DNA mixtures. Samples were mixed and transferred air bubble-free into the Lonza electroporation stripes and nucleofected by means of the Amaxa® 96-well Nucleofection System using the programme EN-158. After 10 min recovery at r/t in the electroporation cuvettes, cells were mixed with 80 µL supplemented medium and aliquots of $1 \times 10^5$ Flpe-expressing cells were seeded into

12-well plates, which already contained $3 \times 10^5$ non-modified NIH/3T3. Plates were incubated at 37 °C for 5-7 days, before cells were fixed and processed for microscopic analysis.

## 2.7 Virological methods

### 2.7.1 Virus reconstitution from BAC DNA

To reconstitute virus from viral BACs, BAC DNA was transfected into MEF using SuperFect® Transfection Reagent.

MEF were thawed and seeded on 10 cm cell culture dishes. Once they reached confluence, they were split 1:3 on 6 cm dishes. For transfection, 1.5 μg of the appropriate BAC DNA was suspended in non-supplemented DMEM in a total volume of 150 μL and 10 μL of ice cold SuperFect® was added. After 10-15 min incubation at room temperature, 1 mL of fully supplemented DMEM was added to the transfection mixture and placed on the cells, which had been washed with PBS during the incubation time. Following 2.5-3 hours of incubation at 37 °C/5% $CO_2$, the transfection mix was replaced by fully supplemented medium as listed in Table 2.10.

One day post-infection, cells as well as supernatants were transferred from 6 cm to 10 cm cell culture dishes and further passaged in 1:2 splits every 7 days from then on. Development of viral plaques was monitored by light microscopy (Axiovert 25, Carl Zeiss AG) as well as fluorescence microscopy (Olympus IX17, Olympus Corp., Tokyo, Japan). After complete lysis, cells were harvested together with the supernatants and stored at -80 °C.

A reconstitution experiment was considered valid if the transfection with wt MCMV BAC produced plaques after one week (positive control), pSM3fr-ΔM53-EM53K128A BAC resulted in plaque formation between two and four weeks post-transfection (attenuated virus control), and no plaques were detected upon transfection with the ΔM53 BAC for six weeks (negative control). Likewise, a viral element was assumed to be essential if no viral progeny was detected for six weeks after transfection.

## 2.7.2 Preparation of MCMV stocks

To prepare concentrated virus inocula for infection experiments, 6 confluent 14.5 cm cell culture dishes of M2-10B4 cells were harvested, mixed with 10 mL inoculum of either a reconstitution (section 2.7.1) or a previous virus stock and re-seeded onto 20 dishes. Upon complete lysis, cells were harvested together with the supernatants and viruses purified as described below. Optional, the suspension could be stored at -80 °C until virus preparation.

Unless indicated otherwise, all subsequent steps were performed on ice or in centrifuges cooled to 4 °C. Virus suspension was centrifuged at $6,000 \times g$ for 20 min (Beckman Coulter™ Avanti™, JLA 16.250). The supernatant was collected and stored on ice until use. The pellet was resuspended in 5 mL non-supplemented DMEM and cells disrupted by three cycles of freezing (20-30 min at -80 °C) and thawing (10 min at 37 °C). Cellular debris was removed by centrifugation at 3,500 rpm for 5 min (Heraeus Multifuge 3 S-R). The supernatants were combined and virus particles were harvested by centrifugation at $30,000 \times g$ for 3.5 hours (Beckman Coulter™ Avanti™, JLA 16.250). The pellet was resuspended in 1.5 mL PBS and virus particles separated by douncing 20 times. The remaining cell debris was precipitated by triple sequential centrifugation at 3,500 rpm and 4 °C for 5 min (eppendorf 5417 R). Aliquots of 50 µL were stored at -80 °C and virus titre was determined by plaque assay (section 2.7.3).

## 2.7.3 Quantification of virus infectivity by plaque assay

To determine the titre of the virus stocks, a standard plaque assay was performed [133].

For this, MEF were seeded on 48-well plates and grown to confluence. Cells were infected with 200 µL of serial dilutions of the virus prepared in cold, non-supplemented DMEM. After one hour incubation at 37 °C to allow for virus adsorption, infectious medium was removed and medium containing methylcellulose (MEM supplemented with 7.5 g/L carboxy-methylcellulose, 5% FCS, 0.3 mg/mL glutamine, 5% of 100x non-essential amino acids, 0.6% (w/v) penicillin, 1.3% (w/v) streptomycin, 7.5% $NaHCO_3$) added. Using methylcellulose, secondary plaque formation is prevented, as infectious particles are unable to diffuse into medium of such high viscosity. After 4 days, plaque

formation was monitored using phase contrast microscopy and virus titre determined according to the following equation

$$virus\ titre\ [pfu\,/\,mL] = \frac{plaques\quad counted\quad \times\quad dilution}{volume\quad of\quad infectious\quad dilution}$$

Virus titration was performed in triplicate samples for virus stocks and in duplicates for growth curves.

### 2.7.4 Infection of cultured cells with MCMV

For standard infection, cells were trypsinised, cell numbers determined using trypan blue and cells either infected directly or seeded onto multi-well plates and allowed to attach for 5-6 hours. For direct infection, the total number of cells required for one experiment was incubated with the appropriate virus dilutions for 30 min at 37 °C, washed twice with pre-warmed media (1,200 rpm/300 × $g$, 5 min, Heraeus Multifuge 3 S-R) and aliquots seeded in absence and presence of 1 µg/mL dox. To infect adherent cells, virus preparations were added and incubated at 37 °C for one hour.

Where a higher multiplicity of infection (MOI) was required, viruses were added to attached cells and subjected to centrifugation (2,000 rpm/860 × $g$, 30 min, r/t, Heraeus Multifuge 3 S-R) followed by one hour incubation at 37 °C before the inoculum was replaced by fresh medium. Centrifugation enhances infection efficiency approximately 10-fold [59].

### 2.7.5 Preparation of growth curves

The growth kinetics of the generated mutant viruses were compared to each other and to control viruses under multi-step growth conditions. For this, cells were harvested, cell numbers determined using trypan blue and the appropriate number of cells (equalling one aliquot of $1.5 \times 10^5$ per day and condition) was mixed in a Falcon with the required viruses at an MOI of 0.1 and incubated for 30 min at 37 °C. Subsequently, cells were washed twice with pre-warmed medium (300 × $g$, 5 min, Heraeus Multifuge 3 S-R) and seeded in aliquots of $1.5 \times 10^5$ cells per well. If it was required, half of the samples were supplemented with 1 µg/mL dox.

Supernatants were harvested daily over a period of five days and the viral load of the culture supernatants was determined by plaque assay (section 2.7.3). The experiments to assess viral growth kinetics were performed in technical duplicates in two independent experiments.

### 2.7.6 Transmission electron microscopy (TEM)

NIH/3T3 cells were grown on carbon-coated sapphire discs and infected at an MOI of 5 using centrifugal enhancement at $1,000 \times g$ for 30 min. Residual virus was removed one hour post infection and dox applied. Cells were fixed 48 hours post-infection by high-pressure freezing with an *HPF 01* instrument (M. Wohlwend GmbH), freeze-substituted, and plastic embedded as described previously [25]. Embedded samples were sectioned and viewed on a JEOL JEM-1400 transmission electron microscope equipped with an Olympus Veleta CCD camera at an acceleration voltage of 80 kV.

## 2.8 Protein analysis

### 2.8.1 Protein extraction from eukaryotic cells

For protein analysis, cells were scraped from the plates at appropriate time points, washed and resuspended in 1 mL PBS. All subsequent steps were performed on ice.

Transfected cells were harvested 48-72 hpt as described above. Of the cell suspension, 10% were pelleted at maximum speed for 10 min (eppendorf 5417 R) and resuspended in 50 µL total lysis buffer (TLB; 62.5 mM Tris (pH 6.8), 2% SDS, 10% glycerine, 6 M urea, 0.01% bromphenol blue, 0.01% phenol red) freshly supplemented with 5% β-mercaptoethanol (ß-EtSH). Nucleic acids were disintegrated by sonication at 30% amplitude for 5 s. The remaining 90% were pelleted and stored at -80 °C until use. As an exception, the protein samples of FlagM53s168 were stored at 4 °C, since it was instable at -80 °C.

Infected cells from a 6 well plate were lysed in 100 µL TLB and treated as described above.

## 2.8.2 Immunoprecipitation

Immunoprecipitation experiments were performed using proteins from isolated expression upon transfection. All steps were carried out on ice or at 4 °C.

Cells were lysed in 1 mL high salt lysis buffer (HSLB; 400 mM NaCl, 20 mM Tris (pH 8.0), 1% Triton® X-100) supplemented with a protease inhibitor cocktail (PIC) for 90 min at 4 °C on a roller shaker. Cell debris was precipitated by centrifugation at maximum speed for 30 min (eppendorf 5417 R) and supernatant added to anti-Flag matrix (EZview™ Red ANTI-FLAG M2 Affinity Gel; Sigma-Aldrich) that had been washed three times with HSLB/PIC. Samples were incubated on a roller shaker at 4 °C o/n to allow optimal binding. Unbound protein was removed by sequential washing steps (14,000 rpm, 1 min, eppendorf 5417 R, soft acceleration): four times with washing buffer I (400 mM NaCl, 20 mM Tris, pH 8.0), once with washing buffer II (150 mM NaCl, 20 mM Tris, pH 8.0) and once with washing buffer III (20 mM Tris, pH 8.0) all supplemented with PIC. Bound proteins were eluted from the beads with 50 µL TLB/ß-EtSH and incubation at 95 °C for 10 min. Samples were stored at -80 °C until analysis.

## 2.8.3 SDS-polyacrylamide gel electrophoresis

Proteins to be analysed were separated by size using polyacrylamide gel electrophoresis under denaturing conditions. Protein samples were obtained from isolated expression in 293T cells (Section 2.6.3) or from expression in the virus context in M2-10B4 cells (section 2.7.4).

**Table 2.11: Composition of gels for SDS-PAGE**

| Component | Separating gel (10%) | Stacking gel (4.5%) |
|---|---|---|
| acrylamide (Rotiphorese® 30) | 3.3 mL | 500 µL |
| gel buffer (4x)[1] | 2.6 mL | 410 µL |
| $H_2O$ | 4 mL | 2.1 mL |
| TEMED | 4 µL | 3 µL |
| APS (10%) | 100 µL | 30 µL |

[1]The 4x separating gel buffer consisted of 1.5 M Tris (pH 8.8) and 0.4% SDS. The 4x stacking gel buffer was composed of 0.5 M Tris (pH 6.8) and 0.4% SDS.

Polyacrylamide gels were poured in a Mini-PROTEAN® 3 gel system (Bio-Rad) according to the recipes below. Prior to loading, samples were heated at 95 °C for 10 min. Proteins were separated by electrophoresis in 1x Laemmli buffer (2.5 mM Tris, 1% SDS, 25 mM glycine) at 160 V until sufficient separation was achieved. Following separation, proteins of interest were detected by Western blot analysis (section 2.8.4).

### 2.8.4 Western blot analysis

Following separation by SDS-PAGE, proteins were transferred from the SDS-gel to a Hybond®-P membrane (18 V, 45 min) in the presence of blotting buffer (25 mM Tris, 192 mM glycine, 20% methanol) using a Trans-Blot® SD Semi-Dry Electrophoretic Transfer Cell (Bio-Rad). Prior to the transfer, membranes were activated by soaking in methanol and washing with water.

Membranes were blocked in TBS-T (150 mM NaCl, 10 mM Tris-HCl (pH 8.0), 0.05% Tween 20) containing 5% non-fat dry milk for one hour at r/t to saturate unspecific protein binding sites. To detect proteins of interest, membranes were incubated with specific primary antibodies (1/1,000 - 1/2,000 dilution) in TBS-T at 4 °C o/n. Unbound antibodies were removed by three washings with TBS-T. To detect the specific deposition of the primary antibodies the membranes were reacted with horseradish peroxidase-conjugated secondary antibodies (1/8,000 in TBS-T; Dianova). After three washings with TBS-T, proteins were visualised using an ECL Plus™ Western Blotting Detection System and Hyperfilm™ ECL™ detection films (GE Healthcare).

### 2.8.5 Protein Complementation assay (PCA)

To study protein interaction by PCA, $7.5 \times 10^5$ 293T cells were co-transfected with plasmids expressing M50 and M53 versions fused to either the N-terminal or the C-terminal part of the ß-lactamase (BlaN and BlaC, respectively) [152].

Co-transfected 293T were harvested 48 hpt by scraping from the plate, washed once with PBS and lysed in 75 µL luciferase reporter lysis buffer (Promega) for 60 minutes on ice. Following lysate clearing at $21,000 \times g$ at 4 °C for 10 minutes, 50 µL of each sample was added to 135 µL phosphate buffer (pH 7) and 15 µL nitrocefin and Bla

activity was determined on an ELISA plate reader for 30 min at 37 °C by measuring the colour conversion rate of nitrocefin leading to increasing absorption at 495 nm.

### 2.8.6 Confocal laser scanning microscopy

Cells were fixed with 4% paraformaldehyde (PFA) at 36 hpi or hpt for 15 min at 37 °C, washed three times with PBS, permeabilized by treatment with 0.1% Triton X-100 in PBS for 15 min at r/t, washed three times, blocked for 60 min with 5% donkey serum in PBS and stained with specific primary antibodies or antisera (1/100 - 1/200 dilution) at 4 °C o/n and washed again three times. Primary antibodies were in turn reacted with the appropriate Alexa Fluor-coupled secondary antibodies (Molecular Probes; 1/150 dilution) for 60 min at r/t in the dark. To prevent unspecific binding, antibodies were diluted in PBS containing 5% donkey serum and 0.02% Triton X-100. DNA was visualized by staining with TO-PRO-3 iodide (Molecular Probes). Finally, cells were washed three times with PBS and fluorescence images were taken on a Zeiss LSM510 microscope with 488, 543, and 633 nm laser illumination and filter sets appropriate for Alexa Fluor 488, 555, and TO-PRO-3.

Pictures were processed using the ImageJ software (National Institutes of Health; http://rsbweb.nih.gov/ij/).

## 2.9 Bioinformatics

Cloning strategies were planned using the Vector NTI software from Invitrogen. DNA sequencing data were analysed using different programmes of the Vector NTI package. Protein alignments were performed by means of the Vector NTI Align X programme via the BLOSUM 62 similarity matrix.

Statistical analyses were performed using the GraphPad Prism software (GraphPad Software Inc., La Jolla, USA).

# 3 RESULTS

## 3.1 Construction of M53 mutants based on predictions

Random linker-scanning mutagenesis of the MCMV protein pM53 identified numerous insertion and few deletion mutations that were inhibitory for virus replication [130]. The inhibitory pM53 proteins with mutations within their conserved region (CR) 4 could inhibit MCMV replication up to the million-fold. Further analysis of these mutants in the virus context showed that their overexpression phenotype showed impaired nuclear egress and genome cleavage/packaging defects. However, the inhibitory potential of the individual insertion mutations in CR2 was weaker, inhibiting viral growth only by about 100-fold. This degree of inhibition did not allow further studies. Thus, although the random screen indicated a functional site in CR2, it did not produce a DN allele with sufficient inhibitory potential for phenotypic analysis.

The DN effect of a mutant protein can be improved by local insertion, replacement, or deletion of functionally important amino acids or motifs. This notion is supported by previous observations for the viral protein pM50, in which the deletion of a putative domain resulted in a stronger inhibitory phenotype than that observed for subtle insertion mutants [141]. Furthermore, chimeric pM53 proteins comprising the pM50 binding domain fused to the C-terminal domains of other pUL31 family members were not able to complement wt pM53 function [152], indicating that at least one essential motif located within the C-terminal sequences is not conserved among the homologues. Based on those observations, a set of pM53 mutants was generated, in which the conserved regions were either replaced by the respective sequences from a homologous protein, or partly/completely deleted. Both strategies aimed at identifying mutant proteins with strong inhibitory potential. The mutants were studied in a *tet*-based conditional expression system, which allows quantitative assessment of their inhibitory potential [142].

### 3.1.1 Construction of M53 mutants

Alignment of the amino acid sequences of the pUL31 family members indicates four regions with high similarity (Figure 3.1A). Previous studies identified the pM50 binding site in pM53 in CR1 and a nuclear localisation signal (NLS) within the variable N-terminus [95]. Additionally, preliminary data showed that chimeric proteins, which carry CR2 to CR4 domains of alpha- or gamma-herpesvirus homologues, bind pM50 but cannot complement the M53 null mutation [152]. Consequently, to generate pM53 mutants, which might interfere with viral replication, the N-terminal part spanning the NLS and the pM50 binding domain was kept in all cases.
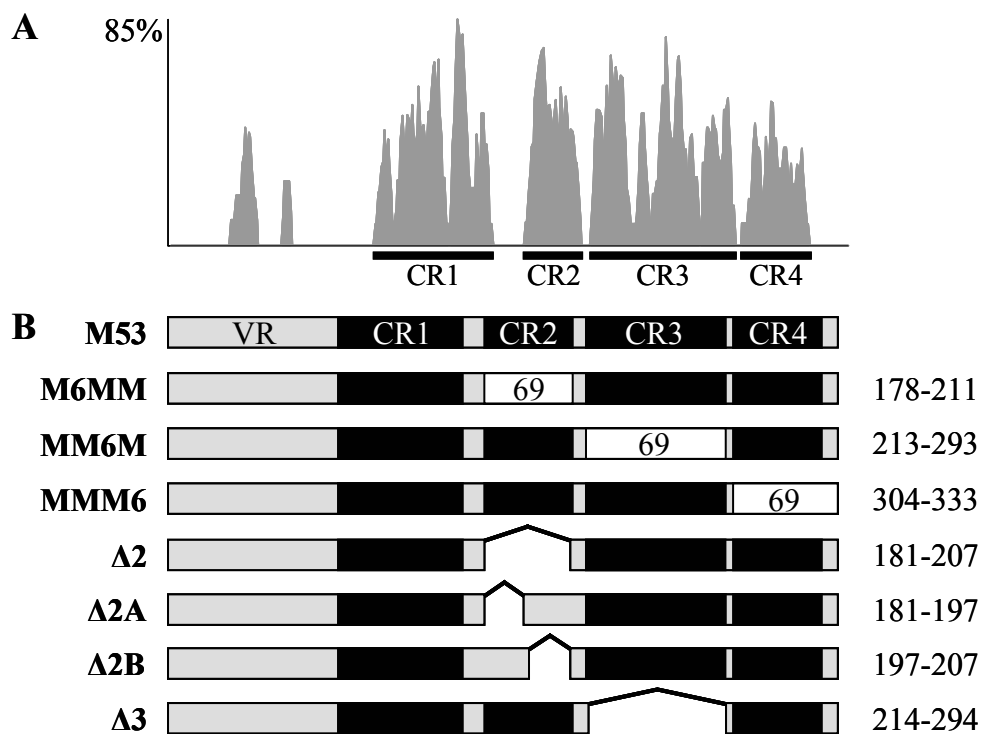


**Figure 3.1: M53 mutants constructed by domain shuffling and domain deletion**

**(A)** The amino acid (aa) sequences of 36 pUL31 homologues were aligned using the Vector NTI AlignX program (Invitrogen) via the BLOSUM 62 similarity matrix. The similarity plot was calculated using a 5 aa window size, with scores for weak and strong similarity and identity of 0.2, 0.5, and 1.0, respectively. The *x* axis represents the number of amino acids in the consensus sequence. Conserved regions (CR) are indicated below the diagram [95]. **(B)** Schematic overview of the pM53 mutants. Proteins are depicted as grey bars, conserved regions are indicated as black boxes. White boxes labelled "69" represent sequences exchanged with the respective stretches of the MHV68 homologue pORF69 (aa 128-161 for M6MM, aa 165-245 for MM6M, aa 253-292 for MMM6). Deletion mutants are shown with bridged spacing. The numbers on the right indicate the amino acids of pM53 affected by the mutation. VR, variable region; CR, conserved region.

Two mutational strategies were exploited in order to generate inhibitory M53 alleles based on the alignment data (Figure 3.1). The first approach consisted of domain shuffling of single CRs by sequence replacement. Thus, three out of the four pM53 CRs were individually replaced with the corresponding coding sequences from pORF69, the M53 homologue of the murine gamma-herpesvirus MHV68, as follows: the coding sequence for amino acids (aa) 128 to 161 of pORF69 replaced the coding sequence of aa 178 to 211 of M53 to yield the protein pM6MM; aa 165 to 245 of pORF69 replaced aa 213 to 294 of pM53 to yield pMM6M; and aa 253 to 292 of pORF69 replaced aa 304 to 333 of pM53 to yield pMMM6.

The second strategy comprised deletion of potential domains. For this, mutants lacking either the complete CR2 coding sequence (aa 181 to 207 ($\Delta$2)), parts of CR2 (aa 181 to 197 ($\Delta$2A) and aa 197 to 207 ($\Delta$2B)), or the complete CR3 (aa 214 to 294 ($\Delta$3)) were generated (Figure 3.1B). A CR4 deletion mutant was not included, as the pM53s309 mutation, truncating the protein close to the beginning of CR4, was already studied extensively [130].

To investigate the effect which the newly generated M53 alleles exhibit on viral replication, they have to be expressed in the viral context. Thus, the mutant expression cassette either has to be delivered *in trans*, or recombinant viruses have to be constructed which selectively express the mutants. Using the latter, the transcription unit encoding the mutant gene needs to be silent during virus reconstitution and switched on when analysis of the phenotype is called for. This permits parallel analysis of the phenotypes resulting from the absence and presence of the mutant protein from the same construct.

To this end, the mutated M53 alleles were placed in a conditional expression cassette in a pOriR6K-derived shuttle vector. This vector contains an FRT site, which allows recombination by the Flp/FRT system. Furthermore, expression of the mutant allele is selectively induced by addition of dox, which neutralises the transcription blockade mediated by the tet repressor (TetR) (Figure 3.2). The TetR is constitutively expressed under control of the CMV promoter and binds to the *tet*-operator sequences (*tetO₂*) in the SV40 promoter region of the mutant gene, which prevents transcription of the mutant gene (OFF). Its expression is turned on by dox addition, which binds to the TetR, thereby blocking it from *tetO₂* binding (ON) [142].
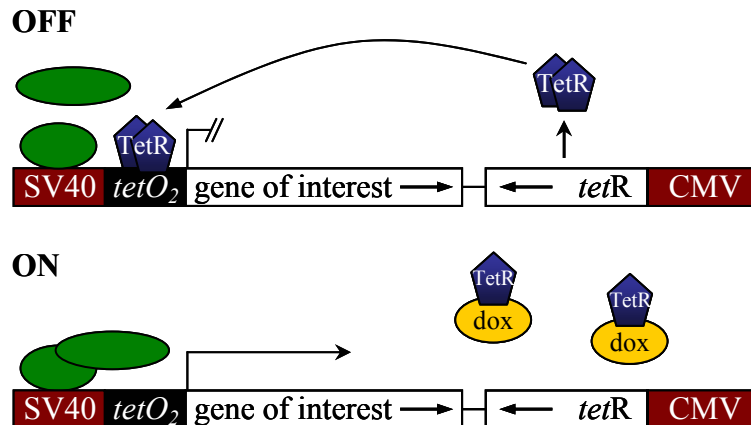
**Figure 3.2: Expression cassette for conditional gene expression in MCMV**

Schematic representation of the dox-inducible expression cassette. The constitutively expressed tet repressor (TetR) binds to the *tet*-operator sequences (*tetO₂*) in the promoter region of the gene of interest, thereby preventing transcription. However, the TetR is bound by dox, allowing assembly of the transcription complex and expression of the gene of interest. Adapted from [142].

### 3.1.2 Analysis of M53 mutants in the viral context

To investigate the inhibitory potential of the chimeric proteins, the expression plasmids were inserted individually into the wt MCMV BAC as an additional M53 allele. To compensate genome overlength, the MCMV genome used as background lacked the genes *m01* to *m16*, which are dispensable for virus replication in cell culture. The growth properties of the virus derived from this BAC are identical to those of a wt virus [97].

Insertion of the expression vectors into the viral BAC was performed using the Flp/FRT recombination system as described in Figure 2.2 (section 2.5.2). The Flp recombinase was expressed from the temperature-sensitive plasmid pCP20 [30]. It recognises and specifically recombines the two FRT sites located on the BAC and the shuttle plasmid harbouring the mutant gene, thereby inserting the plasmid into the MCMV genome. Recombinant BACs were isolated and analysed by restriction enzyme digest to confirm single insertion of the shuttle plasmid, as exemplified in Figure 3.3. Recombinant viruses were then reconstituted from the respective BACs by transfection of MEF in the absence of dox. Virus production was monitored and the inocula were harvested after completion of the cytopathic effect.
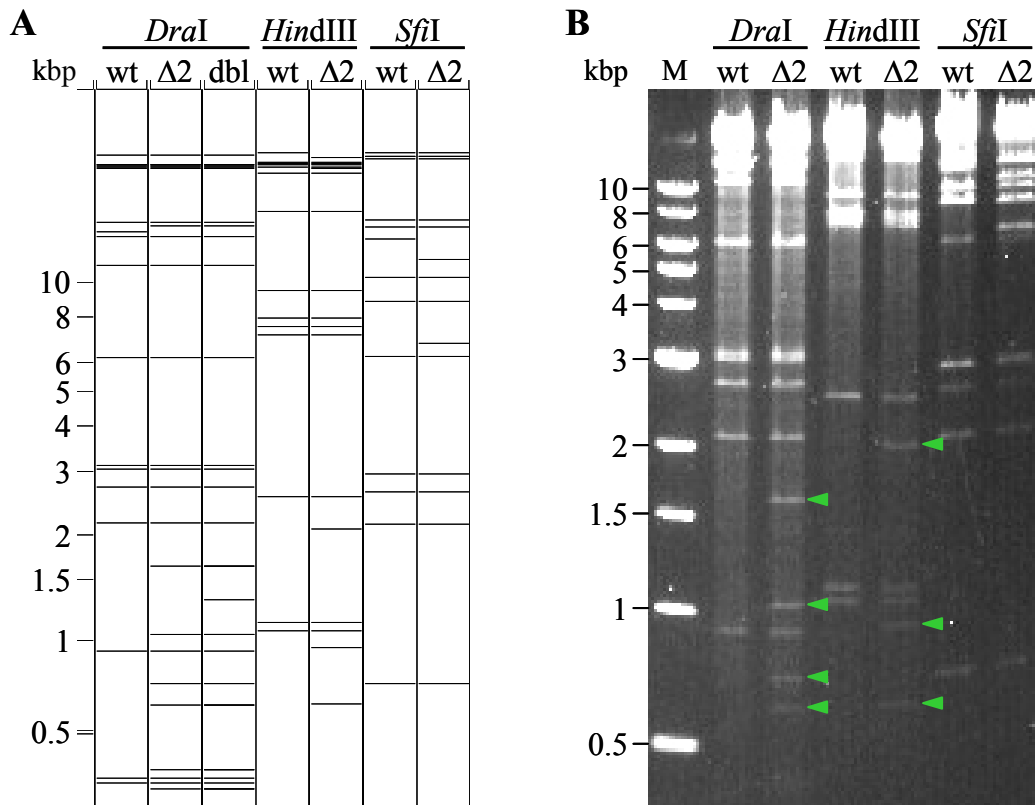
**Figure 3.3: Analysis of the BAC DNA based on restriction patterns**

An example is shown for specific changes in the restriction pattern after flip-in. BAC DNA of wt MCMV (wt) and SVT-Δ2 (Δ2) was digested with *Dra*I, *Hind*III and *Sfi*I (right panel) and the restriction patterns compared to a theoretical digest (left panel). For example, cleavage of wt MCMV with *Dra*I resulted, amongst others, in fragments of 0.9, 2.2, 2.7, 3.0, 3.1 and 6.2 kbp. In contrast, *Dra*I-digested SVT-Δ2 DNA showed, as a result of the flip-in reaction, additional fragments at 0.6, 0.7, 1.0 and 1.6 kbp (indicated with green arrowheads). A double or multiple insertion of the shuttle plasmid could be discriminated by a further fragment at 1.3 kbp, as illustrated in the left panel (dbl). The *Hind*III digest produced additional bands at 0.6, 0.95 and 2.1 kbp for SVT-Δ2 in comparison to wt MCMV, whereas cleavage with *Sfi*I showed an extra fragment at 6.8 kbp.

Subsequently, the inhibitory potential of the mutated pM53 proteins on viral replication was investigated comparing the phenotypes induced in the absence and presence of dox (Figure 3.4). Addition of dox selectively allowed transcription of the mutant allele as illustrated in Figure 3.2.

**A**

Generation of
recombinant BACs

Reconstitution on
murine fibroblasts

**B**

Analysis of the
inhibitory potential
in the viral context

− dox          + dox

no progeny
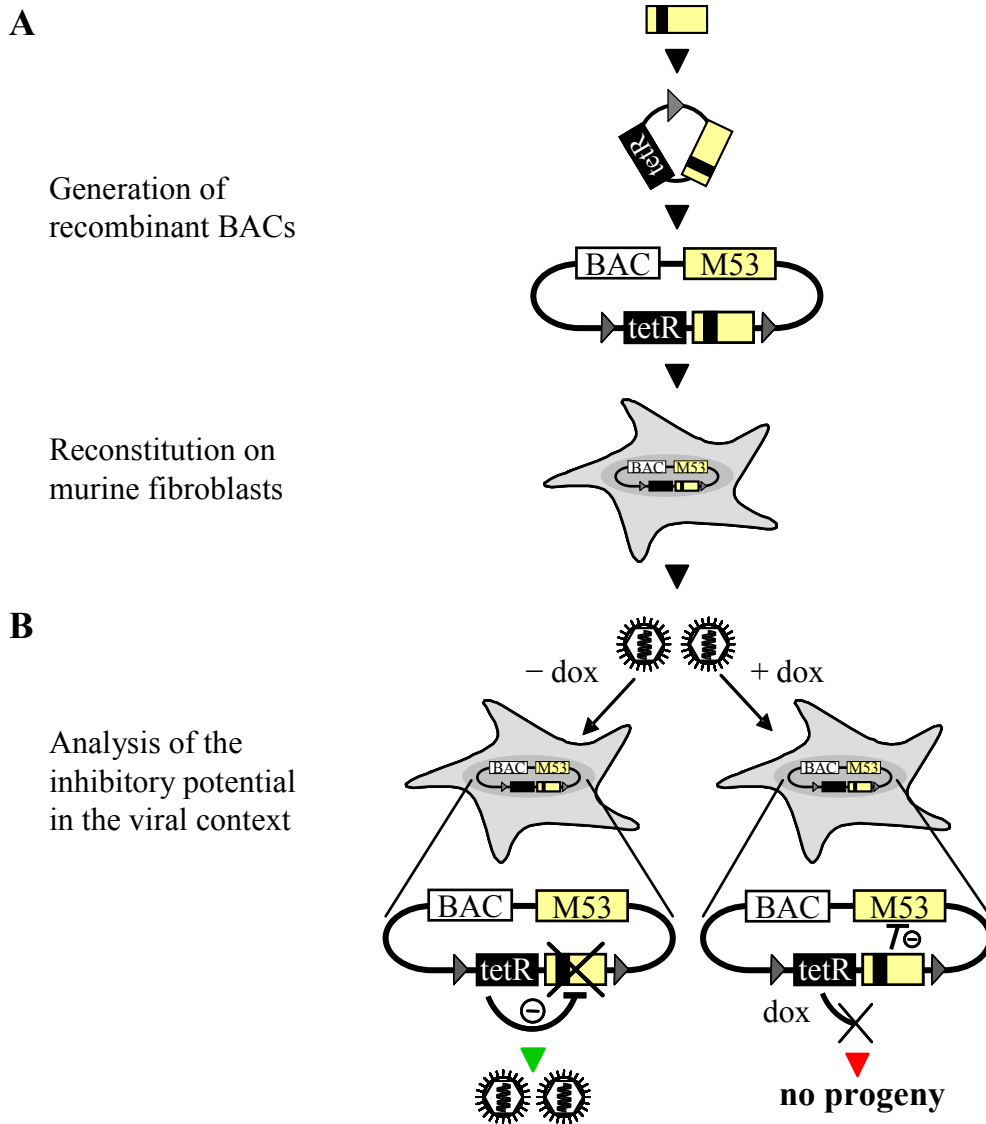
**Figure 3.4: Analysis of the inhibitory effect of the mutant alleles in the viral context**

**(A)** Construction of recombinant viral BACs. The gene of interest (yellow box) is mutated and cloned into an FRT site-containing dox-inducible expression vector, which is subsequently inserted into the wt MCMV BAC by Flp-mediated site-specific recombination via FRT sites (grey arrowheads) in *E. coli*. Recombinant viruses are reconstituted by transfection of murine fibroblasts with BAC DNA in the absence of dox. **(B)** Mutant analysis in the viral context. Cells are infected with MCMV mutant viruses. In the absence of doxycycline (dox; left panel) the constitutively expressed *tet* repressor (tetR, black box) blocks transcription of the mutant gene (grey box with black line), leading to virus replication similar to that observed for wt. The inhibitory potential of the mutant proteins can be analysed upon dox application (right panel), which allows mutant expression by tethering TetR. Adapted from [141].

## 3.1.3 Lack of the correct CR2, but not CR3 sequences results in pM53 mutants with strong inhibitory effects

To investigate the inhibitory potential of the mutant alleles on virus replication, M2-10B4 cells were infected with the mutant viruses in the absence and presence of dox and the release of infectious viruses was analysed under multi-step growth conditions (Figure 3.5). The viruses were named as the corresponding BAC constructs tagged with an "MCMV" prefix.
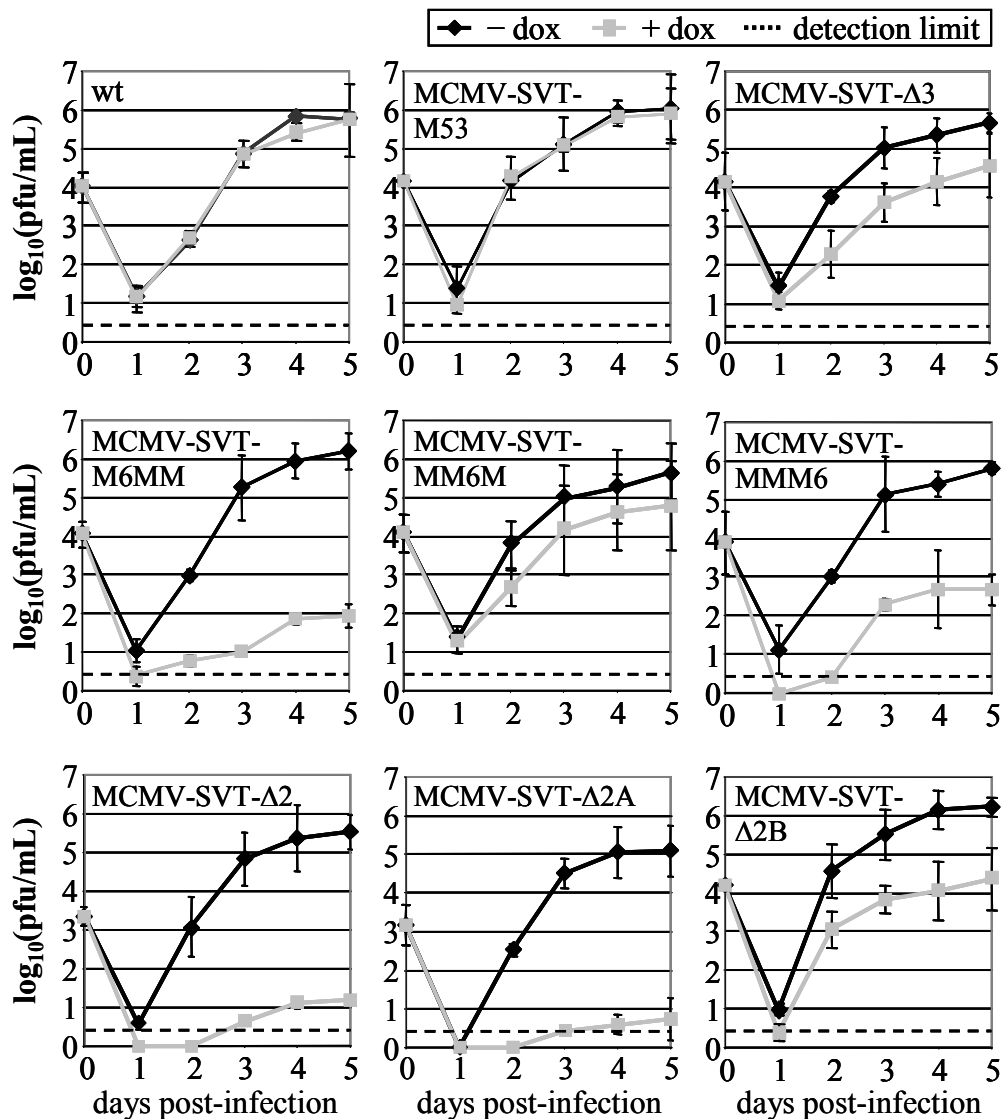


**Figure 3.5: Inhibition of MCMV replication by M53 mutants**

M2-10B4 cells were infected with the indicated viruses at an MOI of 0.1 in the absence (black diamonds) or presence (grey squares) of 1 µg/mL doxycycline (dox) and the viral load in the supernatant was quantified by plaque assay. Error bars represent the standard deviation of duplicate experiments using two separate clones. Dashed line, detection limit.

As expected, in the absence of dox, all mutant viruses produced titres comparable to wt MCMV of at least $10^5$ pfu/mL at 5 days post-infection (dpi). Neither addition of dox to wt MCMV, nor insertion and expression of a second wt gene copy (MCMV-SVT-M53), had any effect on viral titres (Figure 3.5, upper row). However, induction of the mutant alleles led to different results. Expression of pM6MM (MCMV-SVT-M6MM) reduced viral production by about 10,000-fold, which was a clear improvement of the inhibitory potential over the 100-fold effect reported for the i207 mutant derived from a transposon insertion library [130]. In addition, the presence of pMMM6 decreased virus production by about three orders of magnitude (MCMV-SVT-MMM6), whereas expression of pMM6M had only a moderate effect (MCMV-SVT-MM6M) (Figure 3.5, middle row). The latter two findings are in line with the observations reported for the random library, which showed that inhibitory mutations are preferentially located within CR4, and that insertions in CR3 do not inhibit wt protein function [130].

The next step was to study whether the strong inhibitory phenotype of the CR2 replacement could also be achieved by domain deletion. For this, the mutants lacking either the complete CR2 or parts of CR2 (Figure 3.1B) were tested as described above. Again, virus titres in the absence of dox reached ~$10^5$ pfu/mL (Figure 3.5, bottom row), whereas expression of pM53Δ2 severely reduced virus release by approximately four to five orders of magnitude (MCMV-SVT-Δ2). The presence of pM53Δ2A (MCMV-SVT-Δ2A) decreased virus replication to a comparable level as MCMV-SVT-Δ2, while the inhibitory effect of pM53Δ2B was less pronounced, reducing viral titres by about two orders of magnitude (MCMV-SVT-Δ2B).

At last the pM53 mutant lacking CR3 was tested. This served in parallel as control whether the inhibitory phenotype of the CR2 deletion mutants could be specifically attributed to that domain. Induction of the M53Δ3 allele by dox inhibited virus replication minimally (MCMV-SVT-Δ3) (Figure 3.5, upper row). Altogether, from these and previous data it was concluded that deletion or alteration of CR2 and CR4, but not of CR3, results in mutant proteins with a strong inhibitory effect on virus replication.

## 3.1.4 Analysis of the intracellular distribution and expression of the CR2 mutants of pM53

The inhibitory effect of a mutant allele is dominant negative if the mechanism of its interference is specifically connected to the function of the wt allele. Changes in the coding sequence may result in proteins with aberrant folding properties, which are then trapped in compartments designated for degradation. To study whether the pM53 mutants reached the correct cellular compartment where the wt protein is localised, U-2 OS cells were transiently transfected with plasmids expressing the M53 mutants and examined for protein signals 36 hours post-transfection (hpt). Confocal microscopy of the transfected cells revealed that all pM53 mutants correctly localised to the nucleus (Figure 3.6), indicating that all mutant proteins had the potential to obstruct viral maturation in the nucleus. Thus, the functional differences between the pM53 CR2 and CR3 deletion mutants were not due to aberrant protein localisation.
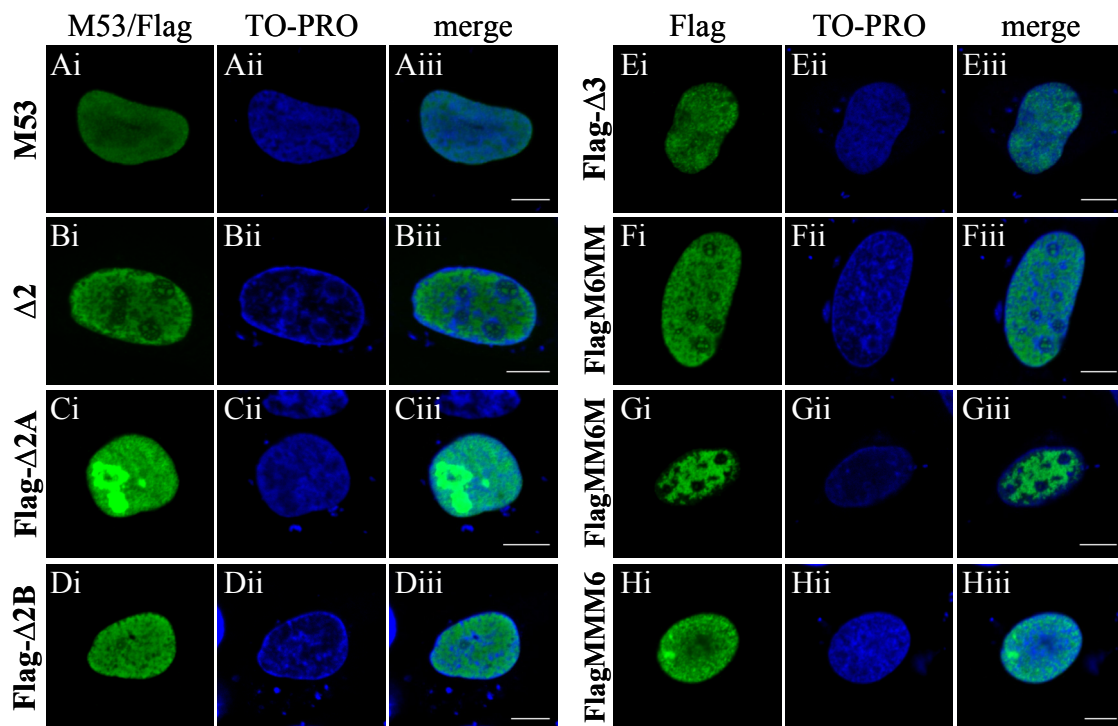


**Figure 3.6: M53 mutants localise to the nucleus**

U-2 OS cells were transiently transfected with plasmids expressing the indicated M53 mutants. Cells were fixed 36 hpt and co-stained with a polyclonal antiserum specific for pM53 (panels A and B) or a monoclonal anti-Flag antibody followed by Alexa-conjugated secondary antibodies and analysed under a confocal immunofluorescence microscope. DNA was stained using TO-PRO 3. Scale bar, 10 μm.

To interfere with viral morphogenesis, a DN protein must be present in sufficient amounts within the cell. To study whether induction of the different mutant alleles resulted in comparable levels of protein expression, M2-10B4 cells were infected at an MOI of 1 with wt MCMV, MCMV-SVT-M53, a virus carrying a second wt M53 allele, MCMV-SVT-Δ2 or MCMV-SVT-Δ3 in the absence and presence of dox. Cell lysates were prepared at 0, 1, 3 and 5 dpi, and subjected to Western blot analysis (Figure 3.7).
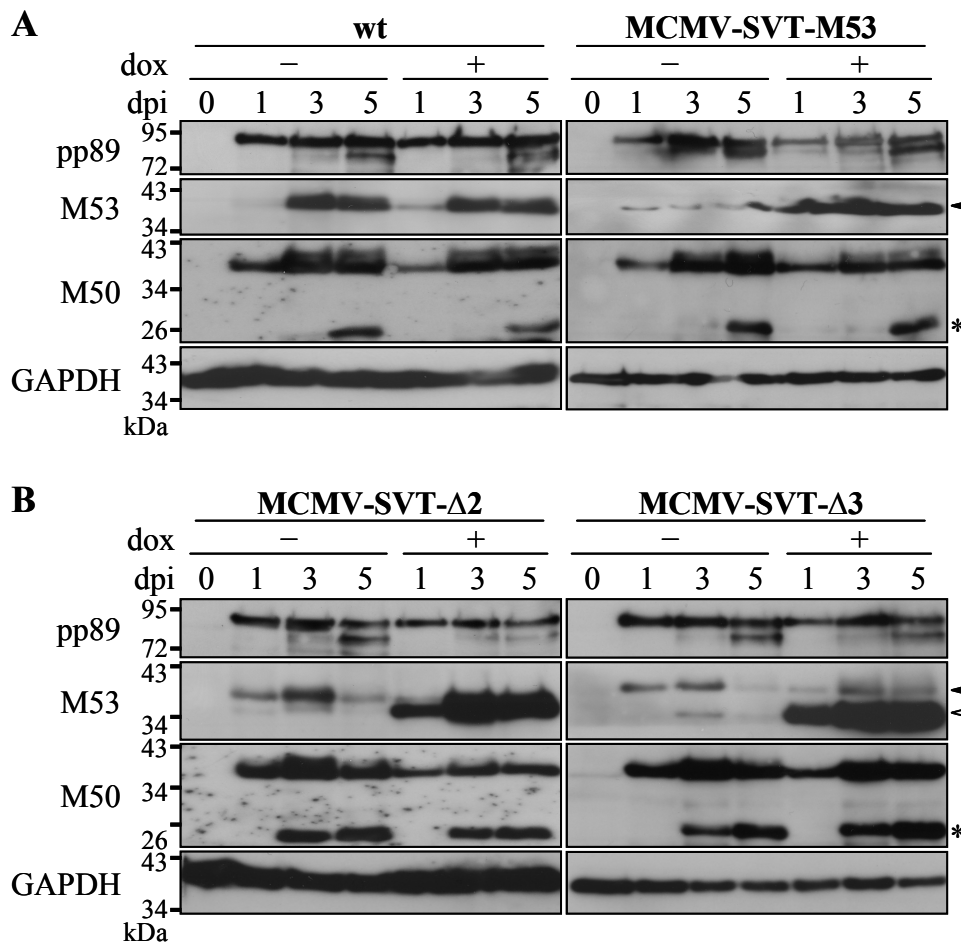


**Figure 3.7: Expression of the wt NEC proteins in presence of pM53 mutants**

M2-10B4 cells were infected with the indicated viruses at an MOI of 1 in the absence (−) or presence (+) of 1 µg/mL doxycycline (dox). Cell lysates were prepared at the indicated time points, and probed for pp89, pM53 and pM50 by Western blotting with specific immune sera. GAPDH was detected using a specific monoclonal antibody. Signals corresponding to wt pM53 are indicated by black arrowheads, signals for the truncated proteins pM53Δ2 and pM53Δ3 by the unfilled arrowheads. The bands for the pM50 degradation products are indicated by an asterisk.

The loading control, pp89, showed comparable levels for all viruses. A faint band representing wt pM53 was observed 24 hours post-infection (hpi), the intensity of which

increased over time (Figure 3.7). While the addition of dox had no effect on pM53 expression in cells infected with wt MCMV, pM53 expression in cells infected with MCMV-SVT-M53 was up-regulated in the presence of dox (Figure 3.7A). Wt pM53 was also detectable in the absence and presence of dox after infection with MCMV-SVT-Δ2 and MCMV-SVT-Δ3 (Figure 3.7B, black arrowhead). Although the endogenous and mutant M53 alleles had no detection tag, the two different pM53 proteins could be discriminated due to size differences. pM53Δ2 (35 kDa) and pM53Δ3 (29 kDa) were strongly expressed upon induction by dox and could be distinguished from the 38 kDa wt pM53 (Figure 3.7B, open arrowhead).

Since pM50 interacts with pM53 [95, 130], the effect of mutant pM53 overexpression on pM50 steady state levels was also investigated. Following infection with each mutant, increasing pM50 signals were detected from 1 dpi, accompanied by accumulating levels of pM50 degradation products. In cells infected with MCMV-SVT-Δ2 and MCMV-SVT-Δ3, the pM50 degradation products appeared earlier (Figure 3.7, asterisk). However, pM53Δ3 had no inhibitory function, therefore the early accumulation of pM50 degradation products did not yet explain the inhibitory effect of pM53Δ2.

## 3.2 Investigation of the M53 CR2 deletion mutant

Partial or complete deletion of M53 CR2 gave rise to DN mutants that strongly interfered with MCMV replication. The growth defects observed upon pM53Δ2 and pM53Δ2A expression were at least 100-fold stronger than the inhibitory potential of i207, the representative inhibitory insertion mutant (harbouring a mutation within M53 CR2) obtained by random linker-scanning mutagenesis [130]. The strong DN effect now allowed a detailed characterisation of the CR2 mutant properties.

### 3.2.1 Deletion of M53 CR2 prevents capsid egress from the nucleus

The NEC, consisting of pM53 and pM50, is involved in MCMV genome cleavage and the nuclear egress of viral capsids [130, 152]. The effect of CR2 deletions on virus morphogenesis was analysed by transmission electron microscopy (TEM).
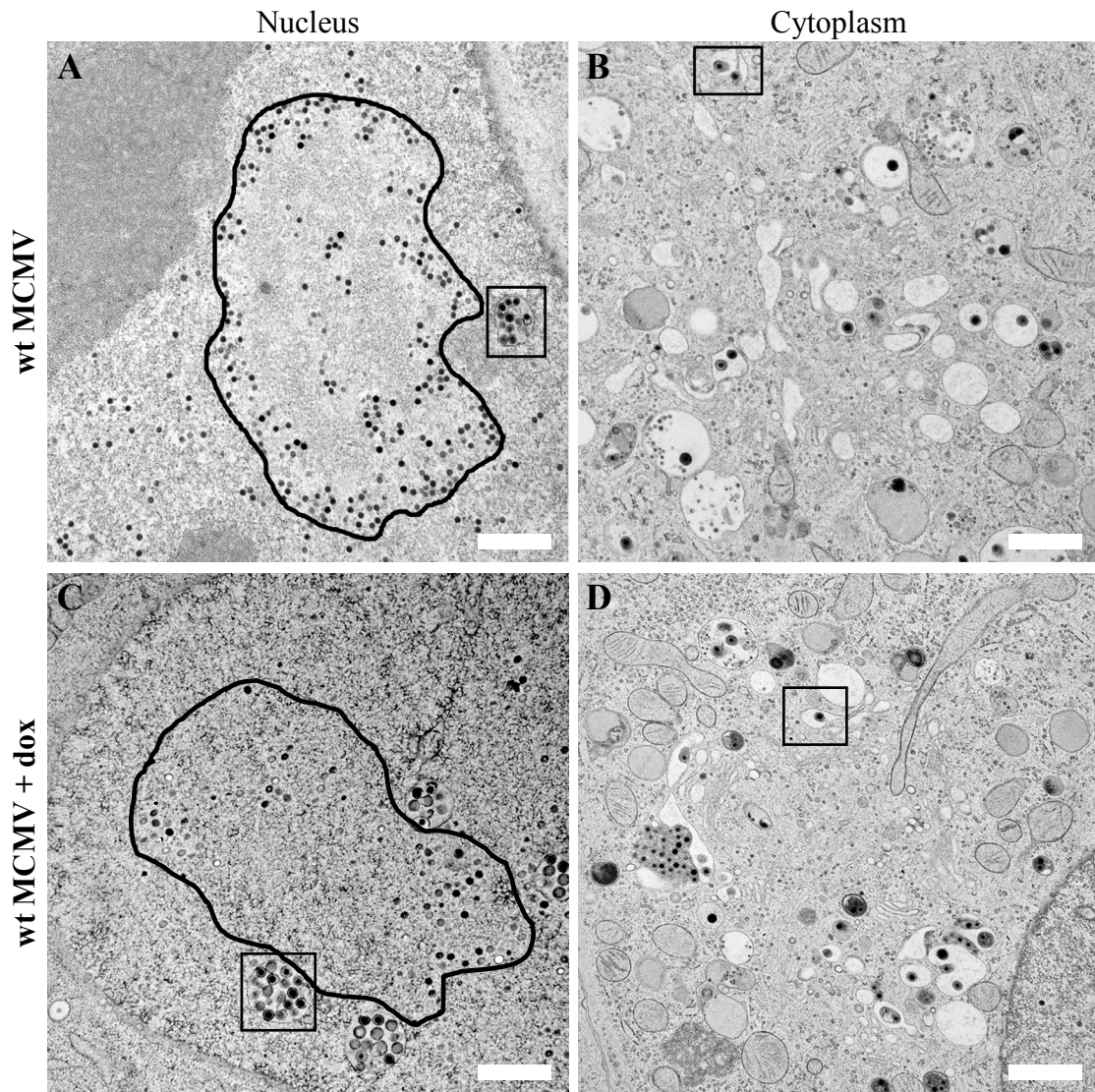
**Figure 3.8: Electron microscopic analysis of wt MCMV**

NIH/3T3 cells were infected with wt MCMV at an MOI of 5 using centrifugal enhancement in the absence (A, B) and presence (C, D) of 1 µg/mL doxycycline (dox). Cells were fixed 48 hpi by high-pressure freezing, freeze-substituted, plastic embedded, and sectioned. Samples were viewed on a JEOL JEM-1400 transmission electron microscope at 80 kV. The rounded outlines indicate the approximate borders of replication compartment-like structures (A, C). The boxes highlight areas of primary (A, C) and secondary envelopment (B, D). Scale bar, 1 µm.

NIH/3T3 cells grown on carbon-coated sapphire discs were infected at an MOI of 5 with wt MCMV, MCMV-SVT-M53 and MCMV-SVT-Δ2 in the absence and presence of dox and examined by TEM after high-pressure freezing at 48 hpi. Viral capsids were observed in the nucleus and cytoplasm of wt MCMV (Figure 3.8) and MCMV-SVT-M53-infected cells (Figure 3.9) as described previously [25].
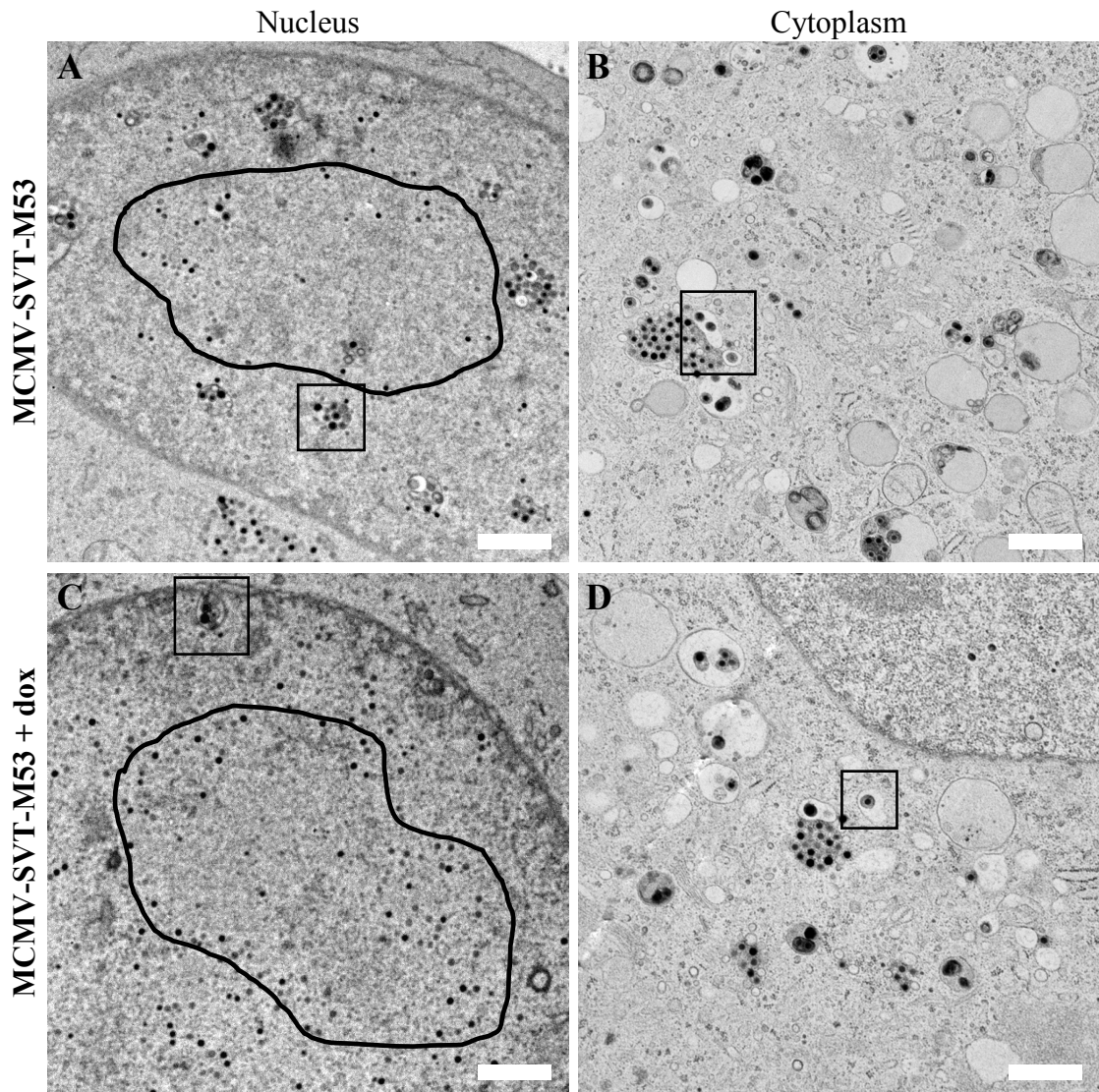
**Figure 3.9: Overexpression of pM53 does not change the infectious phenotype**

NIH/3T3 cells were infected with MCMV-SVT-M53 in the absence (A, B) and presence (C, D) of 1 µg/mL doxycycline (dox) and processed as described in Figure 3.8. The rounded outlines indicate the approximate borders of replication compartment-like structures (A, C). The boxes highlight areas of primary (A, C) and secondary envelopment (B, D). Scale bar, 1 µm.

In the absence of dox, the infection phenotype of MCMV-SVT-Δ2 was similar to that shown by the wt virus. However, the phenotype of dox-treated MCMV-SVT-Δ2-infected cells differed from that of wt-infected cells. In this case, the viral capsids were trapped in the nucleus, indicating the blockade of nuclear maturation, similar to that described for the s309 mutant [130].
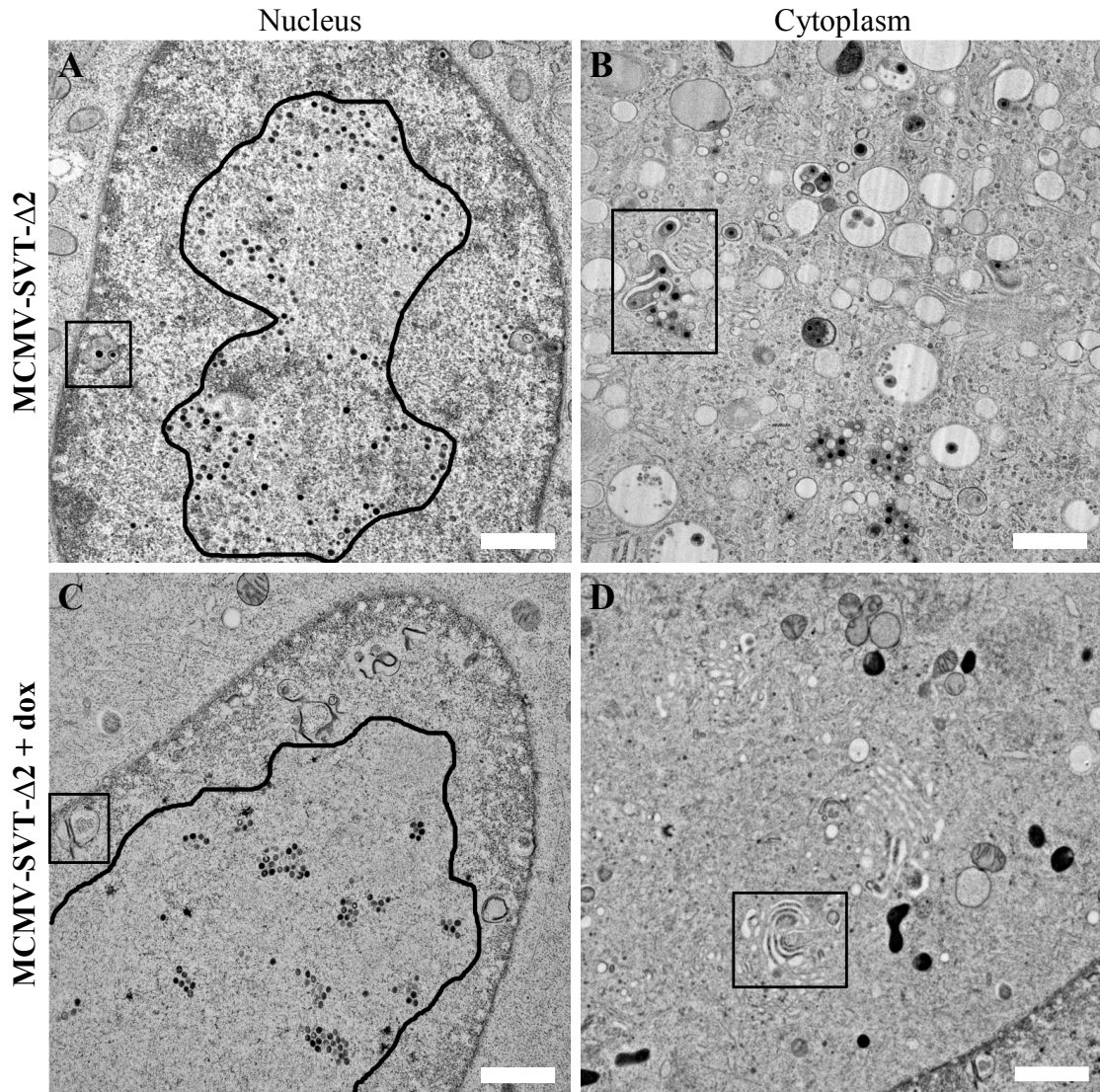
**Figure 3.10: The M53 CR2 deletion virus shows a nuclear egress defect**

NIH/3T3 cells were infected with MCMV-SVT-Δ2 in the absence (A, B) and presence (C, D) of 1 µg/mL doxycycline (dox) and processed as described in Figure 3.8. The rounded outlines indicate the approximate borders of replication compartment-like structures (A, C). The boxes highlight areas of primary (A) and secondary envelopment (B) or membrane accumulations (B, D). Scale bar, 1 µm.

Furthermore, the nuclear capsids in wt-infected cells were dispersed and surrounded an intranuclear structure of altered electron density reminiscent of replication compartments [79] (black lines in Figures 3.8, 3.9 and 3.10 A and C). Upon dox addition, however, the majority of the nuclear capsids clustered in regularly arranged groups within these replication compartment-like structures within MCMV-SVT-Δ2-infected nuclei (Figure 3.10C, black outline), indicating a capsid transport defect.

During nuclear morphogenesis, a complex order of events leads to mature DNA-filled capsids. Viral proteins are assembled into spherical scaffold-containing procapsids. These are believed to mature concurrently with genome packaging into C capsids, with high-density cores and a hexagonal appearance on TEM. In addition, two more products of capsid maturation can be distinguished. B capsids also contain scaffold-like procapsids, but these are icosahedral. They are thought to be the result of premature cleavage of the scaffold protein. The other form appears as A capsids, which are empty capsid shells with an icosahedral symmetry. A and B capsids are believed to be non-functional dead-end products of capsid maturation [188], and an increase in their number reflects disturbances of the processes involved in capsid maturation.

To quantify the influence of pM53Δ2 expression on capsid morphogenesis, the nuclear capsids in the untreated and dox-treated wt MCMV-, MCMV-SVT-M53- and MCMV-SVT-Δ2-infected cells seen on the TEM images were classified according to the stages described above (Figure 3.11). As it is not clear whether the procapsids are preserved by the TEM preparation protocol used here and because they can only be discriminated from B capsids by their shape, all capsids with apparent scaffold ring were classified into one class. Most of the capsids were classified either as procapsids/B capsids or as C capsids in wt- and MCMV-SVT-M53-infected cells in the absence and presence of dox and in cells infected with MCMV-SVT-Δ2 in the absence of dox. There were almost no A capsids. By contrast, induction of the M53Δ2 allele led to a significant increase in the number of immature A capsids from about 1% in the absence of dox to about 7%. There was also a significant increase in the number of immature pro- and B capsids (from about 47% to more than 80%). Accordingly, less than 10% of the nuclear capsids represented mature C capsids (Figure 3.11B).

In addition to inhibiting capsid maturation, expression of the pM53Δ2 mutant induced membrane accumulation in the nucleus, which was distinct from the membrane-surrounded vesicles observed in wt-infected cells, which are formed by invaginations of the INM during capsid egress [25]. This accumulation seemed to comprise membranes folded into each other and connected by a high-staining material (compare black boxes in Figure 3.10 A with that in C). No capsids were found in the cytoplasm of most dox-treated MCMV-SVT-Δ2-infected cells. Furthermore, the cytoplasmic assembly and maturation site [104], where the tegument layer is added and secondary envelopment occurs, was absent in dox-treated MCMV-SVT-Δ2-infected

cells (Figure 3.10, right column). Instead, membrane stacks reminiscent of the Golgi apparatus were often observed, which again seemed to be connected by a high-staining material (Figure 3.10D, black box).

**A**



| virus | dox | A | pro-/B | C | total | n |
|---|---|---|---|---|---|---|
| wt | − | 15 | 2041 | 1390 | 3446 | 23 |
| wt | + | 26 | 1241 | 1152 | 2419 | 21 |
| MCMV-SVT-M53 | − | 9 | 648 | 595 | 1252 | 15 |
| MCMV-SVT-M53 | + | 13 | 1040 | 940 | 1993 | 22 |
| MCMV-SVT-Δ2 | − | 16 | 860 | 941 | 1817 | 28 |
| MCMV-SVT-Δ2 | + | 586 | 6913 | 778 | 8277 | 30 |

**B**
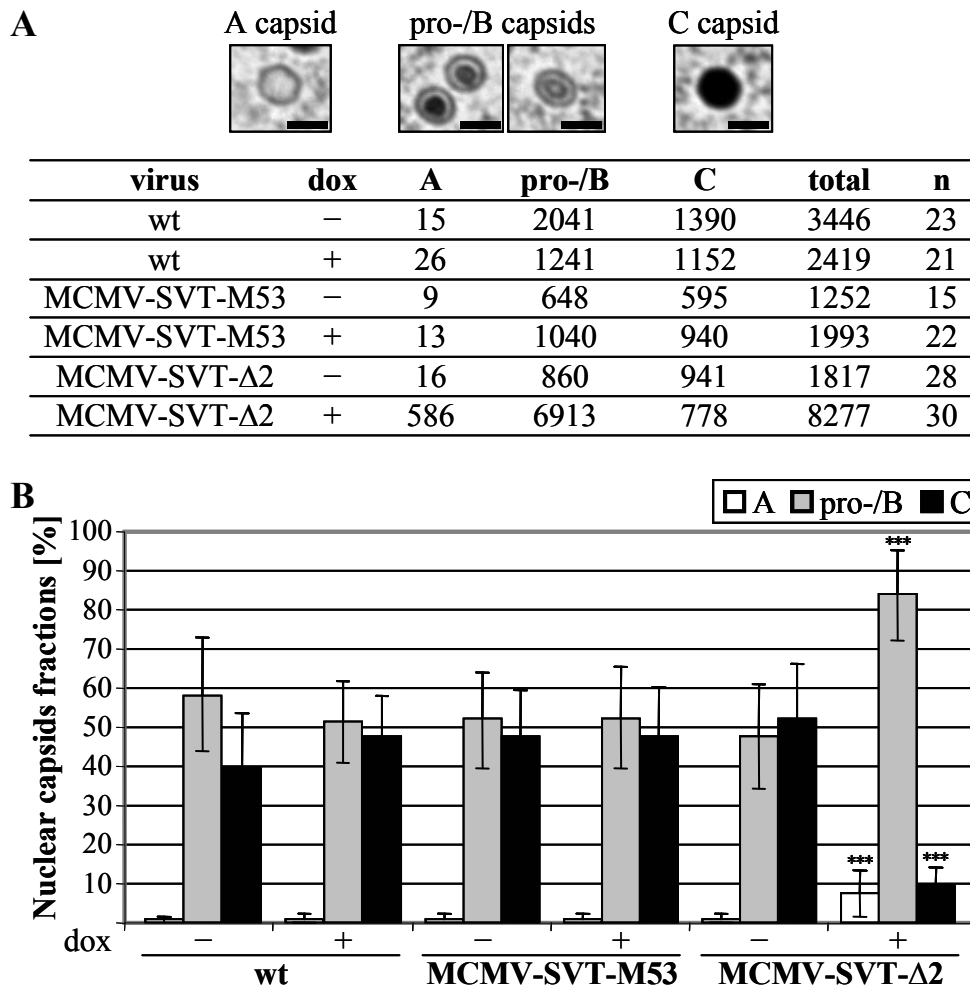


**Figure 3.11: Quantification of the defect in nuclear capsid maturation**

NIH/3T3 cells were infected with the indicated viruses and treated as described in Figure 3.8. (A) Nuclear capsids were categorized according to their morphogenesis stage as shown in the example pictures: immature, unfilled A capsids, scaffold-containing procapsids and B capsids as well as mature C capsids. The capsids were counted for a given number of nuclei (n). Scale bar, 100 nm. (B) Percentage of each category of nuclear capsid. White bars, A capsids; grey bars, procapsids and B capsids; black bars, C capsids. Data are expressed as the mean and standard deviation. ***p < 0.001, unpaired t-test (the two conditions for each virus were compared to each other and to the wt samples; no label means no significant difference).

### 3.2.2 M53 CR2 deletion mutants prevent unit length genome formation

The increased proportion of immature nuclear capsids found in dox-treated MCMV-SVT-Δ2-infected cells indicated a morphogenesis block in viral development at, or prior to, the stage of viral DNA packaging. Therefore, genome cleavage and genome packaging was studied next.

Upon replication, MCMV genomes form concatemers [104]. The head of the viral DNA is inserted into newly assembled procapsids and cleaved into unit length genomes by the viral terminase (pM56 and pM89 in MCMV [131]). The processes of genome encapsidation and cleavage are linked and occur simultaneously. Thus, concatemeric and unit length genomes are present in parallel once viral replication has started.
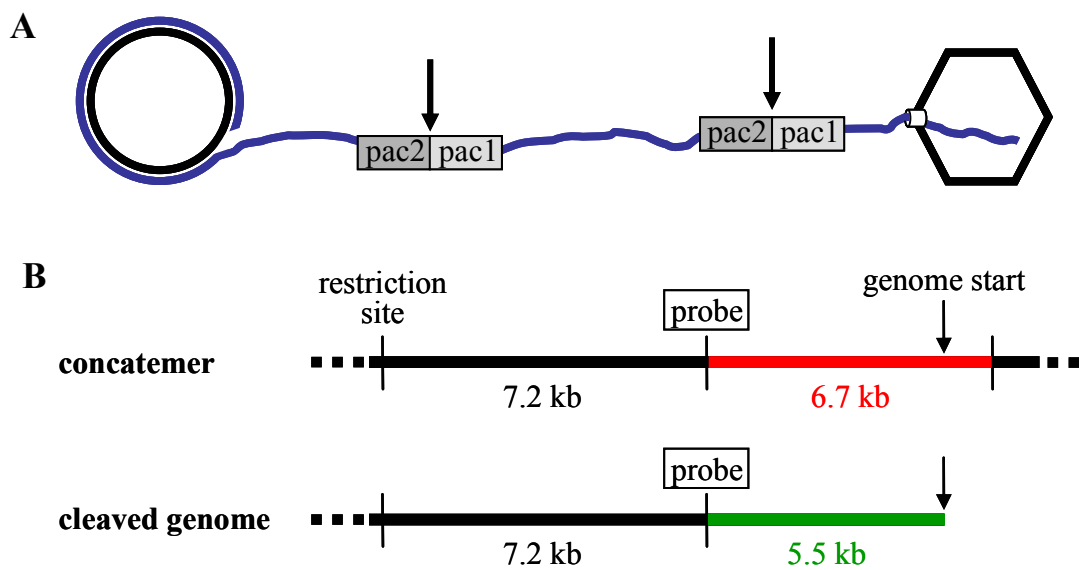


**Figure 3.12: Principle of the packaging assay**

Schematic representation of the Southern blot assay used to analyse MCMV genome cleavage/packaging. **(A)** Upon replication, MCMV genomes are connected head-to-tail. The concatemeric DNA is cleaved by the viral terminase at the indicated site (arrow) and unit length genomes are packaged into newly assembled capsids. **(B)** In the concatemeric form (upper panel), restriction digestion releases a 7.2 kbp control fragment and a 6.7 kbp fragment, which are both recognized by the same probe. By contrast, the unit length genome (bottom panel) gives rise to the 7.2 kbp control fragment, but also gives rise to a 5.5 kbp fragment representing genome cleavage.

To analyse the viral DNA with regard to cleavage/packaging, M2-10B4 cells were either mock-infected or infected with wt MCMV, MCMV-SVT-Δ2, MCMV-SVT-Δ2A or MCMV-SVT-Δ2B in the absence and presence of dox. Total DNA was isolated at 48 hpi, digested using *Apa*LI and subjected to Southern blot analysis. Restriction digest of concatemeric genomes gives rise to a 7.2 kbp control fragment, which was used for normalisation of the genomic load, and a 6.7 kbp fragment representing the uncleaved, concatemeric genome. The same fragments arise from digestion of circular BAC DNA, which mimics the concatemeric genomic form. However, restriction of unit length genomes cleaved by the viral terminase releases a 5.5 kbp fragment of the genome terminus in addition to the 7.2 kbp control fragment (Figure 3.12).

The expected fragments of 7.2 kbp and 6.7 kbp were detected at comparable levels after *Apa*LI digestion of circular wt MCMV BAC DNA (Figure 3.13A). The same pattern was observed for the BAC DNA of the mutant viruses (data not shown). DNA from mock-infected cells gave no signal at all, confirming the specificity of the probe. All three of the expected signals were detected after digestion of DNA from wt- and MCMV-SVT-Δ2-infected cells, although the total amount of viral DNA from dox-treated MCMV-SVT-Δ2-infected cells was less than that from non-treated MCMV-SVT-Δ2- or wt-infected cells. More importantly, expression of pM53Δ2 severely reduced the number of unit length genomes (Figure 3.13A). To quantify this effect, the chemiluminescence signal was measured in a Typhoon scanner and the ratio of cleaved to concatemeric genomes was calculated after normalisation to the control fragments. In absence of dox, MCMV-SVT-Δ2 replicated just like wt MCMV and produced unit length genomes at wt levels. By contrast, induction of pM53Δ2 reduced viral cleavage activity, resulting in a decreased number of unit length genomes and the accumulation of concatemeric DNA (Figure 3.13B). A similar pattern was observed in MCMV-SVT-Δ2A-infected cells, i.e. wt-like replication in the absence of dox, but a marked reduction in the number of unit length genomes upon induction of pM53Δ2A. Expression of pM53Δ2B also resulted in a decrease of unit length genomes, but the effect was less pronounced, possibly reflecting the data observed for the growth kinetics.
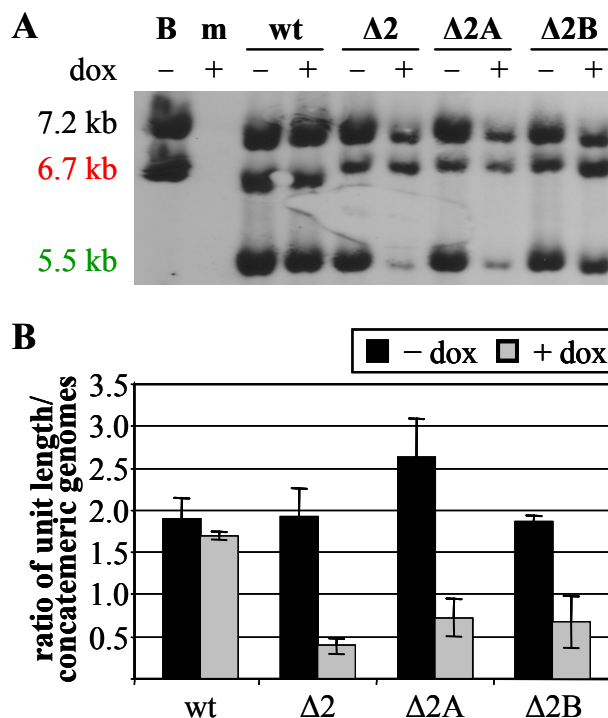
**Figure 3.13: M53 CR2 mutants inhibit the generation of unit length genomes**

**(A)** M2-10B4 cells were mock-infected (m) or infected with wt MCMV (wt), MCMV-SVT-Δ2 (Δ2), MCMV-SVT-Δ2A (Δ2A) or MCMV-SVT-Δ2B (Δ2B) at an MOI of 0.1 for 48 hours in the absence (−) or presence (+) of 1 μg/mL doxycycline (dox). Total DNA was purified, digested with *Apa*LI for 16 hours and subjected to Southern blot analysis. B, BAC DNA. **(B)** The chemiluminescence signal generated in the Southern blot assay was measured in a Typhoon scanner, quantified using ImageJ software (http://rsbweb.nih.gov/ij/) and then plotted as the ratio of unit length genomes to concatemeric genomes normalised to the control fragment. Error bars represent the standard deviation of at least two independent experiments.

Taken together, the results obtained thus far suggest that expression of the CR2 mutants of pM53 inhibits both capsid egress and genome cleavage/packaging, findings very similar to those observed for CR4 mutants [130].

### 3.2.3 M53 CR2 mutants have a DNA replication defect

Quantification of the capsid types observed by TEM revealed a marked increase in the number of aberrant A capsids upon expression of the M53Δ2 allele (Figure 3.11). In wt infection, cleavage and encapsidation of the viral DNA into procapsids proceeds concomitantly, resulting in mature capsids filled with one unit length genome each. An increase in the number of A capsids indicates a maturation defect. It is believed that more A capsids accumulate when the internal scaffold protein is processed before viral DNA has been recruited to the procapsid [188]. This could happen if the virus fails to

produce enough DNA to be inserted. A hint in this direction was already observed in the packaging assay, where in dox-treated MCMV-SVT-Δ2-infected cells the viral DNA load was decreased (Figure 3.13).

To investigate whether the viruses expressing M53 alleles defective in CR2 replicate their DNA as wt MCMV, M2-10B4 cells were infected at an MOI of 0.1 in the absence and presence of dox. Total DNA was purified at 48 hpi, digested using *Pae*I and analysed by semi-quantitative PCR (qPCR). The samples were probed for the M54 gene, encoding the catalytic subunit of the viral polymerase [131], and normalised to the cellular lamin B receptor (LBR) gene (Figure 3.14).
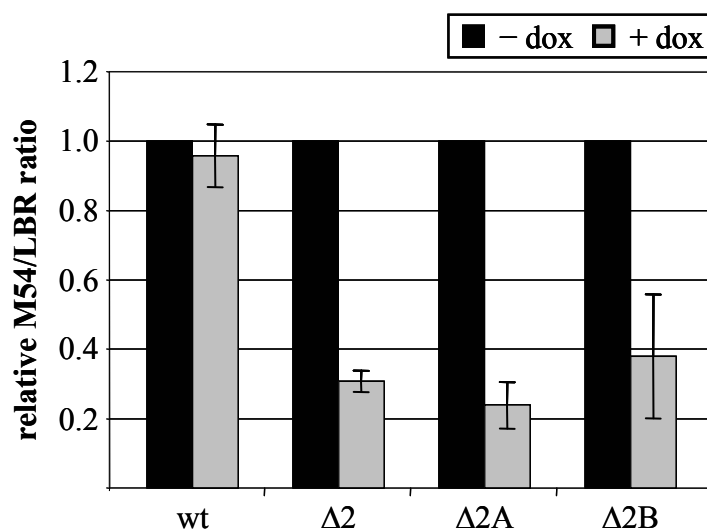


**Figure 3.14: Viral DNA replication is reduced upon induction of the CR2 mutants**

M2-10B4 cells were infected at an MOI of 0.1 with wt MCMV (wt), MCMV-SVT-Δ2 (Δ2), MCMV-SVT-Δ2A (Δ2A) or MCMV-SVT-Δ2B (Δ2B) for 48 hours in the absence (−) or presence (+) of 1 μg/mL doxycycline (dox). Total DNA was purified and digested using *Pae*I, before 20 ng of it were analysed by qPCR, probing for *lbr* as cellular and M54 as viral reference gene. Depicted are mean and standard deviation of duplicate samples of two independent experiments.

Confirmative to the observation in the packaging assay, a 3-fold reduction of viral DNA was detected in the qPCR analysis in MCMV-SVT-Δ2-infected cells with induced DN expression. Similar results were obtained upon expression of the partial deletion mutants pM53Δ2A and pM53Δ2B (ranging between 24% and 38% total DNA levels compared to non-treated cells), supporting the assumption that overexpression of M53 deletion mutants not only interferes with DNA cleavage and encapsidation, but also with the upstream process of DNA replication.

### 3.2.4 The wt NEC is formed in the presence of the inhibitory pM53 mutants

In addition to the interaction between pM53 and pM50, previous reports suggest that pM53 homologues show self-interacting homotypic activity [47, 148, 175, 179]. To study the protein-protein interactions between pM53 subunits in more detail, 293 cells were co-transfected with plasmids expressing Flag-tagged wt M53 together with either wt M53 or a CR2 or CR4 deletion mutant in the presence or absence of M50. Protein complexes were then precipitated using an anti-Flag matrix and analysed by Western blotting. In this setting, the anti-M53 antiserum detected both the Flag-tagged and untagged versions of pM53. As shown in Figure 3.15A, all proteins of interest were expressed at comparable levels (Figure 3.15A, Total).

Following immunoprecipitation (IP) with the anti-Flag matrix, a signal for wt pM53 was detected in addition to a signal for pFlagM53, whereas co-precipitation of the pM53 CR2 deletion was almost lost, giving only a minute amount of residual signal, and the CR4 truncation mutant was not co-precipitated (Figure 3.15A, Flag-IP, lanes 3 to 5). When pM50 was co-expressed, the same pattern was observed, i.e. the signal for wt pM53 was present, but the signals for pM53Δ2 and pM53s309 were not (Figure 3.15A, Flag-IP, lanes 7 to 9). The NEC proteins, pM53 and pM50, and their homologues in other herpesviruses, interact with each other and the complex can be precipitated via either protein partner [22, 95]. In this setting, pM50 was immunoprecipitated with pFlagM53 at comparable levels in presence of pM53, pM53Δ2 or pM53s309. This indicated that the wt NEC was formed regardless of the presence of the inhibitory deletion mutants (Figure 3.15A, Flag-IP, lanes 7 to 9). Unfortunately, wt pM53 had a propensity to bind the matrix non-specifically (Figure 3.15B). Therefore, it could not be clarified whether the failure to co-precipitate the deletion mutants reflected their lost capacity to interact with wt pM53, or whether the mutations simply prevented them from binding to the matrix.
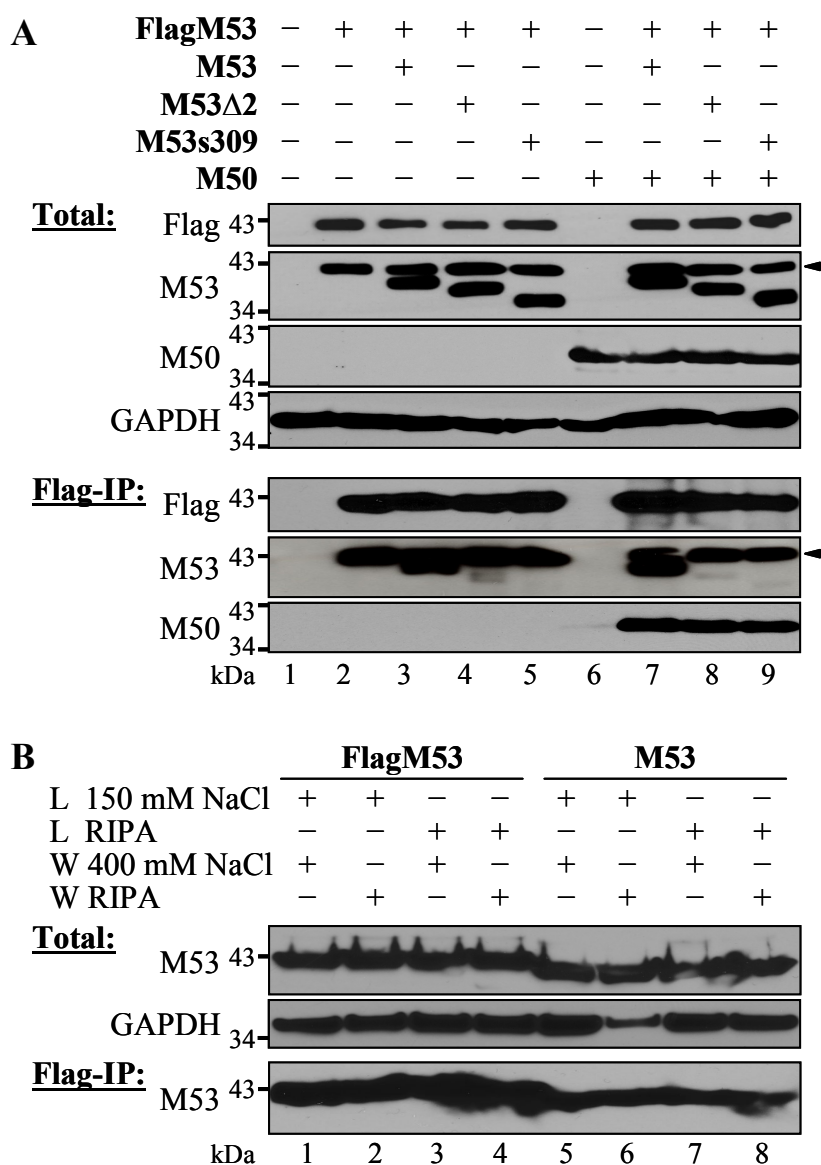
**Figure 3.15: Expression of DN mutants of pM53 does not influence the wt pM53/pM50 interaction**

**(A)** 293 cells were transfected with an empty expression plasmid (lane 1) or plasmids expressing Flag-tagged M53 (lanes 2 to 5 and 7 to 9) in combination with wt M53 (lanes 3 and 7) or the mutants M53Δ2 (lanes 4 and 8) or M53s309 (lanes 5 and 9) in the absence (lane 2 to 5) or presence of M50 (lanes 7 to 9). Cells were harvested 48 hpt and 10% of each sample (lysed in TLB) was used to detect total protein levels (Total). The remaining 90% was subjected to immunoprecipitation using an anti-Flag matrix (Flag-IP). The pFlagM53 band is indicated by a black arrowhead on the M53 blots. **(B)** 293 cells were transfected with plasmids expressing Flag-tagged (lanes 1 to 4) and untagged M53 (lanes 5 to 8). Cells were harvested 48 hpt and 10% of each sample was lysed in TLB and checked for pM53 protein expression. GAPDH was used as loading control (Total). The remaining 90% was subjected to immunoprecipitation with an anti-Flag matrix using different lysis (L) and washing (W) conditions. The eluates were probed for M53 (lower panel; indicated by Flag-IP).

## 3.2.5 CR2 mutations affect the nuclear distribution of the NEC

To characterise the fate of the wt NEC further, immunofluorescence analysis was performed to detect the intracellular localisation of pM53 and pM50 in M2-10B4 cells at 36 hpi. The homologues of the HSV-1 pUL31 and pUL34 proteins form a complex at the INM, thereby affecting the curvature of the membrane and allowing capsid translocation into the cytoplasm [46, 75, 118, 140]. In accordance with these reports, pM53 and pM50 co-localised at the nuclear rim to form the NEC in wt-infected cells; addition of dox did not change this localisation pattern (Figure 3.16A and B). A wt-like appearance was observed in the absence of dox in cells infected with MCMV-SVT-M53, a mutant expressing a second wt M53 allele (Figure 3.16C). Overexpression of the second M53 allele increased the amount of nucleosolic pM53 protein with no apparent change in the co-localisation with pM50 at the nuclear rim (Figure 3.16D). In MCMV-SVT-Δ2-infected cells, pM53 and pM50 showed a pattern comparable to that observed after wt infection in the absence of dox (Figure 3.16E). Additionally, a few pM53 aggregates, indicative for basal mutant expression, were already present in the absence of dox. Upon induction of the mutant M53 allele, the normal distribution of the NEC was disturbed and large aggregates containing pM53 and pM50 were formed at the nuclear periphery (Figure 3.16F). This granular appearance of the NEC after pM53Δ2 overexpression was similar to the accumulation of NEC in the presence of the CR4 truncation mutant s309 [130]. Based on these findings, it was hypothesised that the C-terminal tail of pM53 forms a functional unit and induces similar phenotypes when its overall integrity is disturbed.
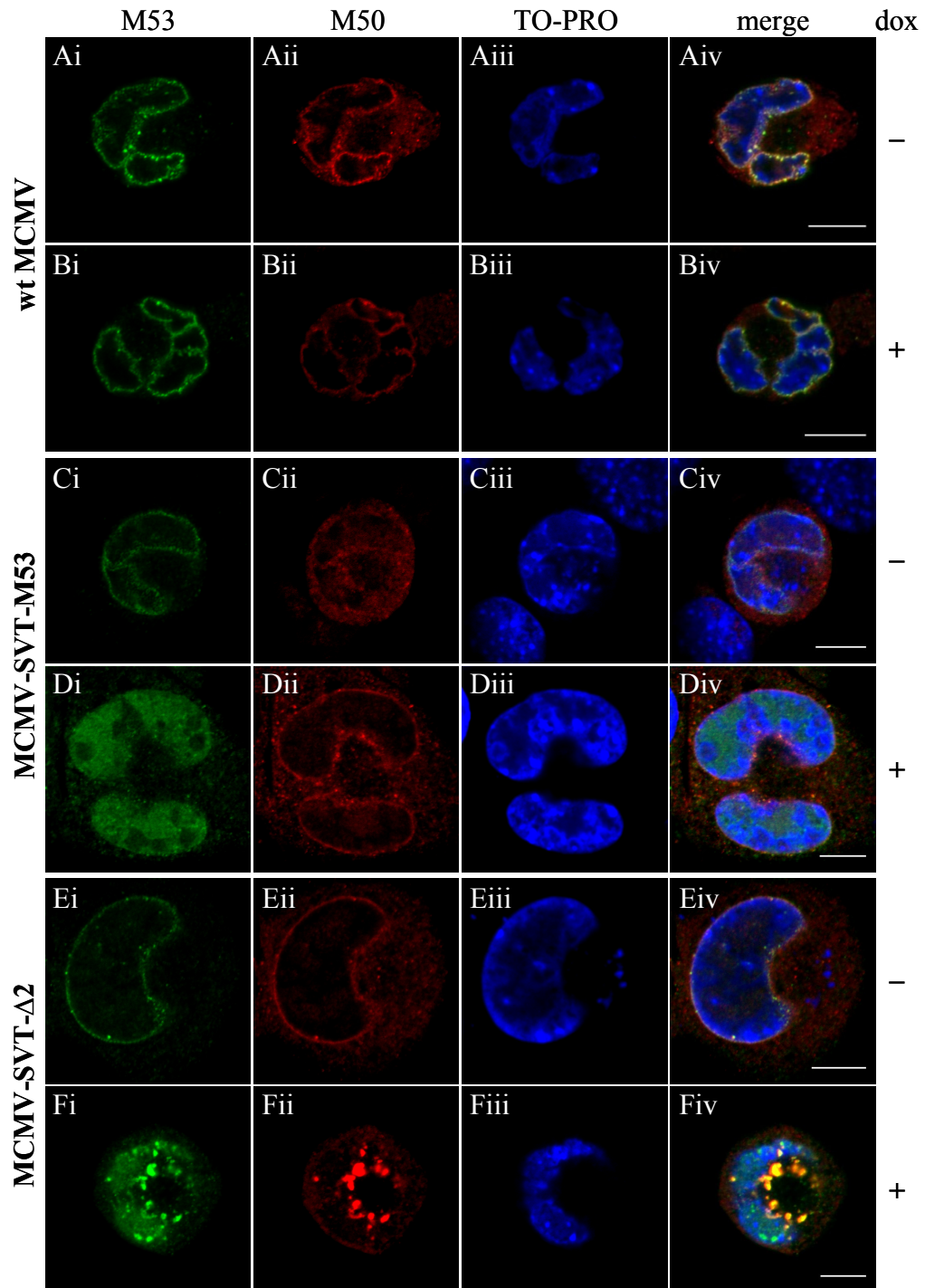
**Figure 3.16: Cellular localisation of the NEC proteins in the presence of mutant pM53 in infected cells**

M2-10B4 cells were infected with wt MCMV (panels A, B), MCMV-SVT-M53 (panels C, D) or MCMV-SVT-Δ2 (panels E, F) at an MOI of 0.5 in the absence (−) or presence (+) of 1 µg/mL doxycycline (dox) and fixed 36 hpi. Cells were co-stained with polyclonal antisera specific for pM53 and pM50 followed by Alexa-conjugated secondary antibodies and analysed using a confocal immunofluorescence microscope. DNA was visualized using TO-PRO 3. Scale bar, 10 µm.

To confirm that the NEC aggregates were formed selectively after overexpression of pM53Δ2 and not as a consequence of inhibiting nuclear capsid maturation in general, M2-10B4 cells were infected with a mutant virus harbouring an inducible GFP-coupled DN allele of the smallest capsid protein, SCP (MCMV-SVT-gfpSCP), which interferes with capsid maturation at an early stage [18, 142; unpublished observations] and analysed using confocal microscopy. While the signal generated by GFP-SCP appeared as granules in the nuclear interior, pM53 co-localised with pM50 was evenly distributed at the nuclear rim, as observed for wt MCMV infection. This distribution was observed in absence and presence of dox (Figure 3.17), indicating that NEC aggregation in MCMV-SVT-Δ2-infected cells was caused specifically by pM53Δ2 expression.
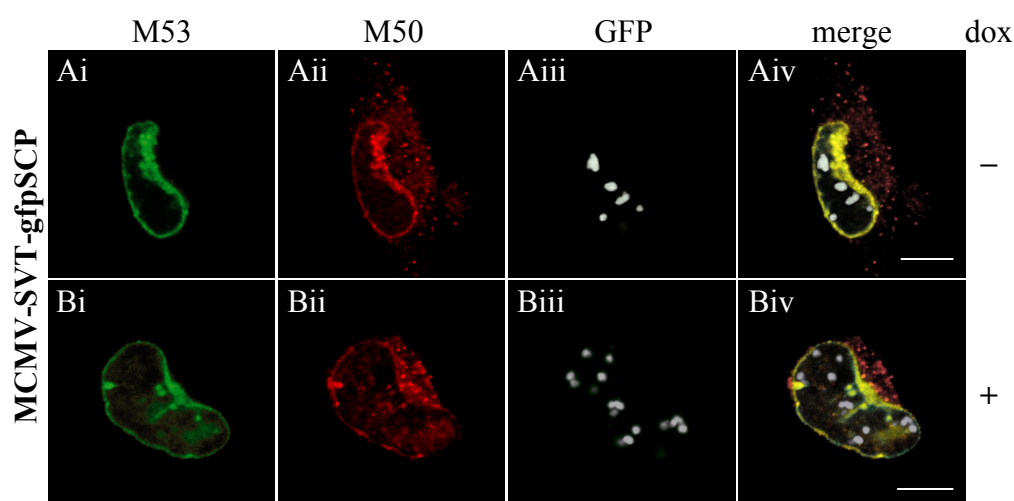


**Figure 3.17: Localisation of the wt NEC proteins in the presence of DN GFP-SCP**

M2-10B4 cells were infected with MCMV-SVT-gfpSCP at an MOI of 0.5 in the absence (−) or presence (+) of 1 μg/mL doxycycline (dox) and fixed at 36 hpi. Cells were co-stained with polyclonal antisera specific for pM53 and pM50 followed by Alexa-conjugated secondary antibodies and analysed using a confocal immunofluorescence microscope. Scale bar, 10 μm.

Many proteins use multiple interactions to facilitate their function. Therefore, to investigate whether NEC aggregation was the direct result of pM53Δ2 overexpression, and independent of other viral proteins except pM50, U-2 OS cells were transiently transfected with plasmids expressing either M50 or M50 together with M53 or M53Δ2. The cells were then stained with polyclonal antisera against pM50 and pM53 at 36 hpi.

When expressed individually, pM53 and pM53Δ2 were evenly distributed throughout the nucleosol (Figure 3.6), whereas pM50 alone was observed at the nuclear membrane and in the ER (Figure 3.18A). Co-expression of wt pM53 and pM50

localised both proteins to the nuclear rim due to formation of the NEC (Figure 3.18B). In the case of pM53Δ2 co-expression with pM50, a proportion of both proteins co-localised at the nuclear membrane, as did the wt proteins. However, a substantial proportion did not show the well-described nuclear rim staining, instead forming aggregates comparable to those observed in infected cells (Figure 3.18C). Based on these data, it was concluded that overexpression of a DN CR2 mutant of pM53 affected the nuclear distribution of the wt NEC in the absence of any other viral protein.
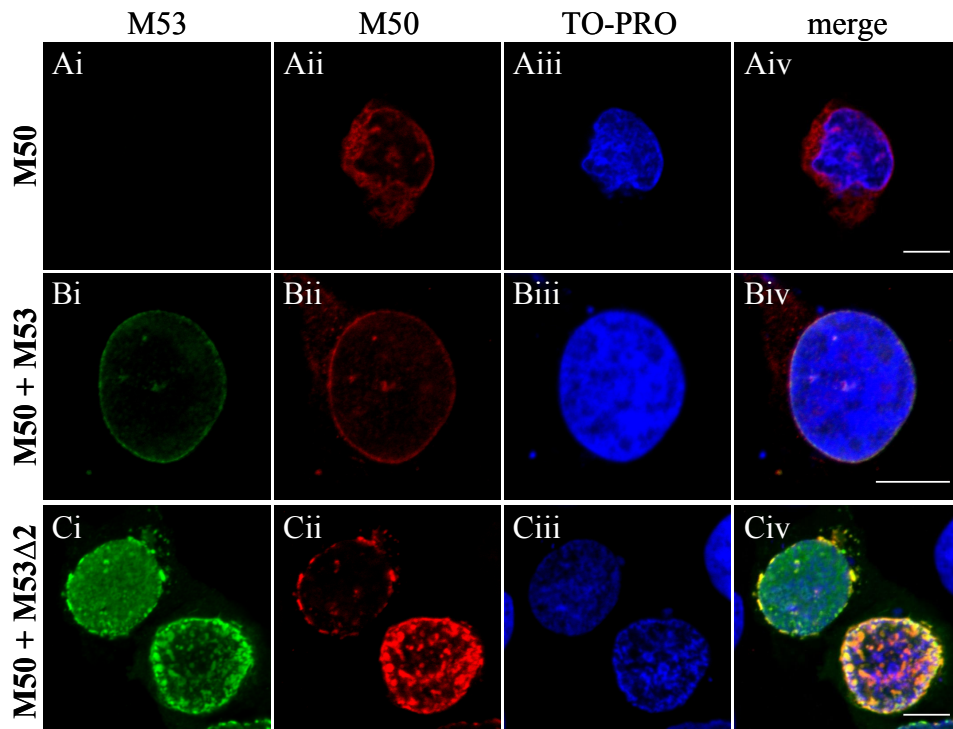


**Figure 3.18: Cellular localisation of pM50 in the presence of mutant pM53**

U-2 OS cells were transiently transfected with plasmids expressing M50 (panel A), M53 and M50 (panel B) or M53ΔCR2 and M50 (panel C) and fixed at 36 hpi. Cells were co-stained with polyclonal antisera specific for pM53 and pM50 followed by Alexa-conjugated secondary antibodies and analysed using a confocal immunofluorescence microscope. DNA was stained using TO-PRO 3. Scale bar, 10 μm.

### 3.2.6 pM53Δ2 binds poorly to pM50

Since formation of NEC aggregates simply requires the presence of both pM50 and the pM53 CR2 deletion mutant, the interaction between pM53Δ2 and pM50 was analysed in more detail. For this, 293 cells were transfected for 48 hours with plasmids expressing M50 together with different Flag-tagged M53 mutants and 90% of the cells

were processed by co-immunoprecipitation with anti-Flag matrix, whereas the remaining 10% were used to check protein expression.

Western blotting (Figure 3.19) confirmed that pFlagM53 proteins and the pM50 protein were expressed at comparable levels. However, the amount of pM50 precipitated by the pM53 proteins differed markedly. As expected, high levels of pM50 were precipitated by wt pM53 and the truncation mutant pM53s168, which consists of the variable region and the pM50 binding site in CR1.
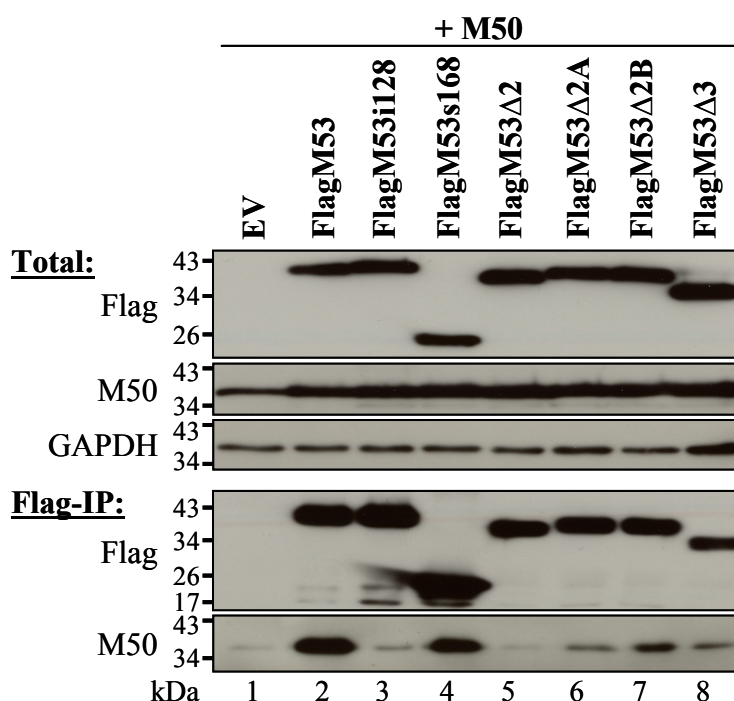


**Figure 3.19: Interaction of the pM53 CR deletion mutants with pM50**

293 cells were transiently transfected with plasmids expressing M50 together with different Flag-tagged M53 versions and harvested 48 hpt. Ten percent of each sample was lysed in TLB to detect total protein levels (Total). The remaining 90% were subjected to immunoprecipitation with an anti-Flag matrix and analysed by Western blotting with specific immune sera (Flag-IP). The Flag signal was detected with a monoclonal anti-Flag antibody directly coupled to horseradish peroxidase. EV, empty vector.

As shown previously [95], the binding-deficient mutant pM53i128 only bound background quantities of pM50. Remarkably, reduced pM50 binding was observed for the CR2 deletion mutants. The strength of pM50 binding declined from pM53Δ2B to pM53Δ2A to pM53Δ2, which precipitated almost no pM50 (Figure 3.19).

To confirm that pM53Δ2 was defective in pM50 binding, the protein-protein interaction was further studied using the protein fragment complementation assay

(PCA) established for the pM50/pM53 interaction [152]. In this assay, the N- and C-terminal parts of the TEM-1 ß-lactamase (BlaN and BlaC, respectively) are fused to pM50 and pM53. When wt pM50 and pM53 interact, the two Bla fragments are in close proximity and ß-lactamase activity is restored. Bla activity is quantified according to its nitrocefin hydrolysis rate (Figure 3.20).
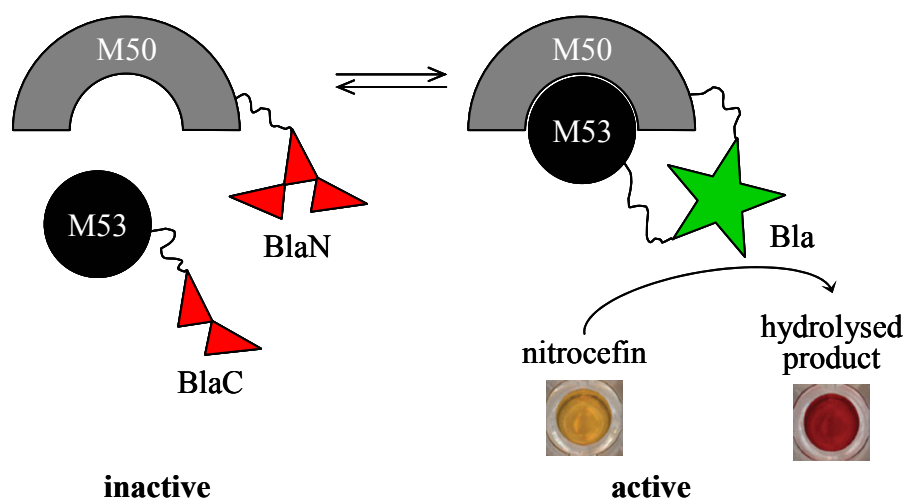


**Figure 3.20: Principle of the protein fragment complementation assay (PCA)**

Schematic representation of the principle of the protein complementation assay (PCA). The N- and C-terminal parts of the TEM-1 ß-lactamase (Bla) as reporter enzyme are fused to pM50 and pM53. Upon interaction of these two proteins, the proximity of the enzyme fragments BlaN and BlaC allows reconstitution of the active enzyme (green star). Adapted from [152].

To assess the pM50 binding, 293T cells were transfected with plasmids expressing different combinations of BlaC-tagged M53 versions together with different M50 versions fused to BlaN. Cells were lysed at 48 hpt and Bla activity was determined by nitrocefin conversion and absorbance measurement at 495 nm (Figure 3.21). The combination of pBlaC-M53 with pBlaN-M50 served as a positive control and yielded the maximum hydrolysis rate ($v_{max}$) of about 12 milliabsorption units/min. The negative control, consisting of pBlaC-M53 and pBlaN-M50DM, a mutant unable to bind pM53 [22], generated a background signal of about 2 milliabsorption units/min. When pBlaC-M53Δ2 was expressed together with pBlaN-M50, the nitrocefin hydrolysis rate was significantly reduced to approximately 50% of the control value, confirming the poor binding of pM53Δ2 to pM50 (as observed in the Flag-IP experiments). A similar reduction in the rate of nitrocefin conversion was observed for pBlaC-M53Δ3. By

contrast, BlaC-s309 together with BlaN-M50 yielded a nitrocefin hydrolysis rate similar to the wt value, indicating an appropriate interaction between these two proteins.
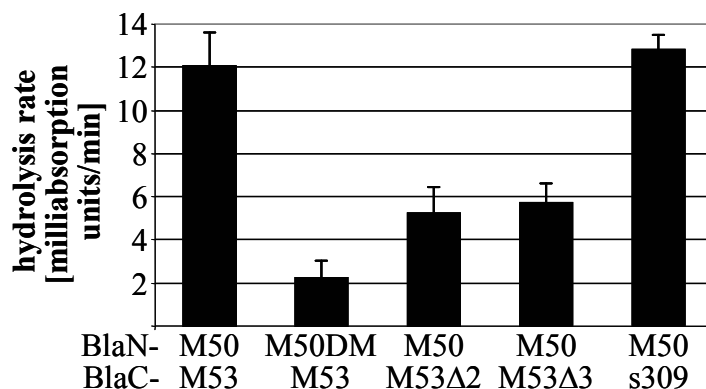


**Figure 3.21: Interaction of the pM53 deletion mutants with pM50 in the PCA**

293T cells were transiently transfected with plasmids expressing BlaN-tagged M50 or M53 binding-deficient M50 (M50DM) together with different versions of BlaC-tagged M53 proteins (wt M53, CR mutants Δ2 and Δ3, CR4 mutant s309). Cell lysates were prepared at 48 hpt and beta-lactamase activity determined by nitrocefin conversion. Absorption was measured at 495 nm. Error bars represent the standard deviation of duplicate samples of at least three separate experiments.

In conclusion, pM53Δ2 had a reduced capacity to bind pM50. As overexpression of this DN mutant led to impaired genome cleavage/packaging and membranous intranuclear NEC accumulation, it is likely that the CR2 of M53 plays a role in coupling genome cleavage with membrane deformation. Taken together, these data show that, despite their phenotypic similarities, the pM53Δ2 and pM53Δ3 mutants must act mechanistically different from the pM53s309 mutant.

# 3.3 Establishment of a high-throughput screening system for MCMV mutant alleles

Although DN mutants are potent tools in genetic analyses, their identification using the classical strategy of two random genetic screens, which are both based on individual flip-in in *E. coli* followed by BAC selection and virus reconstitution, is time-consuming and labour-intensive. Thus, new approaches are called for that decrease the screening effort.

## 3.3.1 Principle of the in-cell Flp-assisted (ICFA) complementation assay

To enable a simplified high-throughput screening, the classical approach had to be modified at several stages. A schematic screen is depicted in Figure 3.22. The basis for this assay was to test whether the recombination of an MCMV BAC with a shuttle plasmid by Flp-mediated recombination can even be performed in MCMV permissive host cells instead of *E. coli*. To this end, a cell line of murine fibroblasts derived from NIH/3T3 was generated, which was stably transfected to express enhanced Flp recombinase (Flpe). Flpe is a modified form of the original Flp evolved by cycling mutagenesis, which catalyses the recombination reaction more efficiently at 37 °C [24]. These cells were co-transfected by electroporation in 96-well format using the Nucleofector™ technology (Lonza AG) with an MCMV BAC lacking the essential gene of interest and a plasmid constitutively expressing either that gene, to test for its complementation at the ectopic position by reconstitution, or a mutated version of this gene. Nucleofection is a novel, non-viral transfection technology to modify primary cells and cell lines which are difficult to transfect. It permits direct entry of the transfected DNA into the nucleus, thus providing the possibility to transfect even non-dividing cells [12, 100, 173].

Following nucleofection, the Flpe-expressing cells were mixed with regular NIH/3T3 fibroblasts at a defined ratio. By site-specific recombination between two FRT sites oriented in the same direction, Flp catalyses both, the insertion of genetic elements into target DNA, but also the excision of such stretches. Under non-selective conditions, the excision reaction is kinetically favoured over the integration [3]. To avoid
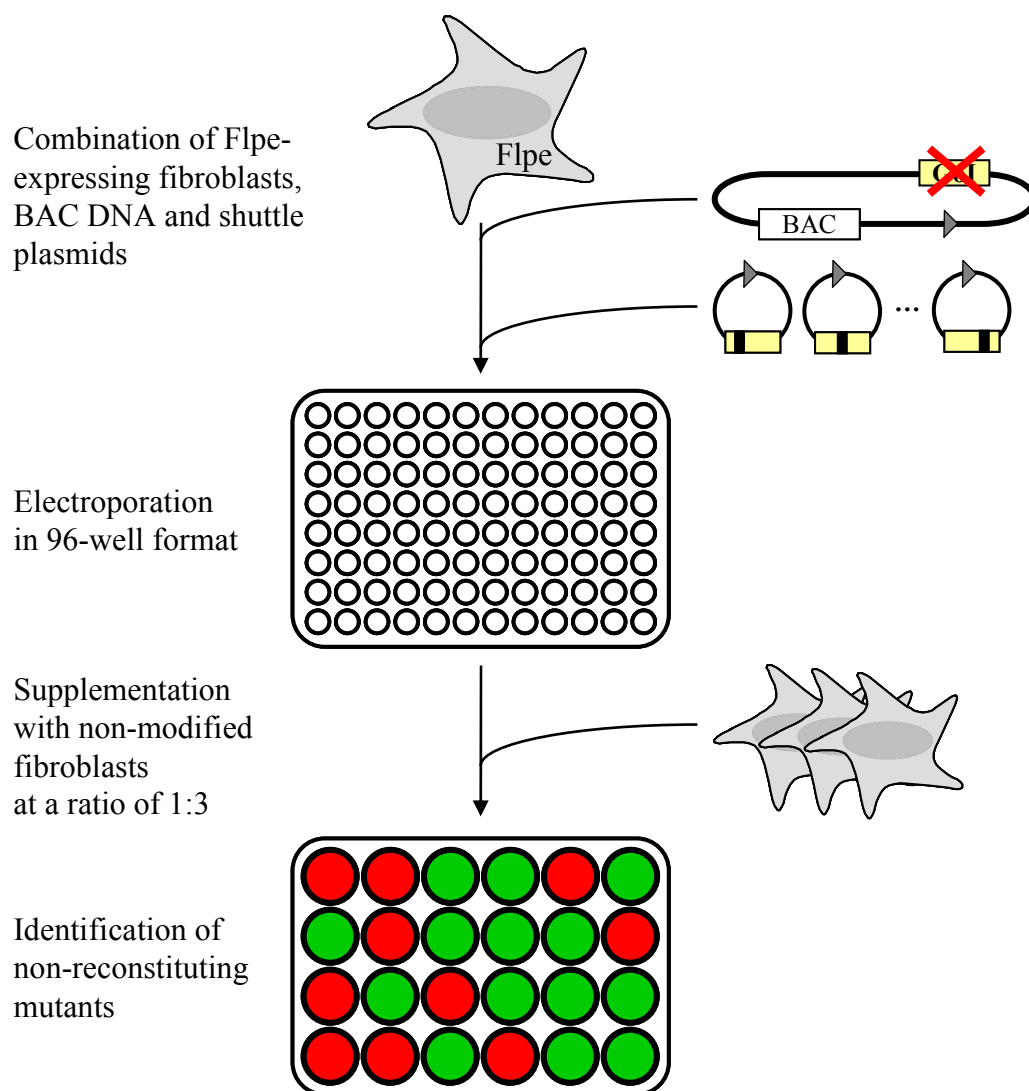
**Figure 3.22: Principle of the in-cell Flp-assisted (ICFA) complementation screen**

Murine fibroblasts stably expressing enhanced eukaryotic Flp recombinase (Flpe) were mixed with BAC DNA, which lacked the gene of interest (GoI, yellow box), and the respective shuttle plasmid carrying a mutated form of the GoI and transfected by nucleofection. Transformed cells were mixed with non-modified fibroblasts at a ratio of 1:3, seeded on multi-well plates and viral plaque formation monitored. Viral reconstitution (formation of plaques) was expected if the mutated gene was able to complement the wt protein function (depicted as green wells), whereas the absence of plaque formation using the same conditions would indicate non-complementing mutants (red wells). Since the unification of the shuttle plasmid and the target genome takes place within the host cell in the presence of Flpe expression, this new test was named in-cell Flp-assisted recombination-based (ICFAR) complementation assay.

overwhelming excision of the newly inserted shuttle plasmid from the BAC, non-Flpe-expressing cells were added in excess to provide sufficient target cells for viral propagation. Thus, by transmission of reconstituted viruses to neighbouring cells without Flpe, the viral genome containing the shuttle plasmid should be maintained, since in Flpe-negative cells it is not exposed to further Flp-specific modifications.

As in the previous recombination based systems in bacteria, the ability of the (mutated) gene expressed from the shuttle plasmid to complement the endogenous wt gene was tested first and assessed by viral plaque formation. This new assay should eventually replace the viability screen.

## 3.3.2 Complementation of essential genes using ICFA recombination (ICFAR)

At first it was tested whether the Flp-assisted recombination mediated directly in eukaryotic cells was indeed sufficient to restore reconstitution of MCMV BACs lacking essential genes. Three essential viral genes were chosen to validate the system, namely M53, M56 and M104. The M53 gene is known to be essential and was subjected to all ectopic complementation-based screens published before [95, 130], and thus provided a possibility to compare the fidelity of the new assay to the established complementation system. The essentiality of pM56, the MCMV homologue of the pUL28 herpesvirus protein family encoding the large subunit of the viral terminase [170], for MCMV replication was examined by transfecting MEF with an MCMV BAC lacking the M56 ORF (ΔM56). No viral progeny was detected for more than six weeks, supporting the crucial role of pM56 during virus production. The third gene, which was deleted from the MCMV genome, M104, encodes the portal protein required for translocation of the viral DNA into newly assembled capsids [120]. This protein is essential in all tested herpesviruses [124].

To test the complementation of these three genes in the ICFA recombination assay, Flpe-expressing cells were co-transfected with MCMV BACs lacking one of those genes and either an empty expression vector or a shuttle plasmid expressing the respective gene and seeded together with unmodified NIH/3T3 on 24-well plates. Six dpt the samples were stained with an antibody specific for the IE1 protein pp89 and the number of fluorescent foci was quantified (Figure 3.23).

No IE1-positive plaques were detected after nucleofection with the three deletion BACs, confirming the essentiality of those genes for viral reconstitution. Conversely, co-transfection of each deletion BAC with its respective rescue plasmid resulted in robust production of viral progeny at 6 dpt. Whereas for the complementation of the M53 and the M56 deletion an average of 32 fluorescent foci was detected, complementation of the M104 deletion resulted in an average of 47 plaques (Figure

3.23A). This confirmed that the in-cell Flp-assisted complementation assay was feasible for virus reconstitution.
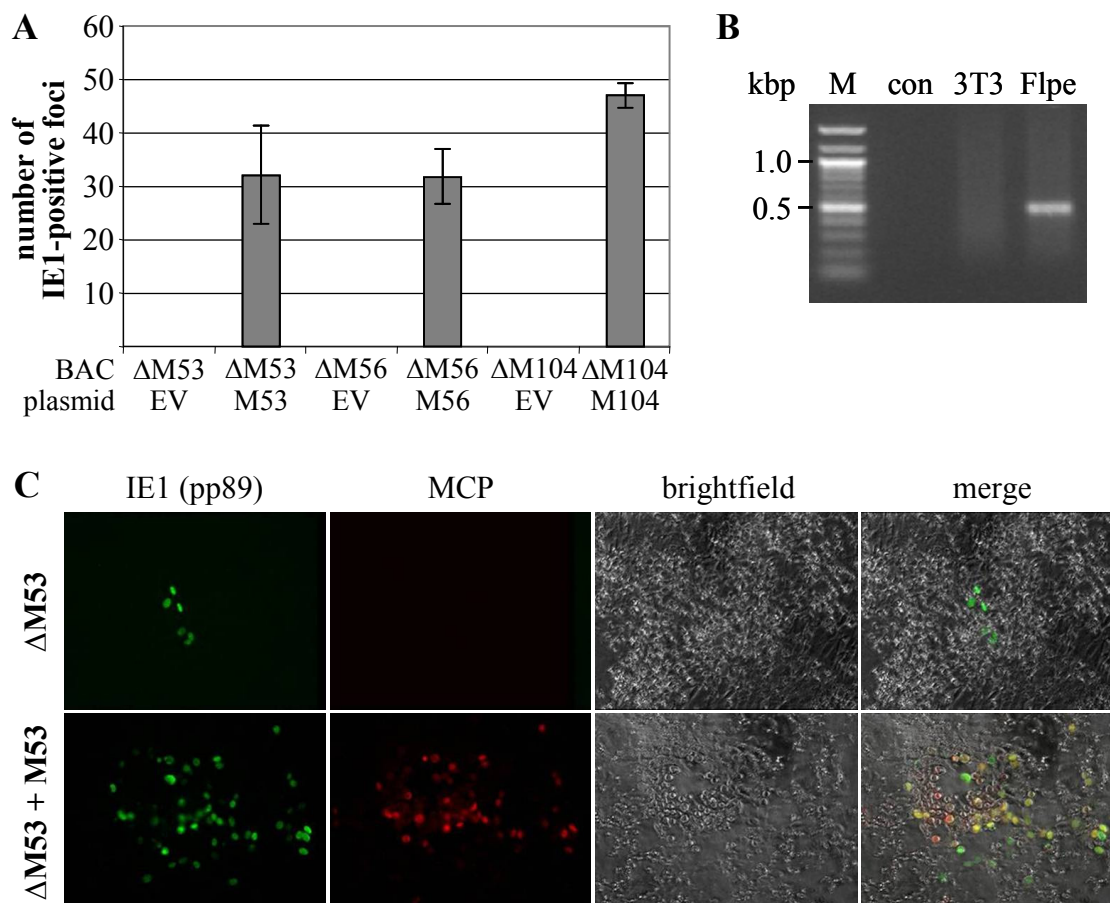


**Figure 3.23: Verification of the ICFAR complementation assay**

**(A)** Flpe-expressing cells were nucleofected with indicated BACs and plasmids and mixed with NIH/3T3. Samples were fixed at 6 dpt, stained with an antibody specific for the IE1 protein and IE1-positive plaques were quantified. Depicted are mean and standard deviation of triplicate samples of two to three independent experiments. EV, empty vector. **(B)** Total RNA was isolated from NIH/3T3 (3T3) and Flpe cells (Flpe), reverse transcribed and PCRed with primers specific for the *flpe* gene. The control reaction (con) did not contain any template. M, 100 bp DNA ladder. **(C)** Flpe-expressing cells were treated as in (A), stained with antibodies specific for the IE1 (pp89) and the major capsid protein (MCP) and images taken using a fluorescence microscope.

In addition to the staining to detect pp89, a sample of M53 was probed with an antibody specific for the major capsid protein (MCP), a gene product expressed late in the replication cycle [142]. Few single cells containing the IE protein pp89 were detected by immunofluorescence microscopy in cells transfected with the ΔM53 BAC, but no MCP-specific signal was observed, verifying that no viral progeny was produced

in the absence of M53. In contrast, the cells surrounding the viral plaques in the sample co-transfected with the M53-expressing rescue plasmid displayed strong signals for both pp89 and MCP, confirming the production of infectious virions (Figure 3.23C).

To verify the expression of Flpe recombinase, the total RNA content was purified from an aliquot of NIH/3T3 and Flpe-expressing cells in each experiment, the mRNAs were reverse transcribed and the resulting cDNA was probed by PCR for transcripts of the *flpe* gene. A representative result is depicted in Figure 3.23B. The expected amplicon of 500 bp, which covers the 5' half of the ORF, was detected exclusively in samples derived from Flpe-expressing cells, indicating that the *flpe* gene was actively expressed in these cells.

### 3.3.3 The ICFAR complementation assay can be used to identify non-complementing mutants

The previous experiments indicated that the ICFA recombination resulted in the ectopic insertion of the co-transfected shuttle plasmid, leading to the production of infectious viral progeny. The next step was to investigate whether this system could be used to screen a mutant library with regard to its complementation capacity. For this, a number of mutants of the M53 library generated by transposon mutagenesis was selected and tested as described above (Figure 3.24). The M53 mutant library has been studied extensively and the capacity to complement the M53 deletion was known of each mutant used [95, 130].

As previously, few IE1-positive foci were detected upon co-transfection of the ΔM53 BAC with an empty shuttle plasmid, but viral reconstitution was not observed, whereas complementation of the M53 deletion with wt pM53 resulted in robust virus production. Expression of the complementation-competent mutants i43 and i104 also led to the formation of viral progeny, albeit the numbers of plaques formed were about half times lower than with wt pM53 in this experiment. The mutants i128, i207, i212 and s309 failed in the previous screen to complement the M53 deletion [95]. This observation was also confirmed using the ICFA recombination-based assay, where no viral reconstitution was detected for any of these mutants. Furthermore, the plaque numbers obtained by phase contrast microscopy matched well with the quantification based on IE1-specific fluorescence. Thus, quantification of viral reconstitution was

possible without the requirement to specifically stain the samples for viral proteins (Figure 3.24B).

**A**

| mutant | i43 | i104 | i128 | i207 | i212 | s309 |
|---|---|---|---|---|---|---|
| **complementation of M53 deletion** | + | + | − | − | − | − |
| **inhibition of wt M53 function** | nd | nd | − | + | − | + |

**B**
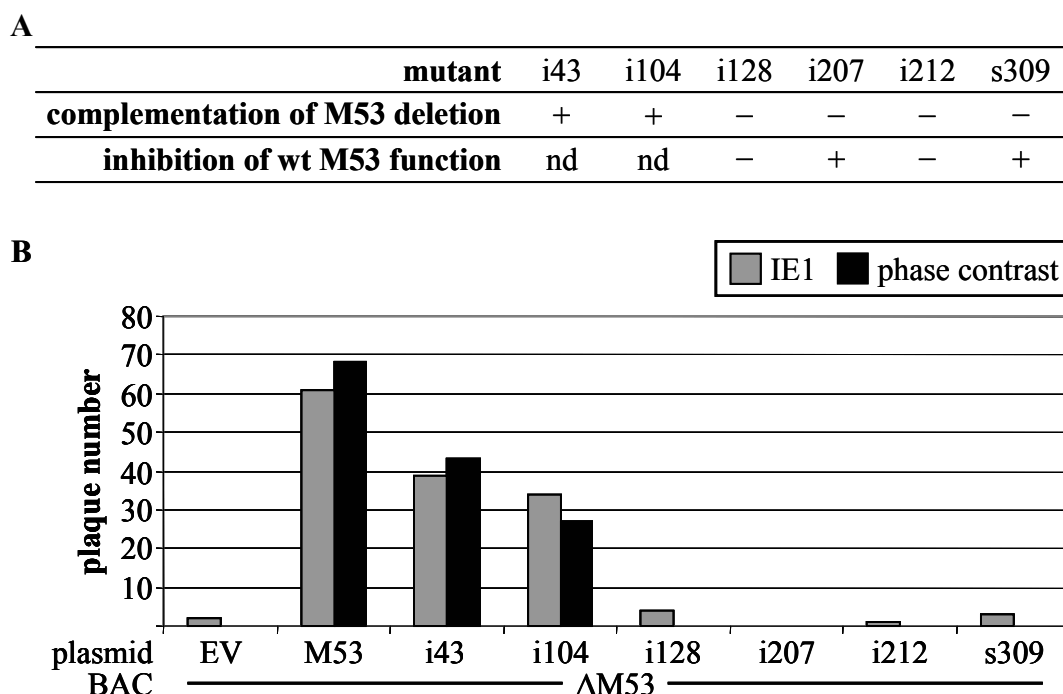


**Figure 3.24: Validation of the ICFAR complementation assay using pM53 mutants of the Tn mutagenesis library**

**(A)** Overview of selected M53 mutants generated by transposon mutagenesis with regard to their ability (+) or failure (−) to either complement an M53 deletion BAC (middle row) or to inhibit the function of the wt pM53 during viral replication [95, 130]. nd, not determined. **(B)** Flpe-expressing cells were nucleofected with the ΔM53 BAC and the indicated shuttle plasmids and supplemented with NIH/3T3. Samples were fixed at 6 dpt and stained with an antibody specific for the IE1 protein. Plaques were quantified in parallel using fluorescence (grey bars) and phase contrast microscopy (black bars). EV, empty vector; i, insertion of five amino acids; s, stop mutation at this position.

Using the M53 mutant library as reference set, the results observed in this screen correlated exactly with the findings published before. Thus, the ICFA recombination assay can be used for the identification of non-complementing mutations. Consequently, this screen was named ICFAR complementation assay.

### 3.3.4 Principle and validation of the ICFAR inhibitory assay

The ICFAR complementation screen aimed also at identifying mutants that fail to restore viral reconstitution. Only such non-complementing mutants have the potential to functionally inhibit the wt protein by a DN mechanism. However, most of the non-

complementing mutants are simply non-functional and lack the potential to inhibit the wt function. To identify the few inhibitory mutants, they have to be re-analysed in a second assay, previously coined "inhibitory screen" (Figure 3.25).
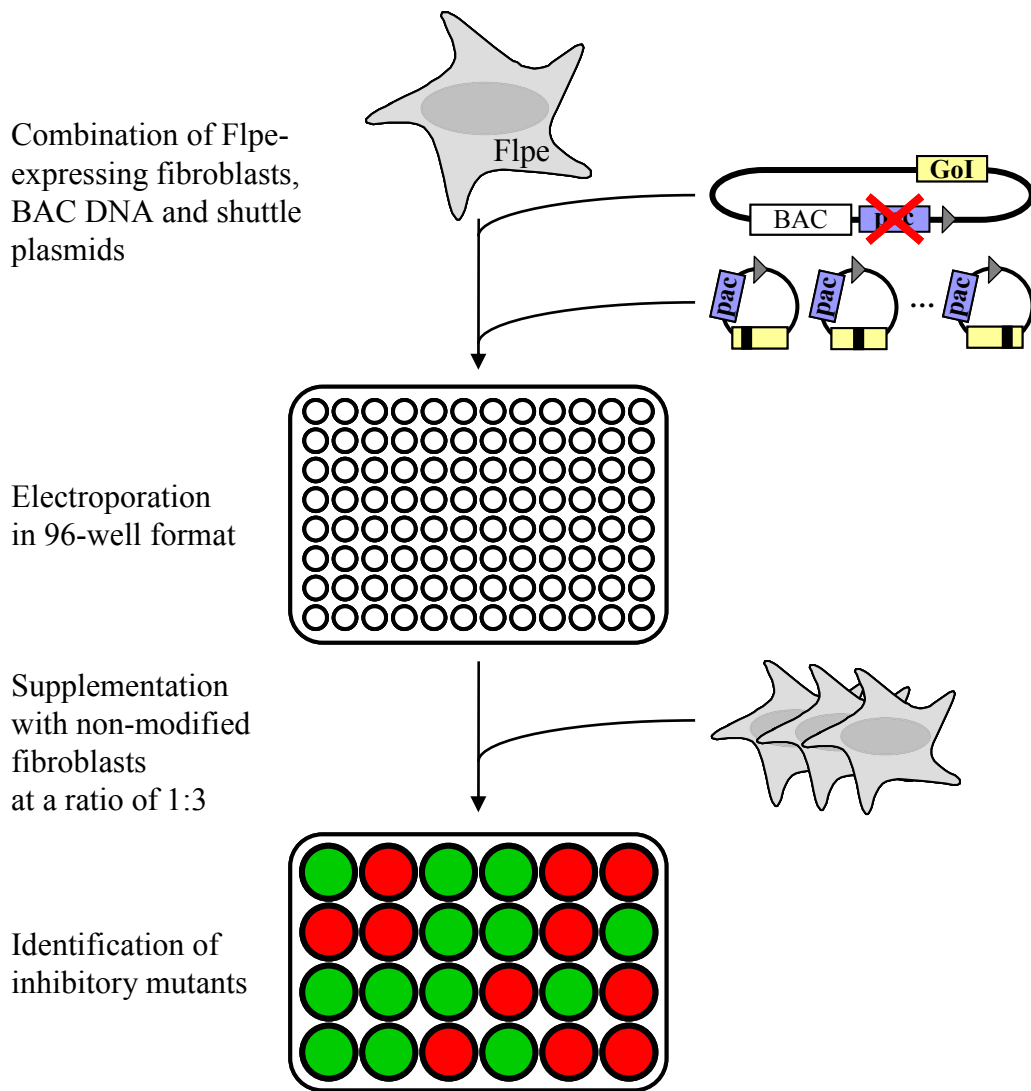


**Figure 3.25: Principle of the ICFAR inhibitory screen**

Murine fibroblasts stably expressing enhanced eukaryotic Flp recombinase (Flpe) were mixed with BAC DNA lacking the packaging signal (*pac*) and the respective shuttle plasmid carrying a mutated form of the GoI plus the complementing *pac* sequence, and transfected by nucleofection. Transformed cells were mixed with non-modified fibroblasts at a ratio of 1:3, seeded on multi-well plates and viral plaque formation was monitored. Reduced viral reconstitution was expected when the mutated form of the GoI was inhibitory for the wt protein (depicted as red wells), whereas non-inhibitory mutants would allow wt-like reconstitution (green wells).

This assay was developed similar to the complementation screen described above with the exception that the gene under study was still present in the acceptor BAC.

However, using a complete MCMV genome as acceptor BAC would not require Flp-mediated ectopic insertion of the shuttle plasmid to enable virus production. Consequently, the escape of non-recombined BACs from the inhibitory function encoded by the shuttle plasmid remained possible. To ensure that only recombinants could be reconstituted, an additional essential genetic marker was transferred to the shuttle plasmid that could not be complemented *in trans*. Such an essential *cis* element is provided by the packaging signals (*pac*). Each MCMV genome is terminally flanked by two *pac* sequences (schematically depicted in Figure 3.12). These are recognised by the viral terminase during the encapsidation process, which induces cleavage of the concatemeric viral DNA, resulting in a unit length genome that is finally packaged [105]. To ensure proper cleavage, the *pac* sequences have to be present in the genome, i.e. the plasmid providing them needs to be part of the genome.

To establish the ICFAR inhibitory screen, the terminal region spanning the two *pac* signals was removed from the MCMV BAC and cloned into a shuttle vector (Figure 3.26A). The shuttle plasmid further comprised two Gateway™ cloning-compatible DNA recombination sites (*att*R sites), which would allow to utilise this vector for the fast generation of a plasmid library. The inserted GoI was expressed under control of the promoter of the eukaryotic elongation factor 1α (EF-1α), which has been shown to be superior to the HCMV IE1 promoter in long-term application, since it is not silenced [171].

First it was investigated whether virus reconstitution was possible from *pac*-lacking genomes. To test this, MEF were transfected with two independent Δ*pac* BAC clones and the production of viral progeny monitored. In both cases no viral plaques were observed for six weeks, confirming that the *pac* sequences are crucial for virus formation. Next it was examined whether the *pac*-containing shuttle plasmid was able to complement the *pac* deletion in the MCMV genome. For this, Flpe-expressing cells were nucleofected with the Δ*pac* BAC and either an empty vector or the *pac*-harbouring rescue plasmid and viral plaques quantified at 6 dpt (Figure 3.26B). No viral plaques were detected after nucleofection with the Δ*pac* BAC and an empty vector. In contrast, complementation using the *pac*-containing shuttle plasmid resulted in robust plaque formation, ranging between 40 and 60 plaques per sample due to recombination.
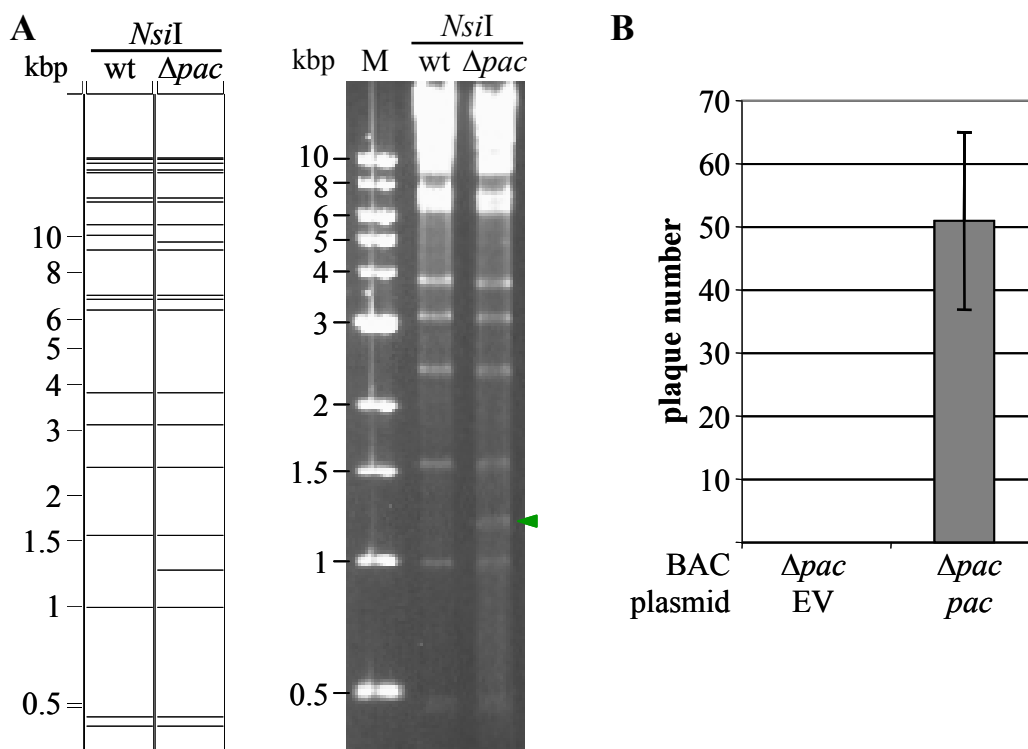
**Figure 3.26: Complementation of the *pac* deletion using the IFCAR system**

**(A)** Construction of an MCMV BAC lacking the terminal packaging signals (*pac*). Schematic (left column) and observed (right column) restriction fragment pattern of wt MCMV (wt) and the *pac* deletion BAC (Δ*pac*) using *Nsi*I. Digest of wt MCMV resulted, amongst others, in fragments of 1, 1.5, 2.4, 3.1 and 3.8 kbp. In contrast, digest of the Δ*pac* BAC gave rise to an additional fragment of 1.25 kbp (green arrowhead). Numbers on the left side indicate size of the DNA fragments. M, 1 kbp DNA ladder. **(B)** IFCAR complementation of the *pac* deletion. Flpe-expressing cells were nucleofected with the Δ*pac* BAC and a shuttle plasmid carrying the *pac* sequence and supplemented with NIH/3T3. Viral plaques were quantified at 6 dpt using phase contrast microscopy. Depicted are mean and standard deviation of two independent experiments. EV, empty vector.

Since it was shown that the *pac* signals were indeed crucial for viral reconstitution and that their deletion from the MCMV genome could be complemented using the ICFAR assay, the system had to be validated. Again the M53 mutant library was used as reference set. A couple of mutants known to be unable to complement the M53 deletion BAC [95], but harbouring the potential to inhibit the wt pM53 function upon their overexpression [130] were chosen and tested using the *pac*-based ICFAR assay (Figure 3.27).

As before, no virus was reconstituted upon nucleofection of the Δ*pac* BAC together with an empty vector (containing no *pac*). Between 30 and 60 IE1-positive plaques were observed upon expression of wt M53 from the shuttle plasmid in addition to the

endogenous M53. The mutants i115, i128 and i146 were non-functional, yet did not interfere with wt pM53 in a DN mechanism. According to these expectations, plaque numbers comparable to the wt control were detected for the i115 and i128 mutants. Unexpectedly, only about half as much plaques formed in the presence of i146. The mutants i207 and i220 were known to be partially inhibitory during viral replication, i.e. reconstitution was delayed. In the presence of either mutant less than half of the plaque numbers of the wt M53 control were observed, confirming the partial inhibitory potential of these proteins. Conversely, about 10 plaques could be detected in the presence of the i313 and s309 mutants. However, both proteins have a strong DN potential and were completely inhibitory for virus production when expressed in the wt genome context [130]. Consequently, no vial progeny was expected for these samples.

**A**

| mutant | i115 | i128 | i146 | i207 | i220 | i313 | s309 |
|---|---|---|---|---|---|---|---|
| **complementation of M53 deletion** | − | − | − | − | − | − | − |
| **inhibition of wt M53 function** | − | − | − | + | + | ++ | ++ |

**B**
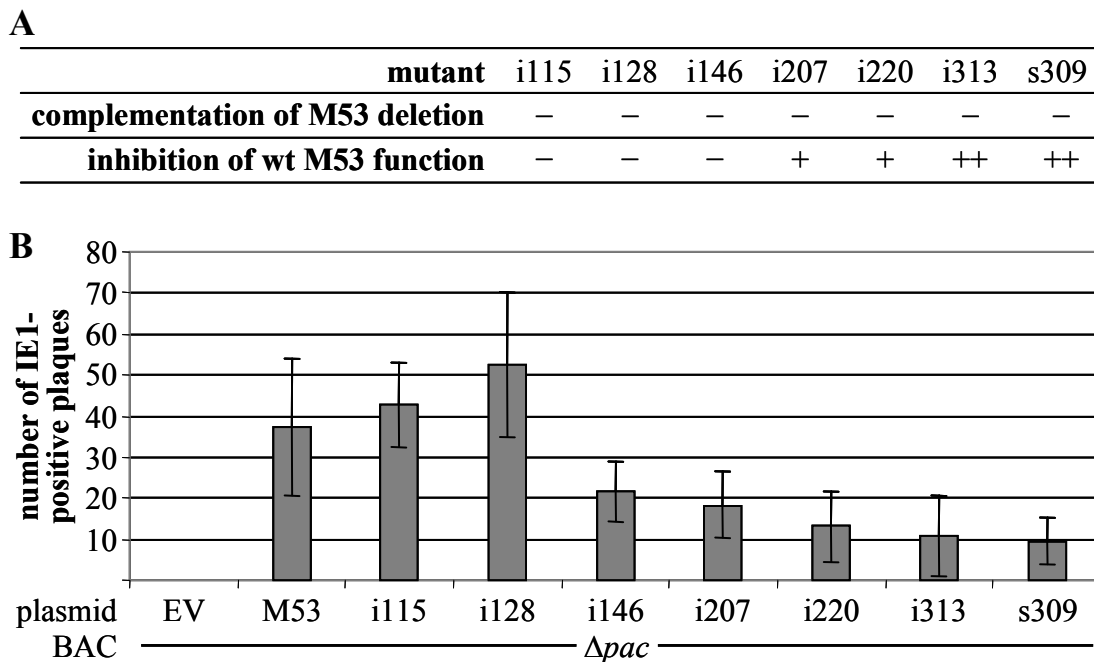


**Figure 3.27: Validation of the in-cell Flp-assisted inhibitory screen**

**(A)** Overview of selected M53 mutants generated by transposon mutagenesis with regard to their ability (+) or failure (−) to either complement an M53 deletion BAC (middle row) or to inhibit the function of the wt pM53 during viral replication [95, 130]. Double pluses indicate complete inhibition of wt pM53. **(B)** Flpe-expressing cells were nucleofected with the Δ*pac* BAC and the indicated shuttle plasmids and supplemented with NIH/3T3. Samples were fixed 6 dpt and stained with an antibody specific for the IE1 protein. Depicted are mean and standard deviation of triplicate samples of two independent experiments. EV, empty vector; i, insertion of five amino acids; s, stop mutation at this position.

To exclude that the DN mutant expression under control of the EF-1α promoter was too weak to provide sufficient protein amounts to inhibit virus production, the EF-1α promoter in the shuttle plasmid was replaced by the HCMV IE1 promoter and the assay repeated using wt M53 and the s309 mutant as examples. Yet again s309 failed to completely block reconstitution, resulting only in reduced plaque numbers between 17 and 37% of the wt M53 control (data not shown).

Taken together, the ICFAR inhibitory assay successfully made use of an essential genetic element that cannot be *trans*-complemented, thereby supporting the integration of the shuttle plasmid. Using the M53 mutant library as reference set, the results were not as clear as expected, as the known strong DN examples i313 and s309 did not completely prevent virus production. However, the plaque numbers quantified for all the inhibitory mutants were considerably less than half of the value of the wt M53 control. Thus, using a cut-off value of 50% of the control (or even less for the identification of strong DNs) should suffice to identify inhibitory mutants. Their proper DN potential has to be analysed subsequently in further assays based on conditional expression.

## 3.4 Application of the ICFAR complementation system to study pM99

To allow the rapid identification of non-complementing mutations, i.e. mutant genes with DN potential, again mutant libraries of the GoI are required. Since the *in vitro* transposon mutagenesis system used in previous studies [95, 97] was not available any more, and an alternative system based on the MuA transposase, obtained from Finnzymes (Thermo Fischer), did not yield the expected mutagenesis frequency (data not shown), novel strategies to generate mutant libraries were demanded. One possibility was exploited by the domain shuffling and deletion approach described above for the M53 gene. However, not all herpesviral proteins show such distinct homology peaks in the sequence alignment with their homologues. For those proteins, the generation of mutant libraries by gene synthesis could be an option. Such a synthetic library should contain a comprehensive set of mutants covering the complete ORF or

part of it. To validate the ICFAR complementation approach further, M99 was chosen for mutagenesis. The M99 ORF is small and information about functionally important motifs were published for its HCMV homologue pUL99 [67, 90, 156], making this gene attractive for a test run. Here it was tested whether M99 complementation is reliable in the new assay. This would also provide a further example for the applicability of the ICFAR system.

### 3.4.1 pM99 is essential for MCMV replication

At first it was tested whether M99, as its HCMV homologue pUL99, is an essential gene [21]. To this end, an M99 deletion BAC (ΔM99) was generated. The first 64 bp of the M99 ORF overlap with the 3'-end of the M98 ORF, consequently the M99 ORF could not be deleted completely. The non-overlapping part was replaced by an amp$^R$ cassette using homologous recombination. To further prevent expression of the pM99 N-terminus from the overlapping stretch, its start codon was modified from ATG to GTG, thereby removing the translational start signal. Since M99 is transcribed in a different reading frame than M98, this mutation did not change the aa sequence of pM98 (Figure 3.28).

To test the replicative capacity of MCMV in the absence of pM99, MEF were transfected with the ΔM99 BAC and plaque formation monitored. Whereas viruses were reconstituted from the wt MCMV BAC within few days, no viral progeny was detected originating from the ΔM99 BAC during six weeks, indicating that pM99 was critical for virus production. To confirm that the observed reconstitution defect was in fact due to the loss of pM99, a pM99 expression plasmid was inserted ectopically into the ΔM99 BAC by Flp/FRT-mediated recombination (ΔM99EPM99) and used to transfect MEF. In this case, viral plaques were detected within 5 dpt and complete cell lysis was reached within two weeks.
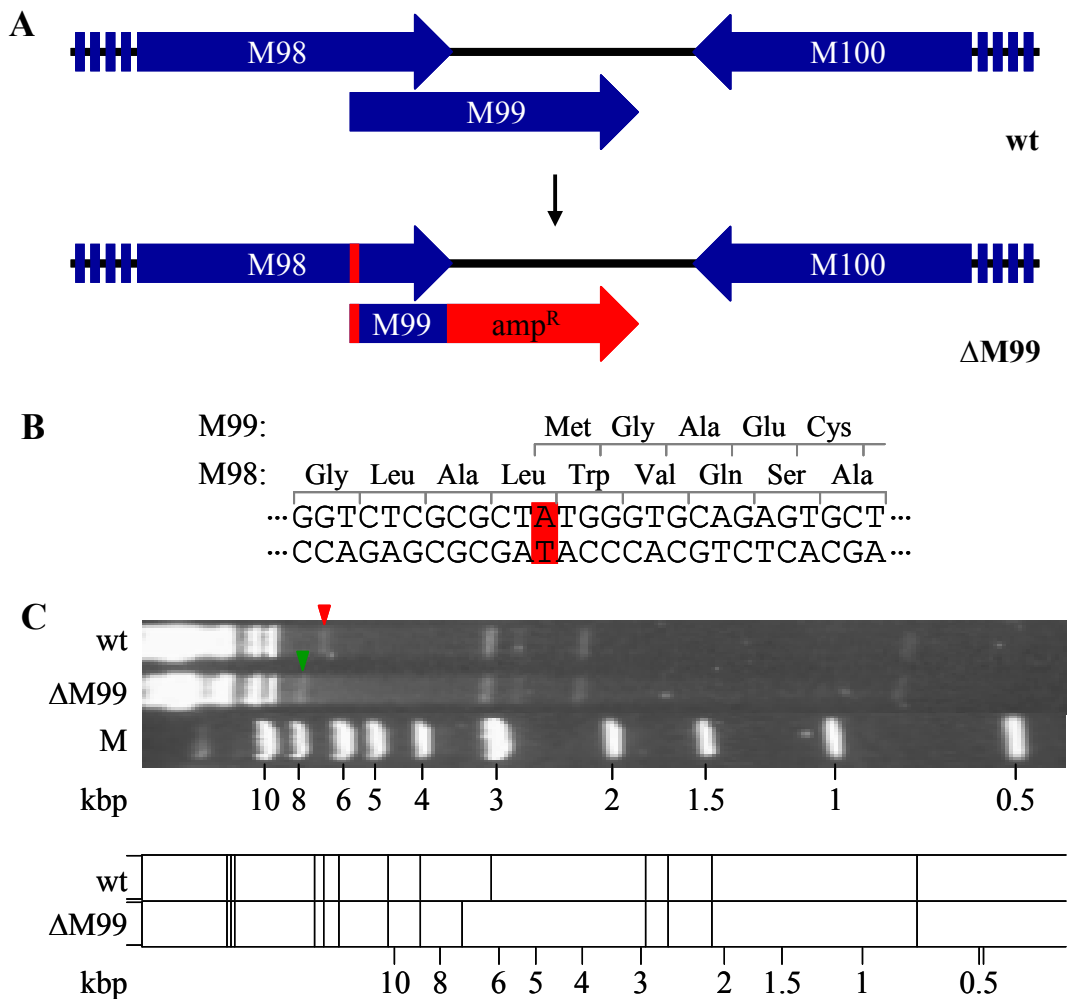
**Figure 3.28: Construction of an M99 deletion BAC**

**(A)** Schematic illustration of the M99 deletion BAC (ΔM99). The M99 ORF overlaps partially with the M98 ORF. The non-overlapping sequence was replaced by an amp[R] cassette using homologous recombination. Expression of the N-terminal part was prevented by exchanging the A in the start codon by a G (red box), which did not change the resulting aa sequence of pM98. **(B)** Wt nucleotide sequence of the M98/M99 overlap. The red box highlights the base pair that was changed. **(C)** Restriction fragment pattern of the wt MCMV and the ΔM99 BAC using *Sfi*I. The 6.2 kbp fragment of the wt genome spanning the M99 ORF (red arrowhead) was replaced by a 7.2 kbp fragment containing the amp[R] cassette (green arrowhead).

## 3.4.2 Flag-tagging of pM99 allows studies in the virus context

Since pM99 appeared to be essential for MCMV replication, it was tested whether Flag-tagging of its C-terminus was possible. Generally, it is preferable to generate a comprehensive mutant set using a tagged protein, as it allows studies on any mutant including those which carry insertions within the epitope for the recognition by the specific anti-serum. Therefore a rescue plasmid was constructed harbouring the

C-terminally tagged M99 ORF and inserted into the ΔM99 BAC (ΔM99EPM99F). MEF were transfected with this modified BAC and the production of viral progeny monitored. Viral plaques were observed within six days and complete lysis within two weeks, indicating that also the Flag-tagged pM99 (pM99F) was functional and successfully complemented the M99 deletion.

To further study whether pM99F can be used as a model of pM99 in biochemical and cell biological assays, the properties of pM99F had to be compared to wt pM99. To do so, pM99 specific antisera were generated by immunising rabbits with two different pM99 peptide epitopes. To test their reactivity and specificity for pM99, lysates of 293 cells transfected with a constitutive expression plasmid for pM99F and wt-infected M2-10B4 cells were subjected to Western blot analysis and probed for a specific pM99 signal using the sera of the different steps of the immunisation process (Figure 3.29). The calculated size of pM99 is 11.8 kDa, of the Flag-tagged protein 13.2 kDa. However, since its homologues are post-translationally myristoylated and palmitoylated [7, 150], its size was expected to be slightly larger. Anti-Flag specific staining of the transfected sample revealed a signal close to 17 kDa, which was in the expected range. A correlating signal was observed for the final (SAB), the large (GP) and the small bleed (PP) of rabbit 700, with the strongest signal for GP700. The pre-immune serum showed a weak reactivity. Endogenous pM99 was also detected in lysates from wt-infected cells using SAB700, GP700 and PP700. GP700 produced strongest pM99 signal, but additionally an unspecific band at ~38 kDa was detected. A specific pM99 signal was also detectable in transfected samples for PP701 and GP701, but only very weakly for SAB701. In contrast, this immune serum failed to recognise pM99 in lysates from wt-infected cells. Interestingly, the small bleed (GP) of both antisera had a higher reactivity than the final bleed.
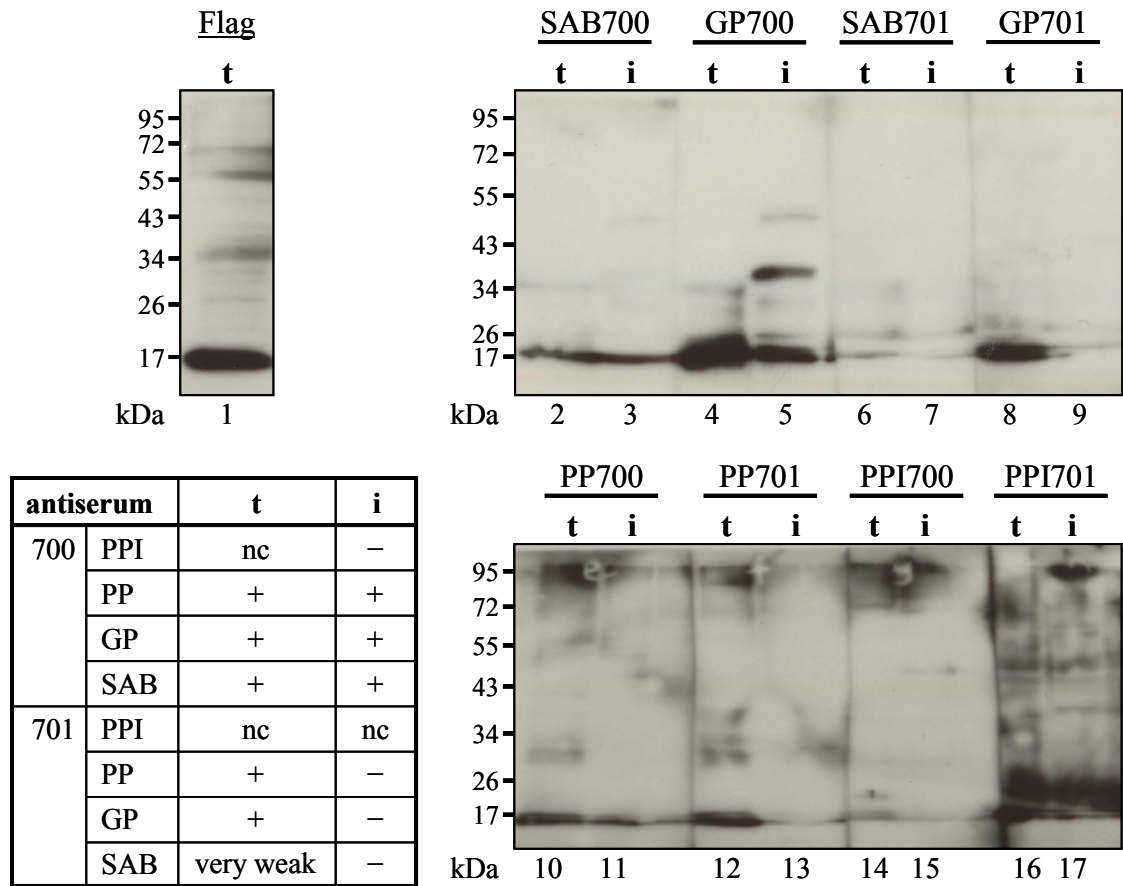
**Figure 3.29: Reactivity of pM99 specific antisera in Western blot**

293 cells transiently transfected with a plasmid expressing Flag-tagged pM99 (t) and M2-10B4 cells infected with wt MCMV (i) were lysed in TLB at 48 hpt/hpi and probed with polyclonal antisera (700, 701) against different pM99 epitopes. pM99 expression in transfected cells was also confirmed using a monoclonal antibody specific for Flag. The observations are summarised in the bottom left table. PPI, pre-immune serum; PP, small bleed; GP, large bleed; SAB, final bleed; nc, not conclusive.

Using the newly available pM99-specific antisera, the expression kinetics of pM99 was investigated using M2-10B4 cells infected with wt MCMV at an MOI of 1 in the absence and presence of phosphonoacetic acid (PAA). PAA specifically prevents the expression of genes that are dependent on active genome replication (true late genes) by inhibiting the viral polymerase [62]. A clear signal for pM99 was detected at 18 hpi and accumulated further until 24 hpi in the absence of PAA, whereas treatment with PAA completely abolished pM99 expression (Figure 3.30). The same pattern was observed for pM53, which is also a known late gene product [95], while expression of the IE protein pp89 was not blocked. Accordingly, pM99 was expressed with late kinetics, similar to the HCMV homologue pUL99 [70].
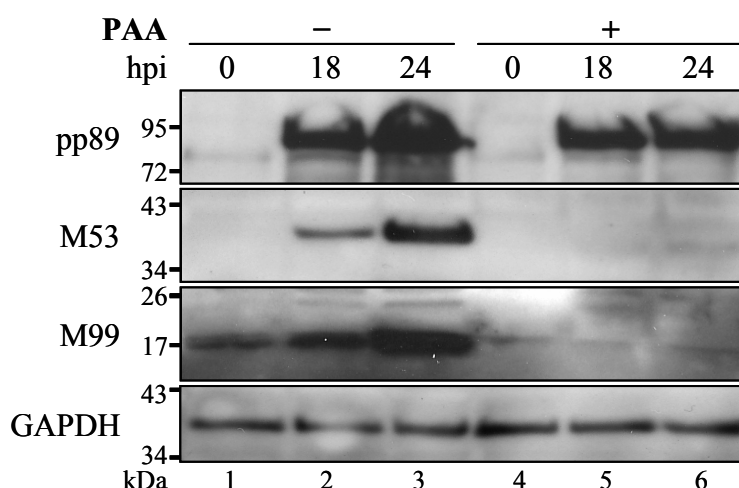
**Figure 3.30: MCMV pM99 is expressed with late kinetics**

M2-10B4 cells were infected with wt MCMV at an MOI of 1 and cultured in the absence (−) and presence (+) of 300 µg/mL PAA. Cell lysates were prepared at indicated time points, separated by SDS-PAGE and probed for pp89, pM53, pM99 and GAPDH by Western blotting with specific immune sera.

In addition to their specificity in Western blotting, the antisera reactivity was tested in immunofluorescence samples. U2-OS cells transfected with a plasmid expressing pM99F were stained with GP700 and GP701, as those gave the strongest signals in the Western blot analysis, as well as anti-Flag antibody. Analysis of the subcellular distribution of pM99 specific signals by confocal immunofluorescence microscopy revealed juxtanuclear punctuate stainings localised predominantly in a limited area. These signals co-localised well with the signal obtained by the anti-Flag staining, indicating that the pM99 antisera indeed detected pM99 *in situ* in transfected cells (data not shown). The same pattern was observed in U2-OS cells transiently expressing pM99F together with HA-tagged pM94 (pHAM94) (Figure 3.31A and B), which is a known interaction partner of pM99 [97]. pM99F and pHAM94 co-localised completely at the juxtanuclear compartment, presumably the endoplasmic reticulum-Golgi intermediate compartment (ERGIC), as was reported previously for their homologues [90, 150], thus confirming this interaction *in situ* in MCMV.

In wt-infected M2-10B4 cells, pM99-specific signals were also detected adjacent to the nucleus (Figure 3.31C), which possibly reflects its localisation within the viral assembly complex, where cytoplasmic maturation of viral particles takes place [149, 155]. A similar juxtanuclear pattern was observed for pM99F and its binding partner

pM94 in M2-10B4 cells infected with a virus expressing Flag-tagged pM99 (MCMV-ΔM99EPM99F) (Figure 3.31D), confirming the presence of both pM99 and pM94 at the assembly complex.
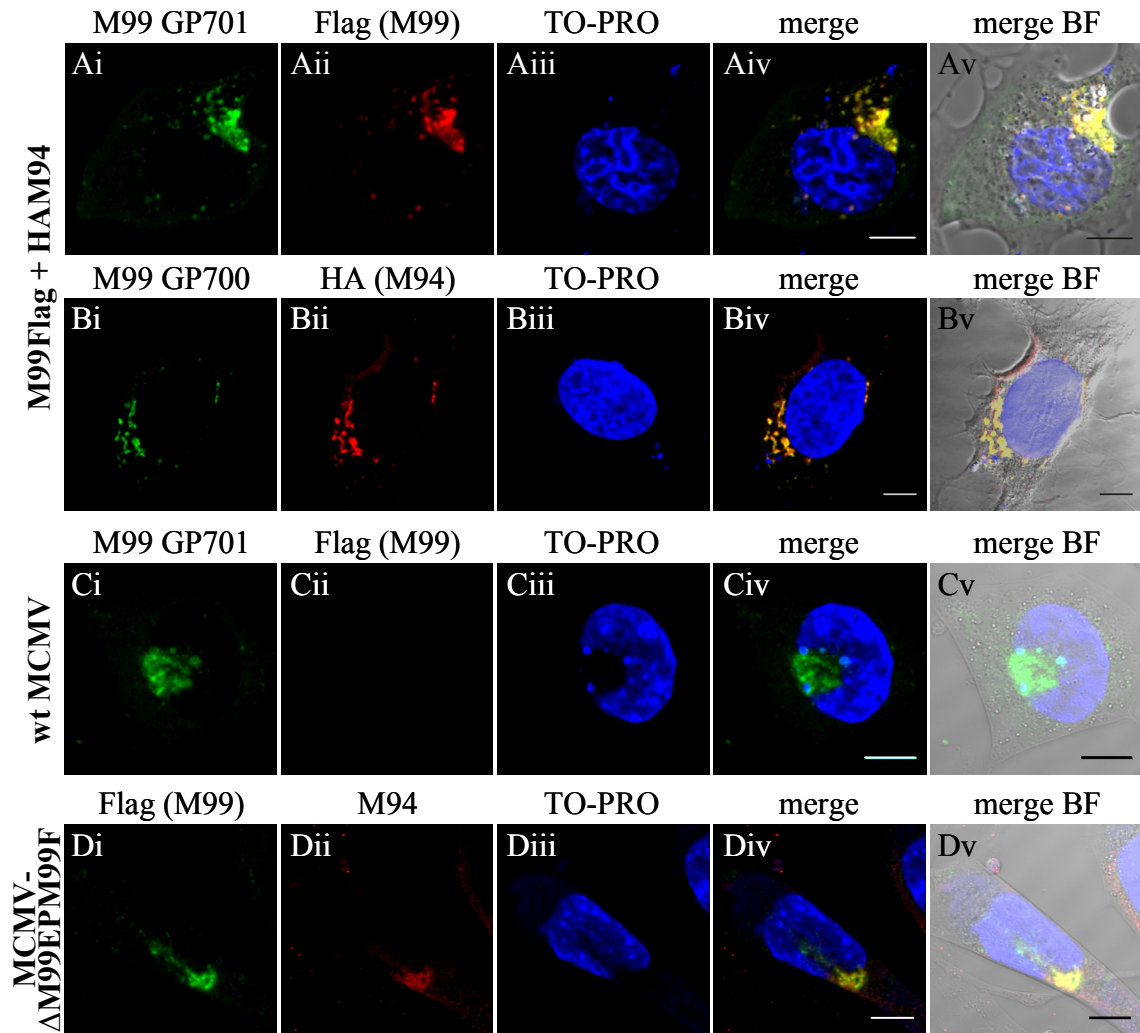


**Figure 3.31: Intracellular localisation of pM99**

U2-OS cells were transiently transfected with plasmids expressing Flag-tagged pM99 and HA-tagged pM94 (A, B), and M2-10B4 cells were infected with indicated viruses (C, D). Cells were fixed at 36 hpt/hpi and probed with polyclonal antisera against pM99 (GP700, GP701) and monoclonal antibodies specific for Flag and HA, followed by Alexa-conjugated secondary antibodies. DNA was visualised using TO-PRO 3. Scale bar, 10 μm. BF, brightfield.

### 3.4.3 ICFAR complementation of the M99 deletion

Since pM99 was essential for MCMV and ectopic insertion by the traditional Flp/FRT technique restored viral growth, it was tested whether the ICFAR

complementation system was applicable to complement the ΔM99 BAC with wt M99. To monitor successful nucleofection and protein expression, expression of pM99 was linked via an internal ribosomal entry site (IRES) to the expression of GFP.
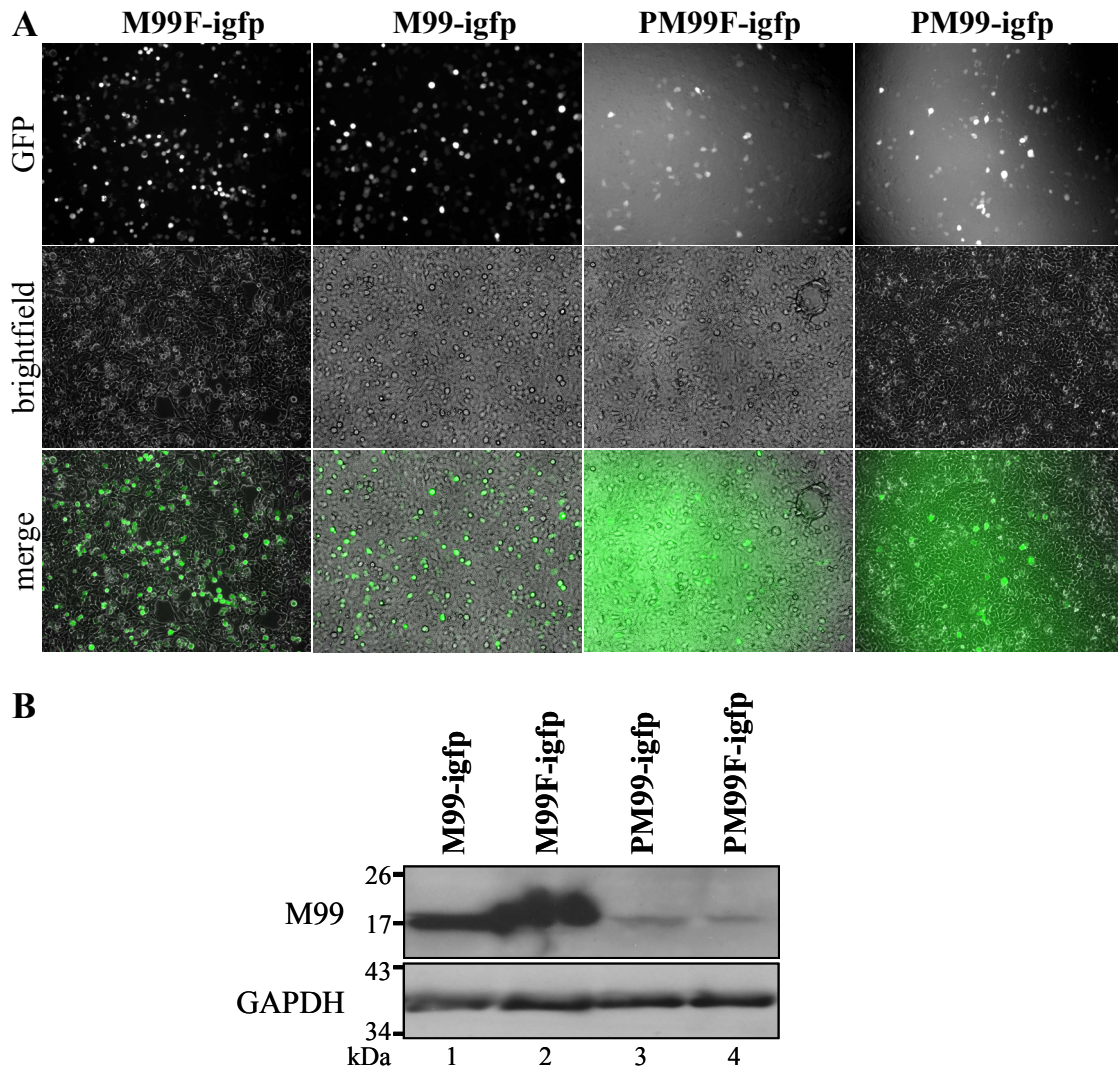


**Figure 3.32: pM99 expression under control of different promoters**

293 cells were transiently transfected with plasmids constitutively expressing the indicated M99-IRES-GFP constructs. pM99 expression in the first two columns was driven by the HCMV IE1 promoter, in the third and fourth column by the endogenous M99 promoter. F, Flag; i, IRES; P, M99 promoter. **(A)** Fluorescent signals emitted by GFP at 48 hpt. **(B)** Cell lysates were analysed by Western blotting and probed for pM99 and GAPDH.

At first it was examined whether pM99 expression rates varied significantly using different promoters. Thus, 293 cells were transiently transfected using plasmids expressing Flag-tagged or untagged pM99 either under control of the HCMV IE1 promoter ($P_{CMV}$) or under control of the endogenous M99 promoter ($P_{M99}$) as well as

GFP in an IRES-induced manner. Fluorescence microscopy revealed that the GFP signal obtained induced by the M99 promoter was strongly reduced as compared to the $P_{CMV}$-induced GFP signal (Figure 3.32A). Assuming that IRES-induced expression is directly dependent on promoter-driven expression, the GFP signal indicated that substantially less pM99 was produced under control of $P_{M99}$ than compared to the HCMV IE1 promoter. This assumption was further confirmed by Western blot analysis probing for pM99 (Figure 3.32B).

Since it was not known whether the amount of pM99 required for viral reconstitution was restricted or whether strong pM99 overexpression would be detrimental for virus production, the $P_{CMV}$ and the $P_{M99}$-driven constructs were tested in the ICFAR complementation assay. To facilitate automated quantification using fluorescent signals, the M99 ORF was deleted as described in Figure 3.28 from an MCMV BAC, in which mCherry expression was coupled by an IRES to the endogenous expression of the smallest capsid protein (SCP), giving rise to SCPiChe-ΔM99. This structural protein is expressed with late kinetics (unpublished observations), therefore an mCherry signal would imply active replication of the viral genome. Flpe-expressing cells were nucleofected with the SCPiChe-ΔM99 BAC together with one of the M99-expressing plasmids and viral plaque formation quantified at 6 dpt.

Whereas no viral progeny was observed upon nucleofection of SCPiChe-ΔM99 together with an empty shuttle vector, co-transfection with each of the M99-expressing constructs resulted in virus reconstitution (Figure 3.33). In comparison, complementation with pM99 expressed under control of $P_{CMV}$, i.e. in high amounts, was less efficient. Only few plaques were detected upon $P_{CMV}$-regulated pM99 and pM99F expression, indicating that excess pM99 obstructed virus production. In contrast, $P_{M99}$-driven expression of pM99 restored viral reconstitution more efficiently, yielding much higher plaque numbers.
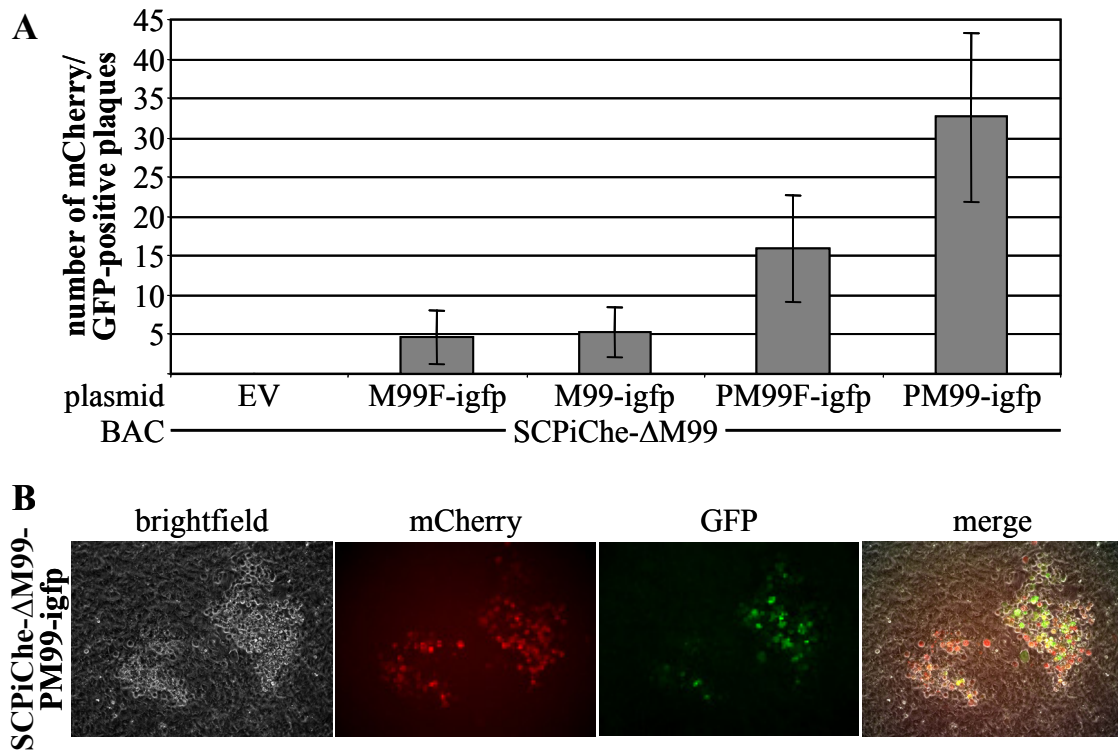
**Figure 3.33: ICFAR complementation of the M99 deletion**

Flpe-expressing murine fibroblasts were nucleofected with the SCPiChe-ΔM99 BAC and the indicated shuttle plasmids. Cells were fixed at 6 dpt and **(A)** viral plaques quantified using fluorescence microscopy. Depicted are mean and standard deviation of two SCPiChe-ΔM99 BAC clones in two separate experiments. **(B)** Plaque appearance exemplified for the complementation with PM99-igfp. F, Flag-tag; i, internal ribosomal entry site; P, M99 promoter.

Both fluorescence signals (mCherry from the BAC, GFP from the plasmid) were detected in all viral plaques examined. Since complementation with $P_{CMV}$-driven pM99 expression yielded only few plaques, most of the analysed plaques originated from $P_{M99}$-regulated pM99 complementation. In these plaques the mCherry signal appeared to dominate (Figure 3.33B). This, however, might be explained with the relatively low GFP expression under control of $P_{M99}$.

Taken together, this analysis successfully established the complementation of the M99 deletion, providing insights into the construction and investigation of potential pM99 mutants, namely to preferentially use constructs expressed under control of the M99 promoter.

### 3.4.4 Application of the ICFAR system to test M99 mutants

Since a comprehensive mutant library covering the M99 ORF is not yet available, a couple of mutants were generated based on the information available for the HCMV pUL99 protein. Alignment of 34 representative pUL11 homologues revealed just one homology peak, designated CR1, although the maximum similarity was quite low (Figure 3.34A). In HCMV pUL99 this region contains the pUL94 binding motif [90]. Furthermore, the N-terminal glycine was shown to be myristoylated and aa 44-57 comprise an acidic cluster (AC). Both features are required for correct localisation of the protein and viral growth, whereas the C-terminal part is dispensable [67]. Corresponding to this, pM99 mutants were generated lacking the first glycine ($\Delta$Gly2), the potential pM94 binding domain ($\Delta$M94) or the acidic cluster ($\Delta$AC) (Figure 3.34B). The expression of all mutants was regulated by $P_{M99}$.

Nucleofection of Flpe-expressing cells with the SCPiChe-$\Delta$M99 BAC together with one of the mutant M99-expressing plasmids repeatedly did not result in the formation of any viral progeny, whereas reconstitution was observed in the control reaction using the wt M99-expressing vector (Figure 3.34C). This indicated that also in MCMV pM99 each of the three deleted features is crucial for the protein functionality. If any of those mutants was inhibitory for MCMV replication would need further testing applying the ICFAR inhibitory assay.
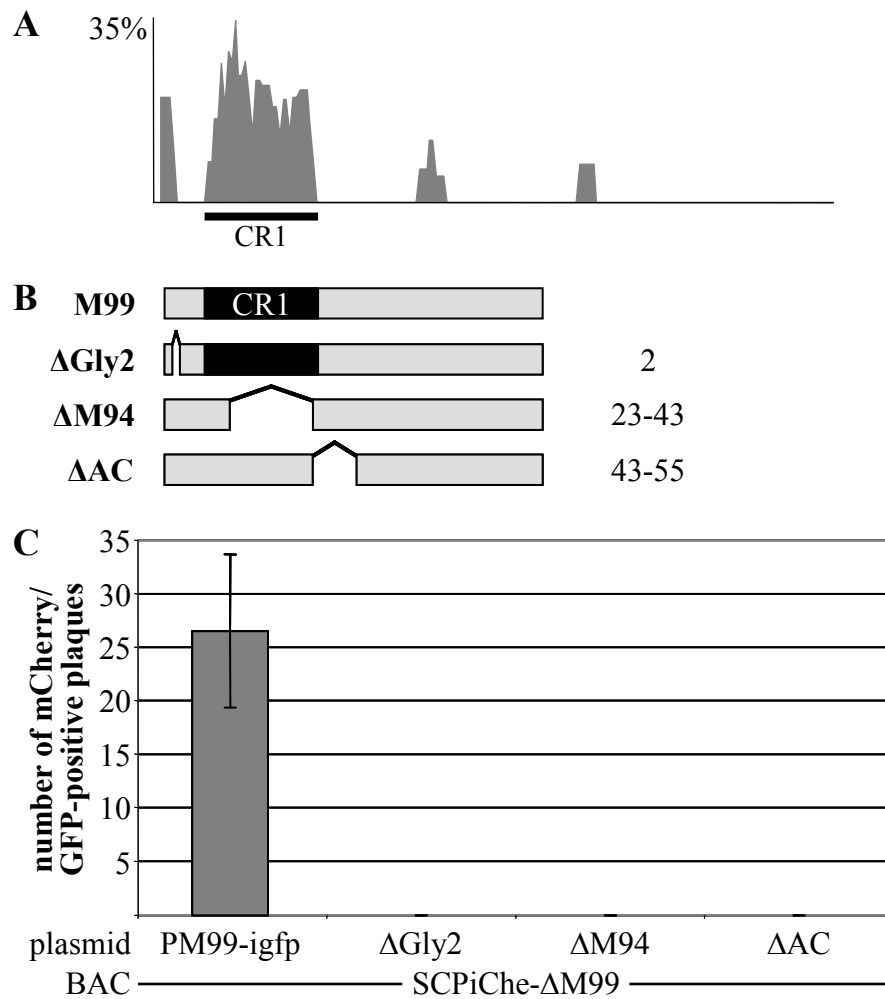
**Figure 3.34: Construction and ICFAR complementation of pM99 mutants**

**(A)** The amino acid sequences of 34 pUL11 homologues (accession numbers are listed in the Supplement, Table 6.2) were aligned using the Vector NTI AlignX program (Invitrogen) via the BLOSUM 62 similarity matrix. The similarity plot was calculated using a 5 aa window size, with scores for weak and strong similarity and identity of 0.2, 0.5, and 1.0, respectively. The *x* axis represents the number of amino acids in the consensus sequence. The conserved region (CR) is indicated below the diagram. **(B)** Schematic overview of the pM99 mutants. Proteins are depicted as grey bars, the conserved region is indicated as black box (aa 12-43 in pM99). Deletion mutants are shown with bridged spacing. Numbers on the right indicate the amino acids of pM99 affected by the mutation. CR, conserved region. **(C)** Flpe-expressing cells were nucleofected with the indicated BAC and plasmids and plaque formation quantified at 6 dpt. Mutants are based on the PM99-igfp plasmid.

# 4 DISCUSSION

Each of the eight existing human herpesviruses is capable of provoking severe or even fatal disease in individuals having an immature or impaired immune system. Herpesvirus disease is almost exclusively controlled by antiviral therapy targeting the replication of the viral DNA [reviewed in 33]. However, novel antiviral strategies exploit the manipulation of protein-protein interactions to suppress viral replication [reviewed in 94]. Targets of this approach are proteins that act in essential complexes. One new possibility to disrupt such viral protein networks and thereby control virus replication is the application of peptides or other small molecules, as shown recently for the NEC of HCMV [153, 180]. Another option is provided by the utilisation of dominant negative mutants. Dominant negative mutants are derived from multi-functional wt proteins that require protein-protein interaction(s) to fulfil at least one of their essential functions. In the DN mutant, a downstream function is inactivated. If the mutant is competitive to the wt allele of the targeted protein-protein interaction, it will enter into the physiological pathway and block it by either not executing its downstream activity or by preventing binding of other downstream targets [58].

## 4.1 Identification of DN mutants

In diploid eukaryotic organisms, gene products can exist in two different versions, as most of them are encoded by two alleles. Cellular DNs are mutants of one allele that inhibit the function of the second, intact protein. In herpesvirus genomes, usually just one allele codes for most of the genes including all core genes, therefore DNs have to be provided either *in cis* by an additional expression cassette or *in trans* by the host cell.

Classically, the function of an unknown gene is investigated by gene knockout. DN proteins possess several advantages that make their application superior to simple gene deletion. One major advantage is that by inactivating the wt protein by a DN the deletion phenotype is accessible in the presence of the wt allele, while *trans-*

complementation of the target gene is not required. In addition, proteins often execute multiple functions in dynamic processes such as varying localisations and/or interaction with different partners. Deletion of such a gene product only reveals its most prominent (usually its most upstream) role, which may actually be a combination of several functions. In contrast, exchanging one domain by an inhibitory one can interfere with just one function and leave the others intact. Thereby different DNs are capable of arresting pathways or complexes at various steps, which is their second big advantage and cannot be achieved by any deletion.

### 4.1.1 Classical approach to identify DNs

Although DN proteins are such valuable tools to dissect cellular as well as viral protein functions, they are not isolated easily. Many cellular DN mutations, such as inhibitory p53 variants in cancer cell lines, were identified by analysing the genotypes of certain diseases [16, 158]. Most of the viral DNs were either generated at random or found by chance. For example, GFP-tagging of the HCMV SCP in order to monitor virus entry by means of fluorescently labelled capsids failed with regard to the original purpose, but gave rise to strong DN proteins [18].

Unfortunately, comprehensive information on structural and functional domains, which would allow a rational design of DN mutants, is at present not available for most of the herpesviral gene products. Proteins of interest have therefore been modified using random mutagenesis techniques. Methods of choice for this are either alanine-scanning [38] or the linker-scanning transposon (Tn) mutagenesis [13, 57]. While in the alanine-scanning single (or multiple) amino acids (aa) are substituted by alanine (or a stretch of alanines), the Tn mutagenesis introduces short additional aa insertions and, depending on the system, even C-terminal truncations.

The second approach has been successfully applied to identify critical regions of cellular and viral gene products [34, 80, 172] or even essential genes [182]. Our group used it to study and isolate DN mutants of the MCMV proteins pM50, pM53 and pM94 [95, 97, 130, 141]. The generation of such mutant libraries is aided by commercially available products and delivers fast results with a good coverage of the ORF. The limiting step, however, is the subsequent analysis and evaluation of the obtained mutants. For example, for a protein of 300 aa, with a coverage of one mutation at every fifth aa, 60 mutants have to be analysed. Using the traditional screening method for

MCMV with bacterial flip-in [22], BAC isolation and transfection, this consumes a lot of time and resources, especially as most likely many of the mutants will be viable, i.e. complement the deletion of the wt gene. To reduce the workload and to quicken the outcome, one could imagine two possibilities. The first could be to decrease the number of mutants to be analysed by identifying important regions of the protein by targeted mutagenesis. These smaller regions can then be subjected to a random mutagenesis to obtain more subtle mutations. The second approach would be the establishment of a laboriously less demanding screening system to test the candidates faster. In this work both alternatives were tested and evaluated regarding their usefulness to generate or improve DN mutants affecting MCMV morphogenesis.

### 4.1.2 DN isolation by targeted mutagenesis

Random screens for DN mutants are time-consuming and labour-intensive. Thus, it was of interest to investigate whether DNs can be constructed on a predictive basis. Usually DN mutants are designed with reference to detailed information about structure-function relationships. However, this knowledge is limited to only few proteins. That rational design of inhibitory mutants can principally work was shown by a genome-wide, systematic screen to identify DN mutants affecting poliovirus. Mutants were tested that resembled previously identified lethal mutations or were predicted by a computer algorithm to be protein destabilising. Several DN mutations were isolated in this study [37]. For herpesviruses, however, there is only sequence information from related viruses to provide a very rough basis for mutant design. Initial clues suggesting that such a sequence-based approach may work, however, could be deduced analysing the data gained by the random screen for DN mutants of the MCMV protein pM53. Analysis of about 100 random mutants indicated the accumulation of potential DNs within two conserved regions (CRs) of the protein, namely CR2 and CR4, which were classified according to the degree of amino acid homology to other members of the pUL31 family [95, 130]. Notably, these regions, however, did not appear to complement pM53 functions if they were derived from a pUL31 homologue belonging to a more distant herpesvirus sub-family [152]. Thus, it was concluded that these domains should code for a binding independent function which may be sub-family specific.

Accordingly, a set of MCMV M53 mutants was constructed in this study in which the above described CRs of pM53 were disrupted by targeted mutagenesis, either by domain shuffling or by domain deletion. Conditional expression of these mutants in a viral context revealed their inhibitory potential. On the whole, the data observed for the designed mutants correlated well with the results of the earlier random screen, indicating that an approach based on sequence comparison can indeed be used to construct inhibitory mutants. Targeting CR2 gave even rise to improved DN effects. These mutants blocked virus production by up to four orders of magnitude, an effect that was about 100-fold stronger than that observed with the insertion mutants generated in the random screen. In addition, shuffling of CR4 also produced the DN mutant expected from the data obtained from the random screen.

Summarising, the M53 data accumulated during this study led to the assumption that it appears possible to design mutants with inhibitory phenotype on an exclusively prediction-based approach, although they might possess less inhibitory capacity compared to the mutants derived from a random mutagenesis. Nevertheless, one cannot conclude a general rule to predict the strength of a DN. If domain replacement leads to the identification of weak DNs, they could be improved by additional subtle mutations within the identified region.

Exchanging conserved regions of related virus subfamilies may always provide functional integrity to some extent, particularly if amino acids critical for enzymatic activity or binding of functional partners are maintained. Thus, the more distantly related the viruses are, which the genetic elements are derived from, the higher the chance to shuffle domains with non-complementing character. Therefore, replacing each conserved domain one by one with the respective domains of the most distant homologue seems to be the best approach to identify regions with inhibitory potential. The alternative to this would be directed deletions of the predicted CRs based on protein alignments. This study confirmed the feasibility of both methodologies.

Even if the mutants constructed by domain shuffling are not as inhibitory as DN mutants with subtle mutations, a great benefit of this approach is that the workload is minimised. Particularly for large ORFs, this issue is of high interest. Since verified sequence information from more than 30 homologues of all herpesvirus core genes are available, we believe that a genome wide screen targeting small conserved regions is

feasible and would probably provide DNs of multiple genes with the workload comparable to that needed to screen one gene with the random approach used so far.

## 4.2 Characterisation of pM53 mutants

UL31 family members are essential multifunctional elements of the herpesvirus life cycle. As described in this study, specific targeting of pM53 CR2 resulted in mutant proteins that blocked viral replication up to 10,000-fold. This stronger inhibitory effect enabled for the first time a more detailed investigation of the role of pM53 in general and its CR2 in particular.

The prominent role of the pUL31 homologues is the formation of the NEC along with pUL34 homologues, and this NEC mediates capsid transport through the nuclear envelope [15, 26, 46, 49, 50, 71, 75, 83, 85, 95, 116, 134, 135, 140, 162, 163]. However, an increasing number of studies have identified additional functions for pUL31 including effects on genome cleavage, capsid targeting to the INM and induction of membrane curvature [130, 138, 184]. Here, M53 alleles lacking CR2 were constructed to further study the putative roles of pM53 during MCMV replication. It was observed that not only CR4- [130] but also CR2-deficient pM53 significantly reduced the number of viral unit length genomes and blocked capsid export from the nucleus. Furthermore, the binding capacity of the CR2 mutant for pM50 was impaired. Nevertheless, the mutant still induced re-localisation of the NEC in infected cells. This strongly indicates that mutations within this region of the protein interfere with the formation of homotypic interactions between NEC subunits, as discussed for HSV-1 [138].

### 4.2.1 Role of pM53 in nuclear maturation

The first UL31 deletion mutants of HSV-1 revealed a defect in viral DNA packaging [29], which was later also confirmed for alpha-, beta- and gamma-herpesviruses [52, 71, 82, 130]. In Epstein-Barr virus (EBV), deletion of the UL31 homologue, BFLF2, results in the accumulation of DNA-lacking A and B capsids, together with a defect in intranuclear distribution, although the defective particles were still exported [52]. This study confirms previous findings in the MCMV system, i.e. that pM53 (the beta-herpesvirus homologue of pUL31) is involved in the DNA cleavage/packaging process.

About 91% of the nuclear capsids in MCMV-SVT-Δ2-infected cells lacked DNA, and there was a marked reduction in the number of unit length genomes. This effect alone does not explain the strong inhibitory effect, but it points out that the NEC is involved in genome cleavage/packaging. Therefore, it is possible that nuclear egress is monitored by a quality control mechanism that preferentially selects mature DNA-filled capsids for primary envelopment rather than DNA-lacking immature forms [25, 53]. Recently, capsid maturation in alpha-herpesviruses was suggested to be linked to nuclear egress by association of pUL31 with viral capsids. While in HSV-1 this interaction depended on pUL25 [184], a constituent of the C-capsid specific complex (CCSC) consisting of pUL17 and pUL25, these were not required for pUL31-capsid interaction in PrV [87]. Capsid-bound pUL31 was observed using a pUL34 deficient PrV, which stabilised the normally transient pUL31-capsid intermediate. Despite its enrichment on C capsids, pUL31 was also detected on A and B capsids, even though the terminase subunits as well as the portal protein were not required for this interaction [87 and unpublished observations]. In a yeast two-hybrid screen in VZV, the pUL31 homologue interacted with several other proteins [175]. Therefore, capsid binding of pUL31 is likely mediated by at least one so far unknown protein-protein interaction. Although the majority of pM53 protein signal was detected at the nuclear envelope using immunofluorescence microscopy, the pUL31 capsid association shows that a fraction of it is present close to the replication centres, thereby supporting viral maturation. An enzymatic function for pUL31 has not been reported yet, indicating that this protein possibly stabilises other protein complexes which then efficiently execute viral DNA cleavage and packaging. Notably, overexpression of pM53Δ2 rapidly saturates its binding sites on pM50 at the nuclear rim, leading to a higher number of free proteins in the nucleosol, ready to attach to capsids. There the surplus might interfere with DNA cleavage either by blocking terminase activity or by de-stabilising a yet uncharacterised maturation complex.

## 4.2.2 Role of pM53 in capsid targeting to the INM

Mature, DNA-filled capsids need to be transported to the nuclear periphery, where they transit through the nuclear envelope. Docking of mature capsids at the INM was abrogated in an HSV-1 UL34 mutant [138], suggesting a role for pUL34 in docking selectivity. In addition, capsids docked to the INM were observed very rarely during DN mutant expression in MCMV-SVT-Δ2-infected cells. This could be a consequence

of impaired capsid maturation associated with reduced genome cleavage. Yet, it could also reflect a defect associated with capsid transport to the egress sites. The first scenario would agree with previous observations showing inefficient primary envelopment of viral mutants, which failed to complete the DNA packaging process [2, 29, 32, 53, 103, 129]. The second explanation is supported by the EM data from the present study, where mature C capsids present in MCMV-SVT-Δ2-infected nuclei were not observed at the INM, but mainly remained associated in capsid clusters formed within the nucleoplasm, arguing for a transport defect caused by the CR2 mutant.

It is believed that capsid-bound pUL31 guides mature DNA-filled capsids to INM-bound pUL34 or pUL34/pUL31 complexes [66]. In this study, capsid-bound pM53Δ2 bound poorly to pM50, and there was no homotypic binding to wt pM53, which might account for the migration/targeting defect of the capsids. We therefore propose that the capsid clusters observed in cells infected with the CR2 deletion mutant in fact represent the DNA packaging sites. These sites cannot be detected by EM in the highly dynamic wt situation, because mature capsids are rapidly transported to the INM. Only the blockade of capsid migration by pM53Δ2 makes this process visible.

### 4.2.3 Role of pM53 in nuclear egress

Strong expression of the CR2 deletion mutant changed the distribution of the NEC and led to the formation of aggregates at the nuclear membrane. It was observed previously that pUL31 homologues are destabilised if they fail to bind to pUL34 homologues [130, 185]. It was proposed that the DN function of pM53 mutants was due to displacement of wt pM53 from the NEC, which renders the wt protein prone to degradation. Yet, overexpression of pM53Δ2 did not destabilise wt pM50. This effect is quite different from the effect of the s309 CR4 mutant, which led to the degradation and loss of both wt NEC proteins [130]. However, the CR2 mutant had no selective effect on the stability of either wt pM53 or wt pM50. This is in line with the reduced binding capacity of pM53Δ2 for pM50. Thus, the DN effect cannot be explained by competition between the mutant and the wt protein for incorporation into the NEC. This suggests that another, as yet unknown protein-protein interaction (mediated by pM53) is required for correct NEC formation at the nuclear rim. It might also explain why s309 has higher DN potential, since both wt pM50 and wt pM53 are degraded in cells infected with s309-expressing viruses.

Studies on a charged cluster DN mutant of HSV-1 pUL34, the homologue of pM50, implicated this protein, together with CR3 of pUL31, in the induction of INM curvature [138]. Notably, no CR3-derived pM53 mutant with inhibitory potential was retrieved from the insertion library [130] or by using the domain shuffling approach. However, despite the lack of functional significance, a reduced binding capacity of the CR2 and CR3 mutants for pM50 was observed, which confirms the data obtained for the HSV-1 homologues. Incidentally, Roller and colleagues discussed a multi-level interaction within the NEC proteins [138]. Although the major binding motif in the MCMV NEC is clearly located in CR1, the present analysis now reveals that the pM53 CR2 region also contributes to the binding of pM50.

Finally, nuclear membrane dynamics contribute substantially to primary envelopment of herpesviruses. When nuclear egress of the capsids was blocked, membrane stacks were formed in MCMV-SVT-Δ2-infected nuclei, as observed with other DN mutants of MCMV NEC proteins [141]. These membrane aberrations were probably derived from the INM, but we did not observe vesicles similar to those monitored in the HSV-1 pUL34 CL13 mutant [139]. Haugo and colleagues observed nuclear envelope blebbing, along with an electron dense layer, upon infection with mutant UL34 HSV-1, which protruded into the cytoplasm [56]. The membrane phenotypes induced by different viruses and mutants in different cell types are remarkably distinct. Yet, they point to the same fact, namely that the NEC alters the membrane dynamics of the nuclear envelope.

Another striking feature of the pM53 DN was the apparent failure to form a cytoplasmic assembly complex. Due to the block in nuclear maturation, hardly any cytoplasmic capsids were observed in MCMV-SVT-Δ2-infected cells. Coincidently, the typical ring-shaped vesicle accumulations derived from the Golgi and TGN compartment, which have been described studying HCMV infected cells [42], could not be detected in MCMV-infected cells expressing the pM53 DN, whereas in cells infected with mutant HCMV or MCMV viruses lacking one of the two SEC proteins, which are blocked in cytoplasmic maturation, a defined assembly site was still observed [97, 161]. This may indicate that the presence of a critical number of cytosolic capsids is required to induce the formation of the viral assembly complex. Alternatively, by vesicle formation and fusion with the outer nuclear membrane the NEC proteins are translocated to the cytoplasm during wt infection. Thus, it is also possible that the NEC,

in addition, executes a further downstream function in the cytoplasm, which is required for the initiation of the assembly complex.

Until recently, the nuclear export pathway exploited by herpesviruses had been thought to be unique to them. However, Speese and colleagues, during their investigation of the *Drosophila* synaptic development, found ribonucleoprotein particles (RNPs) that complexed with lamin C and the C-terminal end of a cellular signalling receptor, DFz2C, which is transported from the plasma membrane to the nucleus. These large granules do not undergo conformational adaptations to fit the nuclear pore complex export machinery as reported for other RNPs [40]. Instead, they also enter the cytoplasm by a mechanism of transition through the nuclear envelope accompanied by envelopment and de-envelopment [168] akin to that described for herpesviruses. Both exit strategies share the disassembly of the lamina underlying the nuclear membrane, which is disrupted by multiple phosphorylation events. In herpesvirus infection, viral and cellular kinases are recruited to the INM to dissolve the lamin layer [15, 27, 73, 115, 118, 123, 136, 144]. The NEC proteins pUL31 and pUL34 are thought to induce membrane curvature, thereby facilitating vesicle formation [71]. Speese *et al.* demonstrated that a cellular kinase, atypical PKC, is required for lamina remodelling and formation of DFz2C granule containing invaginations of the INM [168]. Based on their observations, Speese *et al.* propose that herpesviruses not only hijacked the lamina disassembly pathway operationally during nuclear export, but a complete nuclear exit mechanism used by endogenous RNPs. The data presented here, however, point towards a more general role of the NEC in herpesvirus morphogenesis. Clearly processes other than the nuclear egress were inhibited by the DN mutants of pM53. For the first time a mutant of an NEC protein was described to induce inhibition of DNA synthesis. This may indicate that the role of the NEC is more fundamental in nuclear viral morphogenesis than it was believed before and that the NEC may be required for efficient execution of all functions which require the reorganisation of chromatin dynamics during infection [127]. Supporting this idea it was reported that the HSV-1 homologues affect the late chromatin reorganisation in infected cells [162, 163].

# 4.3 High-throughput screening for essential functions of MCMV

Identification of DN proteins can be separated into consecutive steps. At first, a mutant library of an essential gene of interest is generated. Traditionally, this is carried out using random Tn mutagenesis, yielding numerous candidate genes. These are inserted into a viral BAC deficient for this gene, and analysed with respect to their ability to restore virus reconstitution. Mutants that fail to complement the wt gene point out key regions of the protein. The DN potential of those mutants is then tested by their expression in the wt genome context. The time expenses of this scheme can be reduced in two aspects. First of all, the number of mutants to begin with can be reduced by disrupting different regions of the protein by targeted mutagenesis as described for pM53 in the current study. Thereby, essential domains are identified by investigating only a limited number of mutants, which can then be subjected on demand to a more thorough mutagenesis with an even higher coverage of the parts of interest.

Where a targeted mutagenesis is not possible, for example for proteins without distinct sequence homology peaks such as pM94, the second approach to reduce the effort will be valuable, namely to rapidly test many mutants in a high-throughput screening system. To this end we developed a host cell based flip-in system that omits the necessity of the manipulation of the MCMV genome in bacteria.

## 4.3.1 Evaluation of the ICFAR system

In the classical approach, the expression cassette encoding the (mutant) gene of interest was inserted into the MCMV BAC via site-specific recombination, which was performed in bacteria and demanded the subsequent purification of recombinant BACs from bacterial cultures. In the new system, the in-cell Flp-assisted recombination (ICFAR) system, this step was replaced by allowing recombination to take place within the mammalian target cells, which were modified to stably express Flpe recombinase, an evolved form of the original Flp recombinase better adapted to catalyse the recombination reaction at 37 °C [24]. The presence of the Flpe-encoding mRNA, i.e. the indicator for active transcription, was confirmed by reverse transcription of isolated RNA and PCR of the resulting cDNA in parallel to each experiment and was detectable for several weeks of sub-culturing. The Flpe-expressing cells were transfected using a

technology established recently by the Lonza AG termed nucleofection, which facilitates the direct ingress of the transfected DNA into the nucleus of the treated cell [12, 100, 173]. This provides the chance to transfect even non-dividing cells, which is not an issue for the NIH/3T3 cell line, from which the Flpe-expressing cells are derived, but which is quite useful for MEF, which do not divide any more after reaching confluence. Another advantage of this technique is that it reduces the effort to transfect high numbers of samples under comparable conditions. In comparison, for transfection reactions utilising lipids or liposomes the DNA has to be mixed with the transfection reagent and added onto the cells or into the cell culture medium. This requires the successive preparation of one reaction mix per sample. For nucleofection, cells are harvested and resuspended within the transfection solution, before the whole mixture is added to the DNA preparation. That not only grants analogous treatment and conditions for the cells, which are handled as one block, but also permits to set up up to 96 samples in parallel in a much shorter time frame.

The ICFAR system was successfully tested and evaluated using BACs devoid of an essential viral gene or genetic feature as well as already characterised mutants of an M53 library created by random mutagenesis. Flpe-expressing cells were nucleofected with one of the deletion BACs and its respective rescue plasmid and complementation of the genetic defect assessed by plaque formation. Whereas nucleofection with the ΔM53, the ΔM56 and the ΔM104 BAC together with an empty shuttle vector did not produce viral progeny, the complementation with the respective wt genes reproducibly resulted in plaque formation. The same was true for the complementation of the deletion of the *pac* sequences, which are essential for encapsidation and cleavage of newly replicated MCMV genomes into the viral capsids [105]. Nucleofection with the Δ*pac* BAC and the respective *pac*-containing rescue plasmid successfully restored virus production, resulting in 40 to 60 plaques per sample. This confirmed that the in-cell Flp-assisted complementation assay is feasible for virus reconstitution. Furthermore, the results are quantifiable already at 6 dpt and do not need to be maintained for 6 weeks. Mutations that are partially functional and lead to delayed virus reconstitution may perhaps be negative in this screen. These, however, can be analysed in more detail in the inhibitory screen. All in all, the ICFAR complementation assay is performed much faster than the traditional complementation using the bacterial flip-in, reducing the required time by several weeks.

Since the ICFAR complementation system was not only developed to reconstitute viruses, but to identify non-complementing mutations in a target gene, it was tested with a reference set of M53 mutants [95]. According to the expectations, the complementing mutants (i43, i104) led to the formation of viral progeny, whereas the non-functional mutants (i128, i212) as well as the inhibitory mutants (i207, s309) did not induce virus production. These observations confirmed the applicability of the ICFAR complementation assay to identify non-complementing mutations that might be inhibitory for viral growth.

In the next step, the ICFAR system was applied to isolate inhibitory mutations. For this, a couple of M53 mutants that have been shown to be non-complementing for the M53 deletion BAC [95], but with diverse potential to inhibit the wt pM53 function upon their overexpression [130] were tested using the *pac*-based ICFAR assay. In agreement with the expectations, expression of non-functional but non-inhibitory mutants (i115, i128, i146) did not interfere with viral growth and resulted in plaque numbers comparable to wt pM53 overexpression, whereas expression of the partially inhibitory mutants (i207, i220) decreased viral plaque formation to less than half of the control value. However, the known strong DN proteins (s309, i313) were not able to inhibit virus production completely, as it had been shown previously in other assay systems [130]. The limited inhibitory potential could also not be increased by exchanging the expression-regulating promoter. This might require closer investigation with regard to the expression levels of the mutant gene products, for example by quantitative PCR or Western blot analysis.

Nevertheless, the ICFAR inhibitory assay successfully made use of an essential genetic element that cannot be complemented *in trans* (the *pac* sequences), thereby supporting the integration of the shuttle plasmid. Using the M53 mutant library as reference set, the results were not as clear as expected, as even the known strong DN examples i313 and s309 did not completely prevent virus production. However, the plaque numbers quantified for all the inhibitory mutants were considerably less than half of the value of the wt M53 control. Thus, using a cut-off value of 50% of the control (or even less for the identification of strong DNs) it would be possible to at least identify strong inhibitory mutants. Their DN potential can be quantified subsequently in further assays.

## 4.3.2 Towards an automated readout

The ICFAR complementation system was established using deletion BACs and simple rescue plasmids. To detect virus reconstitution more easily, staining with antisera specific for viral proteins was required, which again added to the expenses of the assay. This drawback was circumvented by fluorescently labelling both the viral backbone as well as the shuttle plasmid. In the viral genome, the mCherry expression cassette was coupled via an IRES to the structural protein SCP. This resulted in a robust fluorescent signal upon the onset of late viral replication, effectively marking productively infected cells. In addition, the gene under investigation on the rescue plasmid was coupled via an IRES to an *egfp* gene. Two advantages are provided by these fluorescence signals, namely infected cells and plaques can be identified by fluorescence microscopy without any protein-specific antibody staining. Furthermore, the plaques could be quantified using an automated detection system fitted with appropriate software.

Expression analysis revealed that protein levels depend on the strength of the promoter used. In some cases, where only a minute amount of a protein is required to facilitate viral growth, the IRES-driven GFP signal was very weak and too weak to be sensed by the automated detection device. In that case the IRES coupling the GFP expression to the weak promoter could be replaced by a poly(A) sequence to complete the expression cassette of the gene under study and GFP expression could be initiated by an alternative, stronger promoter. This modification would greatly enhance the fluorescent signal and fit the construct for automated detection. Then, indeed, the GFP signal would no longer allow an estimation of the expression levels of the protein under study, but this may not always be required during the screening process.

Moreover, complementation of the M99-deficient BAC demonstrated that the rescue plasmid harbouring the *pac* sequences can be utilised in the ICFAR complementation assay as well. Reconstitution of the ΔM99 BAC with an ectopic flip-in of this plasmid (ΔM99EPM99) produced viral progeny that could productively infect a new cell generation, indicating that a second *pac* signal does not result in the formation of defective MCMV genomes. Due to this observation it is possible to use the same rescue plasmid as acceptor for the mutant genes in both ICFAR screens, the complementation and the inhibitory one, which circumvents the re-cloning of non-complementing mutants of the first screen into a new shuttle plasmid for the second screen.

### 4.3.3 Establishment of the ICFAR complementation system to study pM99

Based on previously characterised M53 mutants, it was demonstrated that the ICFAR complementation system was applicable to identify non-complementing mutations within a target gene. However, to show its reliability, we wanted to test the system by screening mutants of a hitherto not analysed gene. For this, the MCMV M99 ORF was chosen, which encodes a small protein of 112 aa, so that a comprehensive mutant library should be manageable.

M99 belongs to the conserved family of UL11 homologues, which were, together with the homologues of pUL16 (pM94), implicated in the process of secondary envelopment of tegumented viral capsids within the cytoplasm [6, 31, 78, 90, 97]. But so far, the role(s) of pM99 in this process have been concluded solely from its homology to pUL11 proteins in other herpesviruses. Thus, a thorough analysis was required to confirm its role in MCMV replication and provided the basic tool-kit for the screening.

Deletion of the M99 ORF from the wt MCMV BAC prevented virus reconstitution in transfected MEF, a defect that was reversed by pM99 expression at an ectopic position in the genome. This indicated that pM99 is crucial for viral growth, which has also been observed for the HCMV homologue pUL99 [45, 187]. This is in contrast to alpha-herpesviruses as well as EBV, where inactivation of the homologous ORFs did not prevent virus formation, only plaque sizes and viral titres were reduced [31, 78, 96, 146], suggesting that the functions required for secondary envelopment are carried out at least in part redundantly in those viruses.

Early studies on HSV-1 demonstrated that pUL11 is expressed with delayed early kinetics [96], whereas pUL99 is a true late gene product [70, 76]. Here it was shown that expression of pM99 depends on viral genome replication as well. Furthermore, infection with HSV-1 resulted in three protein species derived from the UL11 ORF. Propagation of plaque-purified HSV-1 isolates revealed that the original inoculum contained a mixture of two HSV-1 clones, which expressed either the two larger or the smallest protein species, but never all three of them [96]. A similar pattern was not observed for pM99, which was produces as uniform single species of the expected size, confirming that pM99 occurs solely in one post-translationally modified state. The same

was true for pUL99, which has been characterised as 28 kDa protein [110] as well as for pUL11 of PrV [78].

In agreement with previous studies on the HSV-1 and HCMV homologues [4, 78, 92, 149, 150], analysis of the intracellular distribution of pM99 revealed the accumulation at a juxtanuclear compartment. In transiently transfected cells this likely represents the ER-Golgi intermediate compartment (ERGIC), whereas in infected cells the signal possibly reflects its localisation at the viral assembly compartment, where cytoplasmic capsids accumulate and secondary envelopment takes place [156]. The location of the assembly compartment was also pointed out by the staining visualising DNA that is detectable outside the nucleus. A previous study detected pUL11-specific stainings abundantly in nuclear bodies of infected cells [4]. This was not the case for pM99, which was observed exclusively in the cytoplasm. Furthermore, several studies have identified pUL16 (pUL94 in HCMV) as binding partner for pUL11 [28, 90, 93, 97, 126, 186]. Accordingly, the intracellular distribution of pM94 was investigated and observed at the same site as pM99 in close proximity to the nucleus. These data support the role of pM99 in secondary envelopment, as it co-localised with pM94 at the assembly complex, possibly targeting mature capsids to the TGN and plasma membrane. Moreover, reconstitution kinetics of this virus similar to wt MCMV and the intracellular distribution of the expressed pM99F akin to wt pM99 confirmed the feasibility to C-terminally tag the pM99 protein by maintaining its biological functionality.

Following the characterisation of the biological and biochemical properties of pM99 including its confirmed essentiality, the M99 deletion was complemented using the ICFAR system. Since it was not known whether pM99 overexpression would be detrimental for the reconstituting virus, expression cassettes using the endogenous M99 promoter ($P_{M99}$) and the strong HCMV IE1 promoter ($P_{CMV}$) were tested. Although complementation with either construct resulted in viral plaque formation, pM99 expression under control of the endogenous $P_{M99}$ was much more efficient in facilitating viral growth. Reconstitution of viruses from isolated DNA may be affected at several stages, possibly due to deregulation of viral gene expression upon overload with viral genomes or due to the toxicity caused by overexpressed viral proteins. Abundant expression of certain viral proteins, particularly early expression of proteins with late kinetics, may interfere with virus replication. The data obtained for the pM99

complementation strongly highlight the necessity of tightly regulated protein expression, as it is achieved in wt MCMV [137]. Supportive observations were made for the bacterial flip-in of a $P_{CMV}$-driven pM99 expression cassette into the ΔM99 BAC. The recombinant BAC failed repeatedly to reconstitute virus (data not shown). Thus, a major conclusion can be drawn from the ICFAR complementation assay, namely that unregulated and early expression of pM99 is inhibitory for virus production. In contrast to that, pM53 and pM94, which are also expressed with late kinetics [95, 97], do not impair viral replication when expressed early and in excess amounts [present study; 97]. In order to identify and study DN mutants of a specific protein, it is crucial to consider the inhibitory potential of protein surplus. In our case, using the $P_{CMV}$-regulated expression cassette to complement the wt M99 deletion would likely give false-negative results solely due to overexpression of the pM99 version.

Plaque formation upon ICFAR ΔM99 complementation was monitored by detecting the fluorescent signals emitted by mCherry (encoded by the BAC) and GFP (encoded by the shuttle plasmid). Both signals were observed in all plaques, although not all infected cells appeared to be GFP-positive. This might, particularly in the case of GFP expression coupled to $P_{M99}$, be explained with the quite low expression levels induced by this promoter. On the other hand, the partial co-localisation of GFP and mCherry could be an indicator that pM99 is expressed only in the initially transfected cells. If the rescue plasmid was not inserted into the BAC efficiently or flipped-out again, the genomic basis for pM99 expression is realised only in the directly transfected cells, but not passed on to the neighbouring cells. In this case it might be that pM99 is packaged into the mature virion [9, 68, 69] and transported to the newly infected cell, which might be sufficient to facilitate further viral growth at the rim of the plaque until the pM99 supply is depleted. This would also imply that, once expressed, pM99 is stable enough to remain functional in the cytoplasm of a newly infected cell. Furthermore, it supports the finding that minute pM99 amounts already suffice to enable virus production. Insufficient Flp/FRT-mediated recombination was also observed using a shuttle plasmid expressing viable GFP-tagged SCP [19], which was co-transfected with the Δ*pac* BAC (data not shown). Virus reconstitution was detectable, though only part of the infected cells were GFP-positive, again hinting at low flip-in levels or preference of the plasmid excision reaction following flip-in. This might also account in part for

the minor virus production in the presence of the pM53 DN mutants in the inhibitory ICFAR screen and requires closer investigation.

A study on the HCMV homologue pUL99 reported on cell-to-cell spread of a pUL99 deficient virus [160]. Although neither infectious particles could be detected in the supernatant nor the cells transfected with ΔM99 BAC DNA did change their morphology to an infected appearance, this possibility cannot be absolutely excluded for M99-deficient MCMV. To investigate this further, a pM99-expressing complementing cell line would be necessary which enables the propagation of viral progeny lacking pM99. Subsequently, MCMV-ΔM99-infected cells could be analysed by EM and the cytoplasmic distribution of viral particles studied.

To validate the new system, a couple of mutants were tested already which were rationally designed. Three mutants were constructed based on functional domains described for the HCMV homologue pUL99 [67, 90], which included the potential myristoylation site, a conserved acidic cluster and the potential pM94 binding domain, and were deleted from the M99 ORF. Repeatedly, none of these mutants was able to complement the wt pM99 function, indicating that those domains are as well important for the functionality of pM99. In the next step, the three mutants should be tested in the inhibitory screen to check whether the mutations result in non-functional proteins, which cannot interfere with wt pM99, or whether the mutant proteins are inhibitory for MCMV replication.

Furthermore, detailed analyses would be required to study the properties of the mutant proteins. For example, the intracellular distribution of the ΔGly2 mutant should be investigated. Since the N-terminal glycine supposedly is the acceptor for the myristic acid, which anchors the pUL11 homologues at membrane surfaces [8, 92, 149], loss of this amino acid should result in a modified protein localisation. Additionally, it needs to be investigated whether the pM94 binding domain deduced from the pUL99 homologue is indeed responsible for the interaction between pM99 and pM94.

## 4.4 Concluding remarks

The data presented here confirm that the domain targeting approach can be successfully applied to identify DN mutants, although this depends on regions in the protein with sequence homology to related proteins. Therefore it cannot be employed on

any viral protein. Incidentally, pM99 seems to be such a candidate, as two of the three mutations introduced (the pM94 binding and the acidic cluster) could have been deduced from the sequence alignment of the homologous proteins. Nonetheless, it is not known yet whether the pM99 mutations have DN potential or whether they are just non-functional.

Focussing on the pM53 CR2 mutant, the data accumulated during this study both confirm and extend the current model of herpesvirus nuclear egress. Apparently, pM53 and its homologues seem to target mature DNA-filled nucleocapsids to the INM, where they transit into the cytoplasm by budding through the nuclear envelope.

The second part of this study described the establishment of a fast and high-throughput-ready complementation system based on Flp/FRT-mediated recombination in mammalian cells. It was shown that the system is indeed suitable for the high-throughput screening to rapidly identify non-complementing mutations, which can then be tested in a second round for their inhibitory potential. Nevertheless, the inhibitory screen demands further improvement with respect to efficient flip-in and genome stabilisation.

# 5 REFERENCES

[1] **Adler, H., M. Messerle, M. Wagner, and U.H. Koszinowski. 2000.** Cloning and Mutagenesis of the Murine Gammaherpesvirus 68 Genome as an Infectious Bacterial Artificial Chromosome. *J Virol*, **74**(15):6964-6974.

[2] **al Kobaisi, M.F., F.J. Rixon, I. McDougall, and V.G. Preston. 1991.** The herpes simplex virus UL33 gene product is required for the assembly of full capsids. *Virology*, **180**(1):380-388.

[3] **Baer, A. and J. Bode. 2001.** Coping with kinetic and thermodynamic barriers: RMCE, an efficient strategy for the targeted integration of transgenes. *Curr Opin Biotechnol*, **12**(5):473-480.

[4] **Baines, J.D., R.J. Jacob, L. Simmerman, and B. Roizman. 1995.** The herpes simplex virus 1 UL11 proteins are associated with cytoplasmic and nuclear membranes and with nuclear bodies of infected cells. *J Virol*, **69**(2):825-833.

[5] **Baines, J.D. and B. Roizman. 1991.** The open reading frames UL3, UL4, UL10, and UL16 are dispensable for the replication of herpes simplex virus 1 in cell culture. *J Virol*, **65**(2):938-944.

[6] **Baines, J.D. and B. Roizman. 1992.** The UL11 gene of herpes simplex virus 1 encodes a function that facilitates nucleocapsid envelopment and egress from cells. *J Virol*, **66**(8):5168-5174.

[7] **Baird, N.L., J.L. Starkey, D.J. Hughes, and J.W. Wills. 2010.** Myristylation and palmitylation of HSV-1 UL11 are not essential for its function. *Virology*, **397**(1):80-88.

[8] **Baird, N.L., P.C. Yeh, R.J. Courtney, and J.W. Wills. 2008.** Sequences in the UL11 tegument protein of herpes simplex virus that control association with detergent-resistant membranes. *Virology*, **374**(2):315-321.

[9] **Baldick, C.J. and T. Shenk. 1996.** Proteins associated with purified human cytomegalovirus particles. *J Virol*, **70**(9):6097-6105.

[10] **Balthesen, M., L. Dreher, P. Lučin, and M.J. Reddehase. 1994.** The establishment of cytomegalovirus latency in organs is not linked to local virus production during primary infection. *J Gen Virol*, **75**(9):2329-2336.

[11] **Bankier, A.T., S. Beck, R. Bohni, C.M. Brown, R. Cerny, M.S. Chee, C.A. Hutchison, 3rd, T. Kouzarides, J.A. Martignetti, E. Preddie, and et al. 1991.** The DNA sequence of the human cytomegalovirus genome. *DNA Seq*, **2**(1):1-12.

[12] **Bertram, B., S. Wiese, and A. von Holst. 2012.** High-efficiency transfection and survival rates of embryonic and adult mouse neural stem cells achieved by electroporation. *J Neurosci Methods*, **209**(2):420-427.

[13] **Biery, M.C., F.J. Stewart, A.E. Stellwagen, E.A. Raleigh, and N.L. Craig. 2000.** A simple in vitro Tn7-based transposition system with low target site selectivity for genome and gene analysis. *Nucleic Acids Res*, **28**(5):1067-1077.

[14] **Bjerke, S.L., J.M. Cowan, J.K. Kerr, A.E. Reynolds, J.D. Baines, and R.J. Roller. 2003.** Effects of Charged Cluster Mutations on the Function of Herpes Simplex Virus Type 1 UL34 Protein. *J Virol*, **77**(13):7601-7610.

[15] **Bjerke, S.L. and R.J. Roller. 2006.** Roles for herpes simplex virus type 1 UL34 and US3 proteins in disrupting the nuclear lamina during herpes simplex virus type 1 egress. *Virology*, **347**(2):261-276.

[16] **Blagosklonny, M.V. 2000.** p53 from complexity to simplicity: mutant p53 stabilization, gain-of-function, and dominant-negative effect. *FASEB J*, **14**(13):1901-1907.

[17] **Borst, E.-M., G. Hahn, U.H. Koszinowski, and M. Messerle. 1999.** Cloning of the Human Cytomegalovirus (HCMV) Genome as an Infectious Bacterial Artificial Chromosome in Escherichia coli: a New Approach for Construction of HCMV Mutants. *J Virol*, **73**(10):8320-8329.

[18] **Borst, E.-M., S. Mathys, M. Wagner, W. Muranyi, and M. Messerle. 2001.** Genetic Evidence of an Essential Role for Cytomegalovirus Small Capsid Protein in Viral Growth. *J Virol*, **75**(3):1450-1458.

[19] **Bosse, J.B., R. Bauerfeind, L. Popilka, L. Marcinowski, M. Taeglich, C. Jung, H. Striebinger, J. von Einem, U. Gaul, P. Walther, U.H. Koszinowski, and Z. Ruzsics. 2012.** A Beta-Herpesvirus with Fluorescent Capsids to Study Transport in Living Cells. *PLoS ONE*, **7**(7):e40585.

[20] **Bresnahan, W.A. and T. Shenk. 2000.** A Subset of Viral Transcripts Packaged Within Human Cytomegalovirus Particles. *Science*, **288**(5475):2373-2376.

[21] **Britt, W.J., M. Jarvis, J.-Y. Seo, D. Drummond, and J. Nelson. 2004.** Rapid Genetic Engineering of Human Cytomegalovirus by Using a Lambda Phage Linear Recombination System: Demonstration that pp28 (UL99) Is Essential for Production of Infectious Virus. *J Virol*, **78**(1):539-543.

[22] **Bubeck, A., M. Wagner, Z. Ruzsics, M. Lotzerich, M. Iglesias, I.R. Singh, and U.H. Koszinowski. 2004.** Comprehensive Mutational Analysis of a Herpesvirus Gene in the Viral Genome Context Reveals a Region Essential for Virus Replication. *J Virol*, **78**(15):8026-8035.

[23] **Bubic, I., M. Wagner, A. Krmpotic, T. Saulig, S. Kim, W.M. Yokoyama, S. Jonjic, and U.H. Koszinowski. 2004.** Gain of virulence caused by loss of a gene in murine cytomegalovirus. *J Virol*, **78**(14):7536-7544.

[24] **Buchholz, F., P.-O. Angrand, and A.F. Stewart. 1998.** Improved properties of FLP recombinase evolved by cycling mutagenesis. *Nat Biotechnol*, **16**(7):657-662.

[25] **Buser, C., P. Walther, T. Mertens, and D. Michel. 2007.** Cytomegalovirus Primary Envelopment Occurs at Large Infoldings of the Inner Nuclear Membrane. *J Virol*, **81**(6):3042-3048.

[26] **Camozzi, D., S. Pignatelli, C. Valvo, G. Lattanzi, C. Capanni, P. Dal Monte, and M.P. Landini. 2008.** Remodelling of the nuclear lamina during human cytomegalovirus infection: role of the viral proteins pUL50 and pUL53. *J Gen Virol*, **89**(3):731-740.

[27] **Cano-Monreal, G.L., K.M. Wylie, F. Cao, J.E. Tavis, and L.A. Morrison. 2009.** Herpes simplex virus 2 UL13 protein kinase disrupts nuclear lamins. *Virology*, **392**(1):137-147.

[28] **Chadha, P., J. Han, J.L. Starkey, and J.W. Wills. 2012.** Regulated interaction of tegument proteins UL16 and UL11 from herpes simplex virus. *J Virol*.

[29] **Chang, Y.E., C. Van Sant, P.W. Krug, A.E. Sears, and B. Roizman. 1997.** The null mutant of the U(L)31 gene of herpes simplex virus 1: construction and phenotype in infected cells. *J Virol*, **71**(11):8307-8315.

[30] **Cherepanov, P.P. and W. Wackernagel. 1995.** Gene disruption in Escherichia coli: TcR and KmR cassettes with the option of Flp-catalyzed excision of the antibiotic-resistance determinant. *Gene*, **158**(1):9-14.

[31] **Chiu, Y.-F., B. Sugden, P.-J. Chang, L.-W. Chen, Y.-J. Lin, Y.-C. Lan, C.-H. Lai, J.-Y. Liou, S.-T. Liu, and C.-H. Hung. 2012.** Characterization and Intracellular Trafficking of Epstein-Barr Virus BBLF1, a Protein Involved in Virion Maturation. *J Virol*, **86**(18):9647-9655.

[32] **Church, G.A. and D.W. Wilson. 1997.** Study of herpes simplex virus maturation during a synchronous wave of assembly. *J Virol*, **71**(5):3603-3612.

[33] **Clercq, E.D. and A. Holy. 2005.** Acyclic nucleoside phosphonates: a key class of antiviral drugs. *Nat Rev Drug Discov*, **4**(11):928-940.

[34] **Cockrell, S.K., M.E. Sanchez, A. Erazo, and F.L. Homa. 2009.** Role of the UL25 Protein in Herpes Simplex Virus DNA Encapsidation. *J Virol*, **83**(1):47-57.

[35] **Connolly, S.A., J.O. Jackson, T.S. Jardetzky, and R. Longnecker. 2011.** Fusing structure and function: a structural view of the herpesvirus entry machinery. *Nat Rev Microbiol*, **9**(5):369-381.

[36] **Craig, N.L. 1997.** Target Site Selection in Transposition. *Annu Rev Biochem*, **66**(1):437-474.

[37] **Crowder, S. and K. Kirkegaard. 2005.** Trans-dominant inhibition of RNA viral replication can slow growth of drug-resistant viruses. *Nat Genet*, **37**(7):701-709.

[38] **Cunningham, B.C. and J.A. Wells. 1989.** High-resolution epitope mapping of hGH-receptor interactions by alanine-scanning mutagenesis. *Science*, **244**(4908):1081-1085.

[39] **Dal Monte, P., S. Pignatelli, N. Zini, N.M. Maraldi, E. Perret, M.C. Prevost, and M.P. Landini. 2002.** Analysis of intracellular and intraviral localization of the human cytomegalovirus UL53 protein. *J Gen Virol*, **83**(5):1005-1012.

[40] **Daneholt, B. 2001.** Assembly and transport of a premessenger RNP particle. *Proc Natl Acad Sci*, **98**(13):7012-7017.

[41] **Darlington, R.W. and L.H. Moss. 1968.** Herpesvirus Envelopment. *J Virol*, **2**(1):48-55.

[42] **Das, S., A. Vasanji, and P.E. Pellett. 2007.** Three-Dimensional Structure of the Human Cytomegalovirus Cytoplasmic Virion Assembly Complex Includes a Reoriented Secretory Apparatus. *J Virol*, **81**(21):11861-11869.

[43] **Delecluse, H.-J., T. Hilsendegen, D. Pich, R. Zeidler, and W. Hammerschmidt. 1998.** Propagation and recovery of intact, infectious Epstein–Barr virus from prokaryotic to human cells. *Proc Natl Acad Sci*, **95**(14):8245-8250.

[44] **Don, R.H., P.T. Cox, B.J. Wainwright, K. Baker, and J.S. Mattick. 1991.** 'Touchdown' PCR to circumvent spurious priming during gene amplification. *Nucleic Acids Res*, **19**(14):4008.

[45] **Dunn, W., C. Chou, H. Li, R. Hai, D. Patterson, V. Stolc, H. Zhu, and F. Liu. 2003.** Functional profiling of a human cytomegalovirus genome. *Proc Natl Acad Sci*, **100**(24):14223-14228.

[46] **Farina, A., R. Feederle, S. Raffa, R. Gonnella, R. Santarelli, L. Frati, A. Angeloni, M.R. Torrisi, A. Faggioni, and H.J. Delecluse. 2005.** BFRF1 of Epstein-Barr Virus Is Essential for Efficient Primary Viral Envelopment and Egress. *J Virol*, **79**(6):3703-3712.

[47] **Fossum, E., C.C. Friedel, S.V. Rajagopala, B. Titz, A. Baiker, T. Schmidt, T. Kraus, T. Stellberger, C. Rutenberg, S. Suthram, S. Bandyopadhyay, D. Rose, A. von Brunn, M. Uhlmann, C. Zeretzke, Y.A. Dong, H. Boulet, M. Koegl, S.M. Bailer, U. Koszinowski, T. Ideker, P. Uetz, R. Zimmer, and J. Haas. 2009.** Evolutionarily Conserved Herpesviral Protein Interaction Networks. *PLoS Pathogens*, **5**(9):e1000570.

[48] **Frame, R. and J.O. Bishop. 1971.** The Number of Sex-Factors per Chromosome in Escherichia coli. *Journal of Biochemistry*, **121**:93-103.

[49] **Fuchs, W., B.G. Klupp, H. Granzow, N. Osterrieder, and T.C. Mettenleiter. 2002.** The Interacting UL31 and UL34 Gene Products of Pseudorabies Virus Are Involved in Egress from the Host-Cell Nucleus and Represent Components of Primary Enveloped but Not Mature Virions. *J Virol*, **76**(1):364-378.

[50] **Gonnella, R., A. Farina, R. Santarelli, S. Raffa, R. Feederle, R. Bei, M. Granato, A. Modesti, L. Frati, H.J. Delecluse, M.R. Torrisi, A. Angeloni, and A. Faggioni. 2005.** Characterization and Intracellular Localization of the Epstein-Barr Virus Protein BFLF2: Interactions with BFRF1 and with the Nuclear Lamina. *J Virol*, **79**(6):3713-3727.

[51] **Goodrum, F., K. Caviness, and P. Zagallo. 2012.** Human cytomegalovirus persistence. *Cell Microbiol*, **14**(5):644-655.

[52] **Granato, M., R. Feederle, A. Farina, R. Gonnella, R. Santarelli, B. Hub, A. Faggioni, and H.J. Delecluse. 2008.** Deletion of Epstein-Barr Virus BFLF2 Leads to Impaired

Viral DNA Packaging and Primary Egress as Well as to the Production of Defective Viral Particles. *J Virol*, **82**(8):4042-4051.

[53] **Granzow, H., B.G. Klupp, W. Fuchs, J. Veits, N. Osterrieder, and T.C. Mettenleiter. 2001.** Egress of alphaherpesviruses: comparative ultrastructural study. *J Virol*, **75**(8):3675-3684.

[54] **Greijer, A.E., C.A.J. Dekkers, and J.M. Middeldorp. 2000.** Human Cytomegalovirus Virions Differentially Incorporate Viral and Host Cell RNA during the Assembly Process. *J Virol*, **74**(19):9078-9082.

[55] **Hall, R.N., J. Meers, E. Fowler, and T. Mahony. 2012.** Back to BAC: The Use of Infectious Clone Technologies for Viral Mutagenesis. *Viruses*, **4**(2):211-235.

[56] **Haugo, A.C., M.L. Szpara, L. Parsons, L.W. Enquist, and R.J. Roller. 2011.** Herpes Simplex Virus 1 pUL34 Plays a Critical Role in Cell-to-Cell Spread of Virus in Addition to Its Role in Virus Replication. *J Virol*, **85**(14):7203-7215.

[57] **Hayes, F. 2003.** Transposon-based strategies for microbial functional genomics and proteomics. *Annu Rev Genet*, **37**:3-29.

[58] **Herskowitz, I. 1987.** Functional inactivation of genes by dominant negative mutations. *Nature*, **329**(6136):219-222.

[59] **Hodgkin, P.D., A.A. Scalzo, N. Swaminathan, P. Price, and G.R. Shellam. 1988.** Murine cytomegalovirus binds reversibly to mouse embryo fibroblasts: implications for quantitation and explanation of centrifugal enhancement. *J Virol Methods*, **22**(2-3):215-230.

[60] **Homman-Loudiyi, M., K. Hultenby, W. Britt, and C. Söderberg-Nauclér. 2003.** Envelopment of Human Cytomegalovirus Occurs by Budding into Golgi-Derived Vacuole Compartments Positive for gB, Rab 3, Trans-Golgi Network 46, and Mannosidase II. *J Virol*, **77**(5):3191-3203.

[61] **Honess, R.W. and B. Roizman. 1975.** Regulation of herpesvirus macromolecular synthesis: sequential transition of polypeptide synthesis requires functional viral polypeptides. *Proc Natl Acad Sci U S A*, **72**(4):1276-1280.

[62] **Huang, E.S., C.H. Huang, S.M. Huong, and M. Selgrade. 1976.** Preferential inhibition of herpes-group viruses by phosphonoacetic acid: effect on virus DNA synthesis and virus-induced DNA polymerase activity. *Yale J Biol Med*, **49**(1):93-99.

[63] **ICTV. 2011.** International Committee on Taxonomy of Viruses, www.ictvonline.org.

[64] **Irmiere, A. and W. Gibson. 1983.** Isolation and characterization of a noninfectious virion-like particle released from cells infected with human strains of cytomegalovirus. *Virology*, **130**(1):118-133.

[65] **Johannessen, I. and D.H. Crawford. 1999.** In vivo models for Epstein–Barr virus (EBV)-associated B cell lymphoproliferative disease (BLPD). *Rev Med Virol*, **9**(4):263-277.

[66] **Johnson, D.C. and J.D. Baines. 2011.** Herpesviruses remodel host membranes for virus egress. *Nat Rev Microbiol*, **9**(5):382-394.

[67] **Jones, T.R. and S.-W. Lee. 2004.** An Acidic Cluster of Human Cytomegalovirus UL99 Tegument Protein Is Required for Trafficking and Function. *J Virol*, **78**(3):1488-1502.

[68] **Kalejta, R.F. 2008.** Tegument Proteins of Human Cytomegalovirus. *Microbiol Mol Biol Rev*, **72**(2):249-265.

[69] **Kattenhorn, L.M., R. Mills, M. Wagner, A. Lomsadze, V. Makeev, M. Borodovsky, H.L. Ploegh, and B.M. Kessler. 2004.** Identification of Proteins Associated with Murine Cytomegalovirus Virions. *J Virol*, **78**(20):11187-11197.

[70] **Kerry, J.A., M.A. Priddy, C.P. Kohler, T.L. Staley, D. Weber, T.R. Jones, and R.M. Stenberg. 1997.** Translational regulation of the human cytomegalovirus pp28 (UL99) late gene. *J Virol*, **71**(2):981-987.

[71] **Klupp, B.G., H. Granzow, W. Fuchs, G.M. Keil, S. Finke, and T.C. Mettenleiter. 2007.** Vesicle formation from the nuclear membrane is induced by coexpression of two conserved herpesvirus proteins. *Proc Natl Acad Sci*, **104**(17):7241-7246.

[72] **Klupp, B.G., H. Granzow, G.M. Keil, and T.C. Mettenleiter. 2006.** The capsid-associated UL25 protein of the alphaherpesvirus pseudorabies virus is nonessential for cleavage and encapsidation of genomic DNA but is required for nuclear egress of capsids. *J Virol*, **80**(13):6235-6246.

[73] **Klupp, B.G., H. Granzow, and T.C. Mettenleiter. 2001.** Effect of the pseudorabies virus US3 protein on nuclear membrane localization of the UL34 protein and virus egress from the nucleus. *J Gen Virol*, **82**(10):2363-2371.

[74] **Klupp, B.G., H. Granzow, and T.C. Mettenleiter. 2011.** Nuclear Envelope Breakdown Can Substitute for Primary Envelopment-Mediated Nuclear Egress of Herpesviruses. *J Virol*, **85**(16):8285-8292.

[75] **Klupp, B.G., H. Granzow, and T.C. Mettenleiter. 2000.** Primary Envelopment of Pseudorabies Virus at the Nuclear Membrane Requires the UL34 Gene Product. *J Virol*, **74**(21):10063-10073.

[76] **Kohler, C.P., J.A. Kerry, M. Carter, V.P. Muzithras, T.R. Jones, and R.M. Stenberg. 1994.** Use of recombinant virus to assess human cytomegalovirus early and late promoters in the context of the viral genome. *J Virol*, **68**(10):6589-6597.

[77] **Kolter, R., M. Inuzuka, and D.R. Helinski. 1978.** Trans-complementation-dependent replication of a low molecular weight origin fragment from plasmid R6K. *Cell*, **15**(4):1199-1208.

[78] **Kopp, M., H. Granzow, W. Fuchs, B.G. Klupp, E. Mundt, A. Karger, and T.C. Mettenleiter. 2003.** The Pseudorabies Virus UL11 Protein Is a Virion Component Involved in Secondary Envelopment in the Cytoplasm. *J Virol*, **77**(9):5339-5351.

[79] **Kops, A.d.B. and D.M. Knipe. 1988.** Formation of DNA replication structures in herpes virus-infected cells requires a viral DNA binding protein. *Cell*, **55**(5):857-868.

[80] **Koso, H., H. Takeda, C.C.K. Yew, J.M. Ward, N. Nariai, K. Ueno, M. Nagasaki, S. Watanabe, A.G. Rust, D.J. Adams, N.G. Copeland, and N.A. Jenkins. 2012.** Transposon mutagenesis identifies genes that transform neural stem cells into glioma-initiating cells. *Proc Natl Acad Sci*, **109**(44):E2998–E3007.

[81] **Krmpotic, A., I. Bubic, B. Polic, P. Lucin, and S. Jonjic. 2003.** Pathogenesis of murine cytomegalovirus infection. *Microbes Infect*, **5**(13):1263-1277.

[82] **Kuhn, J., T. Leege, B.G. Klupp, H. Granzow, W. Fuchs, and T.C. Mettenleiter. 2008.** Partial functional complementation of a pseudorabies virus UL25 deletion mutant by herpes simplex virus type 1 pUL25 indicates overlapping functions of alphaherpesvirus pUL25 proteins. *J Virol*, **82**(12):5725-5734.

[83] **Lake, C.M. and L.M. Hutt-Fletcher. 2004.** The Epstein-Barr virus BFRF1 and BFLF2 proteins interact and coexpression alters their cellular localization. *Virology*, **320**(1):99-106.

[84] **Landolfo, S., M. Gariglio, G. Gribaudo, and D. Lembo. 2003.** The human cytomegalovirus. *Pharmacol Ther*, **98**(3):269-297.

[85] **Leach, N., S.L. Bjerke, D.K. Christensen, J.M. Bouchard, F. Mou, R. Park, J. Baines, T. Haraguchi, and R.J. Roller. 2007.** Emerin Is Hyperphosphorylated and Redistributed in Herpes Simplex Virus Type 1-Infected Cells in a Manner Dependent on both UL34 and US3. *J Virol*, **81**(19):10792-10803.

[86] **Leach, N.R. and R.J. Roller. 2010.** Significance of host cell kinases in herpes simplex virus type 1 egress and lamin-associated protein disassembly from the nuclear lamina. *Virology*, **406**(1):127-137.

[87] **Leelawong, M., D. Guo, and G.A. Smith. 2011.** A Physical Link between the Pseudorabies Virus Capsid and the Nuclear Egress Complex. *J Virol*, **85**(22):11675-11684.

[88] **Leuzinger, H., U. Ziegler, E.M. Schraner, C. Fraefel, D.L. Glauser, I. Heid, M. Ackermann, M. Mueller, and P. Wild. 2005.** Herpes Simplex Virus 1 Envelopment Follows Two Diverse Pathways. *J Virol*, **79**(20):13047-13059.

[89] **Liang, L. and J.D. Baines. 2005.** Identification of an Essential Domain in the Herpes Simplex Virus 1 UL34 Protein That Is Necessary and Sufficient To Interact with UL31 Protein. *J Virol*, **79**(6):3797-3806.

[90] **Liu, Y., Z. Cui, Z. Zhang, H. Wei, Y. Zhou, M. Wang, and X.-E. Zhang. 2009.** The tegument protein UL94 of human cytomegalovirus as a binding partner for tegument protein pp28 identified by intracellular imaging. *Virology*, **388**(1):68-77.

[91] **Liu, Y., Z. Zhang, X. Zhao, H. Wei, J. Deng, Z. Cui, and X.-E. Zhang. 2012.** Human cytomegalovirus UL94 is a nucleocytoplasmic shuttling protein containing two NLSs and one NES. *Virus Res*, **166**(1–2):31-42.

[92] **Loomis, J.S., J.B. Bowzard, R.J. Courtney, and J.W. Wills. 2001.** Intracellular Trafficking of the UL11 Tegument Protein of Herpes Simplex Virus Type 1. *J Virol*, **75**(24):12209-12219.

[93] **Loomis, J.S., R.J. Courtney, and J.W. Wills. 2003.** Binding Partners for the UL11 Tegument Protein of Herpes Simplex Virus Type 1. *J Virol*, **77**(21):11417-11424.

[94] **Loregian, A. and G. Palù. 2005.** Disruption of the interactions between the subunits of herpesvirus DNA polymerases as a novel antiviral strategy. *Clin Microbiol Infect*, **11**(6):437-446.

[95] **Lotzerich, M., Z. Ruzsics, and U.H. Koszinowski. 2006.** Functional Domains of Murine Cytomegalovirus Nuclear Egress Protein M53/p38. *J Virol*, **80**(1):73-84.

[96] **MacLean, C.A., A. Dolan, F.E. Jamieson, and D.J. McGeoch. 1992.** The myristylated virion proteins of herpes simplex virus type 1: investigation of their role in the virus life cycle. *J Gen Virol*, **73**(3):539-547.

[97] **Maninger, S., J.B. Bosse, F. Lemnitzer, M. Pogoda, C.A. Mohr, J. von Einem, P. Walther, U.H. Koszinowski, and Z. Ruzsics. 2011.** M94 is essential for the secondary envelopment of murine cytomegalovirus. *J Virol*, **85**(18):9254-9267.

[98] **Marschall, M., A. Marzi, P.a.d. Siepen, R. Jochmann, M. Kalmer, S. Auerochs, P. Lischka, M. Leis, and T. Stamminger. 2005.** Cellular p32 Recruits Cytomegalovirus Kinase pUL97 to Redistribute the Nuclear Lamina. *J Biol Chem*, **280**(39):33357-33367.

[99] **Maul, G.G. and D. Negorev. 2008.** Differences between mouse and human cytomegalovirus interactions with their respective hosts at immediate early times of the replication cycle. *Med Microbiol Immunol*, **197**(2):241-249.

[100] **Maurisse, R., D. De Semir, H. Emamekhoo, B. Bedayat, A. Abdolmohammadi, H. Parsi, and D.C. Gruenert. 2010.** Comparative transfection of DNA into primary and transformed mammalian cells from different lineages. *BMC Biotechnol*, **10**:9.

[101] **McLauchlan, J. and F.J. Rixon. 1992.** Characterization of enveloped tegument structures (L particles) produced by alphaherpesviruses: integrity of the tegument does not depend on the presence of capsid or envelope. *J Gen Virol*, **73**(2):269-276.

[102] **McLeod, M., S. Craft, and J.R. Broach. 1986.** Identification of the crossover site during FLP-mediated recombination in the Saccharomyces cerevisiae plasmid 2 microns circle. *Mol Cell Biol*, **6**(10):3357-3367.

[103] **McNab, A.R., P. Desai, S. Person, L.L. Roof, D.R. Thomsen, W.W. Newcomb, J.C. Brown, and F.L. Homa. 1998.** The Product of the Herpes Simplex Virus Type 1 UL25 Gene Is Required for Encapsidation but Not for Cleavage of Replicated Viral DNA. *J Virol*, **72**(2):1060-1070.

[104] **McVoy, M.A. and S.P. Adler. 1994.** Human cytomegalovirus DNA replicates after early circularization by concatemer formation, and inversion occurs within the concatemer. *J Virol*, **68**(2):1040-1051.

[105] **McVoy, M.A., D.E. Nixon, S.P. Adler, and E.S. Mocarski. 1998.** Sequences within the Herpesvirus-Conservedpac1 and pac2 Motifs Are Required for Cleavage and Packaging of the Murine Cytomegalovirus Genome. *J Virol*, **72**(1):48-56.

[106] **Meckes, Jr., J.A. Marsh, and J.W. Wills. 2010.** Complex mechanisms for the packaging of the UL16 tegument protein into herpes simplex virus. *Virology*, **398**(2):208-213.

[107] **Messerle, M., I. Crnkovic, W. Hammerschmidt, H. Ziegler, and U.H. Koszinowski. 1997.** Cloning and mutagenesis of a herpesvirus genome as an infectious bacterial artificial chromosome. *Proc Natl Acad Sci*, **94**(26):14759-14763.

[108] **Mettenleiter, T.C. 2004.** Budding events in herpesvirus morphogenesis. *Virus Res*, **106**(2):167-180.

[109] **Mettenleiter, T.C., B.G. Klupp, and H. Granzow. 2009.** Herpesvirus assembly: an update. *Virus Res*, **143**(2):222-234.

[110] **Meyer, H., A.T. Bankier, M.P. Landini, C.M. Brown, B.G. Barrell, B. Rüger, and M. Mach. 1988.** Identification and procaryotic expression of the gene coding for the highly immunogenic 28-kilodalton structural phosphoprotein (pp28) of human cytomegalovirus. *J Virol*, **62**(7):2243-2250.

[111] **Milbradt, J., S. Auerochs, and M. Marschall. 2007.** Cytomegaloviral proteins pUL50 and pUL53 are associated with the nuclear lamina and interact with cellular protein kinase C. *J Gen Virol*, **88**(10):2642-2650.

[112] **Milbradt, J., S. Auerochs, H. Sticht, and M. Marschall. 2009.** Cytomegaloviral proteins that associate with the nuclear lamina: components of a postulated nuclear egress complex. *J Gen Virol*, **90**(3):579-590.

[113] **Milbradt, J., R. Webel, S. Auerochs, H. Sticht, and M. Marschall. 2010.** Novel Mode of Phosphorylation-triggered Reorganization of the Nuclear Lamina during Nuclear Egress of Human Cytomegalovirus. *J Biol Chem*, **285**(18):13979-13989.

[114] **Mocarski, E.S. and M.F. Stinski. 1979.** Persistence of the cytomegalovirus genome in human cells. *J Virol*, **31**(3):761-775.

[115] **Mou, F., T. Forest, and J.D. Baines. 2007.** US3 of Herpes Simplex Virus Type 1 Encodes a Promiscuous Protein Kinase That Phosphorylates and Alters Localization of Lamin A/C in Infected Cells. *J Virol*, **81**(12):6459-6470.

[116] **Mou, F., E. Wills, and J.D. Baines. 2009.** Phosphorylation of the UL31 Protein of Herpes Simplex Virus 1 by the US3-Encoded Kinase Regulates Localization of the Nuclear Envelopment Complex and Egress of Nucleocapsids. *J Virol*, **83**(10):5181-5191.

[117] **Muhlbach, H., C. Mohr, Z. Ruzsics, and U. Koszinowski. 2009.** Dominant-Negative Proteins in Herpesviruses - From Assigning Gene Function to Intracellular Immunization. *Viruses*, **1**(3):420-440.

[118] **Muranyi, W., J. Haas, M. Wagner, G. Krohne, and U.H. Koszinowski. 2002.** Cytomegalovirus recruitment of cellular kinases to dissolve the nuclear lamina. *Science*, **297**(5582):854-857.

[119] **Nash, A.A., B.M. Dutia, J.P. Stewart, and A.J. Davison. 2001.** Natural history of murine γ-herpesvirus infection. *Phil Trans R Soc Lond B*, **356**(1408):569-579.

[120] **Newcomb, W.W., R.M. Juhas, D.R. Thomsen, F.L. Homa, A.D. Burch, S.K. Weller, and J.C. Brown. 2001.** The UL6 Gene Product Forms the Portal for Entry of DNA into the Herpes Simplex Virus Capsid. *J Virol*, **75**(22):10923-10932.

[121] **Oshima, S., T. Daikoku, S. Shibata, H. Yamada, F. Goshima, and Y. Nishiyama. 1998.** Characterization of the UL16 gene product of herpes simplex virus type 2. *Arch Virol*, **143**(5):863-880.

[122] **Panté, N. and M. Kann. 2002.** Nuclear Pore Complex Is Able to Transport Macromolecules with Diameters of 39 nm. *Mol Biol Cell*, **13**(2):425-434.

[123] **Park, R. and J.D. Baines. 2006.** Herpes Simplex Virus Type 1 Infection Induces Activation and Recruitment of Protein Kinase C to the Nuclear Membrane and Increased Phosphorylation of Lamin B. *J Virol*, **80**(1):494-504.

[124] **Patel, A.H., F.J. Rixon, C. Cunningham, and A.J. Davison. 1996.** Isolation and Characterization of Herpes Simplex Virus Type 1 Mutants Defective in the UL6 Gene. *Virology*, **217**(1):111-123.

[125] **Phillips, S.L. and W.A. Bresnahan. 2012.** The Human Cytomegalovirus (HCMV) Tegument Protein UL94 Is Essential for Secondary Envelopment of HCMV Virions. *J Virol*, **86**(5):2523-2532.

[126] **Phillips, S.L., D. Cygnar, A. Thomas, and W.A. Bresnahan. 2012.** Interaction between the Human Cytomegalovirus Tegument Proteins UL94 and UL99 Is Essential for Virus Replication. *J Virol*, **86**(18):9995-10005.

[127] **Placek, B.J. and S.L. Berger. 2010.** Chromatin dynamics during herpes simplex virus-1 lytic infection. *Biochimica et Biophysica Acta (BBA) - Gene Regulatory Mechanisms*, **1799**(3–4):223-227.

[128] **Pomeranz, L.E., A.E. Reynolds, and C.J. Hengartner. 2005.** Molecular Biology of Pseudorabies Virus: Impact on Neurovirology and Veterinary Medicine. *Microbiol Mol Biol Rev*, **69**(3):462-500.

[129] **Poon, A.P. and B. Roizman. 1993.** Characterization of a temperature-sensitive mutant of the UL15 open reading frame of herpes simplex virus 1. *J Virol*, **67**(8):4497-4503.

[130] **Popa, M., Z. Ruzsics, M. Lotzerich, L. Dolken, C. Buser, P. Walther, and U.H. Koszinowski. 2010.** Dominant Negative Mutants of the Murine Cytomegalovirus M53 Gene Block Nuclear Egress and Inhibit Capsid Maturation. *J Virol*, **84**(18):9035-9046.

[131] **Rawlinson, W.D., H.E. Farrell, and B.G. Barrell. 1996.** Analysis of the complete DNA sequence of murine cytomegalovirus. *J Virol*, **70**(12):8833-8849.

[132] **Reddehase, M.J., J. Podlech, and N.K.A. Grzimek. 2002.** Mouse models of cytomegalovirus latency: overview. *Journal of clinical virology : the official publication of the Pan American Society for Clinical Virology*, **25**:23-36.

[133] **Reddehase, M.J., F. Weiland, K. Munch, S. Jonjic, A. Luske, and U.H. Koszinowski. 1985.** Interstitial murine cytomegalovirus pneumonia after irradiation: characterization of cells that limit viral replication during established infection of the lungs. *J Virol*, **55**(2):264-273.

[134] **Reynolds, A.E., L. Liang, and J.D. Baines. 2004.** Conformational Changes in the Nuclear Lamina Induced by Herpes Simplex Virus Type 1 Require Genes UL31 and UL34. *J Virol*, **78**(11):5564-5575.

[135] **Reynolds, A.E., B.J. Ryckman, J.D. Baines, Y. Zhou, L. Liang, and R.J. Roller. 2001.** UL31 and UL34 Proteins of Herpes Simplex Virus Type 1 Form a Complex That Accumulates at the Nuclear Rim and Is Required for Envelopment of Nucleocapsids. *J Virol*, **75**(18):8803-8817.

[136] **Reynolds, A.E., E.G. Wills, R.J. Roller, B.J. Ryckman, and J.D. Baines. 2002.** Ultrastructural Localization of the Herpes Simplex Virus Type 1 UL31, UL34, and US3 Proteins Suggests Specific Roles in Primary Envelopment and Egress of Nucleocapsids. *J Virol*, **76**(17):8939-8952.

[137] **Roizman, B. and P.E. Pellet**, The family of herpesviridae: a brief introduction, in *Fields Virology*, D.M. Knipe and P.M. Howley, Editors. 2001, Lippincott Williams & Wilkins: Philadelphia. p. 2479-2499.

[138] **Roller, R.J., S.L. Bjerke, A.C. Haugo, and S. Hanson. 2010.** Analysis of a Charge Cluster Mutation of Herpes Simplex Virus Type 1 UL34 and Its Extragenic Suppressor Suggests a Novel Interaction between pUL34 and pUL31 That Is Necessary for Membrane Curvature around Capsids. *J Virol*, **84**(8):3921-3934.

[139] **Roller, R.J., A.C. Haugo, and N.J. Kopping. 2011.** Intragenic and Extragenic Suppression of a Mutation in Herpes Simplex Virus 1 UL34 That Affects both Nuclear Envelope Targeting and Membrane Budding. *J Virol*, **85**(22):11615-11625.

[140] **Roller, R.J., Y. Zhou, R. Schnetzer, J. Ferguson, and D. DeSalvo. 2000.** Herpes Simplex Virus Type 1 UL34 Gene Product Is Required for Viral Envelopment. *J Virol*, **74**(1):117-129.

[141] **Rupp, B., Z. Ruzsics, C. Buser, B. Adler, P. Walther, and U.H. Koszinowski. 2007.** Random Screening for Dominant-Negative Mutants of the Cytomegalovirus Nuclear Egress Protein M50. *J Virol*, **81**(11):5508-5517.

[142] **Rupp, B., Z. Ruzsics, T. Sacher, and U.H. Koszinowski. 2005.** Conditional Cytomegalovirus Replication In Vitro and In Vivo. *J Virol*, **79**(1):486-494.

[143] **Ruzsics, Z. and U.H. Koszinowski**, Mutagenesis of the Cytomegalovirus Genome, in *Human Cytomegalovirus*, T.E. Shenk and M.F. Stinski, Editors. 2008, Springer Berlin, Heidelberg. p. 41-61.

[144] **Ryckman, B.J. and R.J. Roller. 2004.** Herpes Simplex Virus Type 1 Primary Envelopment: UL34 Protein Modification and the US3-UL34 Catalytic Relationship. *J Virol*, **78**(1):399-412.

[145] **Sacher, T., J. Podlech, C.A. Mohr, S. Jordan, Z. Ruzsics, M.J. Reddehase, and U.H. Koszinowski. 2008.** The major virus-producing cell type during murine cytomegalovirus infection, the hepatocyte, is not the source of virus dissemination in the host. *Cell Host Microbe*, **3**(4):263-272.

[146] **Sadaoka, T., H. Yoshii, T. Imazawa, K. Yamanishi, and Y. Mori. 2007.** Deletion in Open Reading Frame 49 of Varicella-Zoster Virus Reduces Virus Growth in Human Malignant Melanoma Cells but Not in Human Embryonic Fibroblasts. *J Virol*, **81**(22):12654-12665.

[147] **Saeki, Y., T. Ichikawa, A. Saeki, E.A. Chiocca, K. Tobler, M. Ackermann, X.O. Breakefield, and C. Fraefel. 1998.** Herpes simplex virus type 1 DNA amplified as bacterial artificial chromosome in Escherichia coli: rescue of replication-competent virus progeny and packaging of amplicon vectors. *Hum Gene Ther*, **9**(18):2787-2794.

[148] **Sam, M.D., B.T. Evans, D.M. Coen, and J.M. Hogle. 2009.** Biochemical, Biophysical, and Mutational Analyses of Subunit Interactions of the Human Cytomegalovirus Nuclear Egress Complex. *J Virol*, **83**(7):2996-3006.

[149] **Sanchez, V., K.D. Greis, E. Sztul, and W.J. Britt. 2000.** Accumulation of Virion Tegument and Envelope Proteins in a Stable Cytoplasmic Compartment during Human Cytomegalovirus Replication: Characterization of a Potential Site of Virus Assembly. *J Virol*, **74**(2):975-986.

[150] **Sanchez, V., E. Sztul, and W.J. Britt. 2000.** Human Cytomegalovirus pp28 (UL99) Localizes to a Cytoplasmic Compartment Which Overlaps the Endoplasmic Reticulum-Golgi-Intermediate Compartment. *J Virol*, **74**(8):3842-3851.

[151] **Santarelli, R., A. Farina, M. Granato, R. Gonnella, S. Raffa, L. Leone, R. Bei, A. Modesti, L. Frati, M.R. Torrisi, and A. Faggioni. 2008.** Identification and Characterization of the Product Encoded by ORF69 of Kaposi's Sarcoma-Associated Herpesvirus. *J Virol*, **82**(9):4562-4572.

[152] **Schnee, M., Z. Ruzsics, A. Bubeck, and U.H. Koszinowski. 2006.** Common and Specific Properties of Herpesvirus UL34/UL31 Protein Family Members Revealed by Protein Complementation Assay. *J Virol*, **80**(23):11658-11666.

[153] **Schnee, M., F.M. Wagner, U.H. Koszinowski, and Z. Ruzsics. 2012.** A cell free protein fragment complementation assay for monitoring the core interaction of the human cytomegalovirus nuclear egress complex. *Antivir Res*, **95**(1):12-18.

[154] **Scott, E.S. and P. O'Hare. 2001.** Fate of the Inner Nuclear Membrane Protein Lamin B Receptor and Nuclear Lamins in Herpes Simplex Virus Type 1 Infection. *J Virol*, **75**(18):8818-8830.

[155] **Seo, J.Y. and W.J. Britt. 2007.** Cytoplasmic Envelopment of Human Cytomegalovirus Requires the Postlocalization Function of Tegument Protein pp28 within the Assembly Compartment. *J Virol*, **81**(12):6536-6547.

[156] **Seo, J.Y. and W.J. Britt. 2006.** Sequence Requirements for Localization of Human Cytomegalovirus Tegument Protein pp28 to the Virus Assembly Compartment and for Assembly of Infectious Virus. *J Virol*, **80**(11):5611-5626.

[157] **Serrano, M., A.W. Lin, M.E. McCurrach, D. Beach, and S.W. Lowe. 1997.** Oncogenic ras Provokes Premature Cell Senescence Associated with Accumulation of p53 and p16INK4a. *Cell*, **88**(5):593-602.

[158] **Shaulian, E., A. Zauberman, D. Ginsberg, and M. Oren. 1992.** Identification of a minimal transforming domain of p53: negative dominance through abrogation of sequence-specific DNA binding. *Mol Cell Biol*, **12**(12):5581-5592.

[159] **Shiba, C., T. Daikoku, F. Goshima, H. Takakuwa, Y. Yamauchi, O. Koiwai, and Y. Nishiyama. 2000.** The UL34 gene product of herpes simplex virus type 2 is a tail-anchored type II membrane protein that is significant for virus envelopment. *J Gen Virol*, **81**(10):2397-2405.

[160] **Silva, M.C., J. Schroer, and T. Shenk. 2005.** Human cytomegalovirus cell-to-cell spread in the absence of an essential assembly protein. *Proc Natl Acad Sci U S A*, **102**(6):2081-2086.

[161] **Silva, M.C., Q.C. Yu, L. Enquist, and T. Shenk. 2003.** Human Cytomegalovirus UL99-Encoded pp28 Is Required for the Cytoplasmic Envelopment of Tegument-Associated Capsids. *J Virol*, **77**(19):10594-10605.

[162] **Simpson-Holley, M., J. Baines, R. Roller, and D.M. Knipe. 2004.** Herpes Simplex Virus 1 UL31 and UL34 Gene Products Promote the Late Maturation of Viral Replication Compartments to the Nuclear Periphery. *J Virol*, **78**(11):5591-5600.

[163] **Simpson-Holley, M., R.C. Colgrove, G. Nalepa, J.W. Harper, and D.M. Knipe. 2005.** Identification and Functional Evaluation of Cellular and Viral Factors Involved in the Alteration of Nuclear Architecture during Herpes Simplex Virus 1 Infection. *J Virol*, **79**(20):12840-12851.

[164] **Sinclair, J. and P. Sissons. 2006.** Latency and reactivation of human cytomegalovirus. *J Gen Virol*, **87**(7):1763-1779.

[165] **Smith, G.A. and L.W. Enquist. 1999.** Construction and Transposon Mutagenesis inEscherichia coli of a Full-Length Infectious Clone of Pseudorabies Virus, an Alphaherpesvirus. *J Virol*, **73**(8):6405-6414.

[166] **Sodeik, B., M.W. Ebersold, and A. Helenius. 1997.** Microtubule-mediated Transport of Incoming Herpes Simplex Virus 1 Capsids to the Nucleus. *J Cell Biol*, **136**(5):1007-1021.

[167] **Spear, P.G. and R. Longnecker. 2003.** Herpesvirus Entry: an Update. *J Virol*, **77**(19):10179-10185.

[168] **Speese, Sean D., J. Ashley, V. Jokhi, J. Nunnari, R. Barria, Y. Li, B. Ataman, A. Koon, Y.-T. Chang, Q. Li, Melissa J. Moore, and V. Budnik. 2012.** Nuclear Envelope Budding Enables Large Ribonucleoprotein Particle Export during Synaptic Wnt Signaling. *Cell*, **149**(4):832-846.

[169] **Talbot, P. and J.D. Almeida. 1977.** Human Cytomegalovirus: Purification of Enveloped Virions and Dense Bodies. *J Gen Virol*, **36**(2):345-349.

[170] **Tengelsen, L.A., N.E. Pederson, P.R. Shaver, M.W. Wathen, and F.L. Homa. 1993.** Herpes simplex virus type 1 DNA cleavage and encapsidation require the product of the UL28 gene: isolation and characterization of two UL28 deletion mutants. *J Virol*, **67**(6):3470-3480.

[171] **Teschendorf, C., K.H. Warrington, Jr., D.W. Siemann, and N. Muzyczka. 2002.** Comparison of the EF-1 alpha and the CMV promoter for engineering stable tumor cell lines using recombinant adeno-associated virus. *Anticancer Res*, **22**(6A):3325-3330.

[172] **Thorne, L., D. Bailey, and I. Goodfellow. 2012.** High-Resolution Functional Profiling of the Norovirus Genome. *J Virol*, **86**(21):11441-11456.

[173] **Trompeter, H.-I., S. Weinhold, C. Thiel, P. Wernet, and M. Uhrberg. 2003.** Rapid and highly efficient gene transfer into natural killer cells by nucleofection. *J Immunol Methods*, **274**(1–2):245-256.

[174] **Trus, B.L., W.W. Newcomb, N. Cheng, G. Cardone, L. Marekov, F.L. Homa, J.C. Brown, and A.C. Steven. 2007.** Allosteric Signaling and a Nuclear Exit Strategy: Binding of UL25/UL17 Heterodimers to DNA-Filled HSV-1 Capsids. *Mol Cell*, **26**(4):479-489.

[175] **Uetz, P., Y.A. Dong, C. Zeretzke, C. Atzler, A. Baiker, B. Berger, S.V. Rajagopala, M. Roupelieva, D. Rose, E. Fossum, and J. Haas. 2006.** Herpesviral Protein Networks and Their Interaction with the Human Proteome. *Science*, **311**(5758):239-242.

[176] **van Zijl, M., W. Quint, J. Briaire, T. de Rover, A. Gielkens, and A. Berns. 1988.** Regeneration of herpesviruses from molecularly cloned subgenomic fragments. *J Virol*, **62**(6):2191-2195.

[177] **Vanarsdall, A.L. and D.C. Johnson. 2012.** Human cytomegalovirus entry into cells. *Current Opinion in Virology*, **2**(1):37-42.

[178] **Vittone, V., E. Diefenbach, D. Triffett, M.W. Douglas, A.L. Cunningham, and R.J. Diefenbach. 2005.** Determination of Interactions between Tegument Proteins of Herpes Simplex Virus Type 1. *J Virol*, **79**(15):9566-9571.

[179] **Vizoso Pinto, M.G., V.R. Pothineni, R. Haase, M. Woidy, A.S. Lotz-Havla, S.W. Gersting, A.C. Muntau, J. Haas, M. Sommer, A.M. Arvin, and A. Baiker. 2011.** Varicella Zoster Virus ORF25 Gene Product: An Essential Hub Protein Linking Encapsidation Proteins and the Nuclear Egress Complex. *J Proteome Res*, **10**(12):5374-5382.

[180] Wagner, F.M., *A high-throughput compatible cell-free protein fragment complementation assay monitoring viral protein interactions*, in *Max von Pettenkofer-Institute*2012, Ludwig-Maximilians-University: Munich, Germany.

[181] **Warming, S., N. Costantino, D.L. Court, N.A. Jenkins, and N.G. Copeland. 2005.** Simple and highly efficient BAC recombineering using galK selection. *Nucleic Acids Res*, **33**(4):e36.

[182] **Weber, P.C., M. Levine, and J.C. Glorioso. 1987.** Rapid identification of nonessential genes of herpes simplex virus type 1 by Tn5 mutagenesis. *Science*, **236**(4801):576-579.

[183] **Yamauchi, Y., C. Shiba, F. Goshima, A. Nawa, T. Murata, and Y. Nishiyama. 2001.** Herpes simplex virus type 2 UL34 protein requires UL31 protein for its relocation to the internal nuclear membrane in transfected cells. *J Gen Virol*, **82**(6):1423-1428.

[184] **Yang, K. and J.D. Baines. 2011.** Selection of HSV capsids for envelopment involves interaction between capsid surface components pUL31, pUL17, and pUL25. *Proc Natl Acad Sci*, **108**(34):14276-14281.

[185] **Ye, G.J. and B. Roizman. 2000.** The essential protein encoded by the UL31 gene of herpes simplex virus 1 depends for its stability on the presence of UL34 protein. *Proc Natl Acad Sci U S A*, **97**(20):11002-11007.

[186] **Yeh, P.C., D.G. Meckes, Jr., and J.W. Wills. 2008.** Analysis of the Interaction between the UL11 and UL16 Tegument Proteins of Herpes Simplex Virus. *J Virol*, **82**(21):10693-10700.

[187] **Yu, D., M.C. Silva, and T. Shenk. 2003.** Functional map of human cytomegalovirus AD169 defined by global mutational analysis. *Proc Natl Acad Sci*, **100**(21):12396-12401.

[188] **Yu, X., P. Trang, S. Shah, I. Atanasov, Y.-H. Kim, Y. Bai, Z.H. Zhou, and F. Liu. 2005.** Dissecting human cytomegalovirus gene function and capsid maturation by ribozyme targeting and electron cryomicroscopy. *Proc Natl Acad Sci*, **102**(20):7103-7108.

# 6 SUPPLEMENTARY INFORMATION

## 6.1 Homologous herpesvirus proteins

**Table 6.1: Nomenclature of selected homologous ORFs/proteins in herpesviruses**

| HSV/PrV | HCMV | MCMV | EBV | MHV68 |
|---------|------|------|-----|-------|
| UL11 | UL99 | M99 | BBLF1 | ORF38 |
| UL16 | UL94 | M94 | BGLF2 | ORF33 |
| UL17 | UL93 | M93 | BGLF1 | ORF32 |
| UL25 | UL77 | M77 | BVFR1 | ORF19 |
| UL31 | UL53 | M53 | BFLF2 | ORF69 |
| UL34 | UL50 | M50 | BFRF1 | ORF67 |

**Table 6.2: Accession numbers of pUL11 homologue sequences**

Listed are the accession numbers of the pUL11 homologues used for the alignment depicted in Figure 3.34A. Protein sequences were downloaded from the Protein Knowledgebase (UniProtKB) on http://www.uniprot.org.

| | | | |
|---|---|---|---|
| A5A411_9ALPH | Q5Y0U2_9ALPH | Q9QP14_ILTV | TG11_PSHV1 |
| D1FXX1_FHV1 | Q6X222_9ALPH | Q9YZA4_9ALPH | TG11_SHV21 |
| E2IUF9_SHV1 | Q77CB3_BHV1C | TG11_EHV1B | TG11_VZVO |
| F5HHY1_HHV8P | Q782T5_9ALPH | TG11_GAHVM | UL11_EBVA8 |
| G8H0M3_9BETA | Q806B8_CHV1 | TG11_HHV11 | UL11P_HCMVA |
| G8XT03_9BETA | Q85040_SUHVK | TG11_HHV2H | VG38_ALHV1 |
| G8XUG4_9BETA | Q8QS01_9BETA | TG11_HHV6U | VG38_ICHVA |
| G9CUB8_9ALPH | Q8UZG1_9GAMA | TG11_HHV7J | |
| Q2QBG6_CHV16 | Q9E1H9_MEHV1 | TG11_MUHVK | |

# 6.2 Oligonucleotides

**Table 6.3: Oligonucleotides used for cloning**

| No. | Name | Sequence (5'- 3') |
|---|---|---|
| 01 | Apa2-for | ATCGGGTCACAGTCCTCACGCC |
| 02 | Apa2-rev | CAACATCCGTGGGTCGACACC |
| 03 | CHfor | CGCAAGTTCTACTTCGGGTTCC |
| 04 | CHrev | ACACGCTCGAGGACTCTAGCCGCAGACATCGC |
| 05 | CR4MHVfor | GAGTCCTCGAGCAGAATACCTACCATACCGGCCGA |
| 06 | FlagΔSakM53for | TAAACTTAAGCTTGGCGCGCC |
| 07 | FlagM53SalIrev | GTCGGGGTGGTCGACCTC |
| 08 | LITrev | ATTCAGGCTGCGCAACTGTTGG |
| 09 | M53ΔCR2AB-for | TAAACTTAAGCTTGGCGCGC |
| 10 | M53ΔCR2A-5'rev | Phosphate–CGTCGTCTCCTTGCAGGTGG |
| 11 | M53ΔCR2A-3'for | Phosphate–AACGTGATGAAGCACCGCAAG |
| 12 | M53ΔCR2AB-rev | TCCACCTTCCTCTGCAGCATC |
| 13 | M53ΔCR2B-5'rev | Phosphate–GGTCTGGTTGATGAAGGCCAC |
| 14 | M53ΔCR2B-3'for | Phosphate–GGCTTCCGTAAAAACATGGAAC |
| 15 | M53ΔCR3-5'rev | Phosphate–CATGTTCTTACGGAACCCGAAGTAG |
| 16 | M53ΔCR3-3'for | Phosphate–CGATGTCTGCGGCTAGAGTCG |
| 17 | M56-1for | GTGTGGGTACCACGCGTGGCCACCATGGCCATGAATACGTTACAAAAACTGTG |
| 18 | M56-1rev | GTGTACCGGTGCTCCTCGTAGCACTGAAAAC |
| 19 | M56-2for | GTGTGTACCGGTCTGCTGGCGAGGTTGTGCGA |
| 20 | M56-2rev | GTGTGTAAGCTTTTCCCCTCCTGCCCCGGCCC |
| 21 | M56-3for | GTGTGGATCCCCCCTTTTCAATCGCTTGCACGA |
| 22 | M56-3rev | GTGTGTCGTACGTTATATAGTGCGACGGACAG |
| 23 | M56-4for | GTGTCGTACGGACTGGATGACAGTCGGATACATG |
| 24 | M56-4rev | GTGTGTATGCATGGATCCTCACTTGTACAGGCAAGGAGGC |
| 25 | M99for | GATCGAGGCGCGCCGGTACCCGGTAAGAAGACGGGTCTCG |
| 26 | M99Flagrev | ATCGATCGCGGCCGCTTATTTGTCGTCGTCGTCTTTGTAGTCGCCGGAGCCCAAGGCCCTGACTTTTTTCTTC |
| 27 | M99syn-for | AAGGCGCGCCGCTAGCGGTACCATGGGTGCAGAGTG |
| 28 | M99rev | TTTAGGCCTGTCGACTCACAAGGCCCTGACTTTTTTCTTC |
| 29 | M99ΔGly2-for | GCCGCTAGCGGTACCATGGCAGAGTGCTGTAAACAGC |

**Table 6.3: Oligonucleotides used for cloning, continued**

| No. | Name | Sequence (5'- 3') |
|---|---|---|
| 30 | M99ΔM94-5'rev | CAGGGAGTCCGCGGCGTAGGG |
| 31 | M99ΔM94-3'for | GACGAAGACCAGGTCGGCG |
| 32 | M99ΔAC-5'rev | AGACGTATCCGTCAGCACAGAGAATTCGG |
| 33 | M99ΔAC-3'for | TTCGTGCAGAAACAGCTCACGAC |
| 34 | MCMVpac_for | GTGTGTCGGACCGGGTTTAGATAAAAATGTGACCG |
| 35 | MCMVpac_rev | GTGTGTCATATGAAAACCCTGGACTCCCCGAAC |
| 36 | P(M99)-for | GCTTAATTAACTGTTCCTCAAGGCCGCGTTC |
| 37 | P(M99)-rev | TTTGCTAGCAGCGCGAGACCCGTCTTCTTAC |

**Table 6.4: Primers used for BAC mutagenesis**

| Name | Sequence (5'- 3') | Comments |
|---|---|---|
| H5-DPAC | CTCGTTAACCGAGCACATGTTTTTTTAACGAC TCCTCCACACACATATGATGTGGGCGGACAAA ATAGTTGG | replacement of *pac* sequences by kan[R] cassette by homologous recombination |
| H3-DPAC | GGGTACCGAGCTCGAATTCACTGGCCGTCGTT TTACAACGTCGTGACTGGGTGTGGGCGGACAA TAAAGTCTTAAACTGAA | |
| H5-M99amp | GTGGGTGCAGAGTGCTGTAAACAGCTATGTCG CAGCCTGCATCCCTACGCCGCGGACTCCCTGA GAACCATCACCCTAATCAAGTTT | replacement of M99 ORF by amp[R] cassette by homologous recombination |
| H3-M99amp | CTCTTTCTCCCTTTCTCCCCCCCTCACGGTCG ATCGATAGATAGATATCAGAGTAAACTTGGTC TGACAGTTACC | |

**Table 6.5: Primers used for confirmative and qPCR**

| Name | Sequence (5'- 3') |
|---|---|
| Flpe-for | ATGGCTCCCAAGAAGAAGAG |
| Flpe-rev | GTGATCTCCCAGATGCTTTC |
| LBR-for | GGAAGTTTGTTGAGGGTGAAGTGGT |
| LBR-rev | CCAGTTCGGTGCCATCTTTGTATTT |
| 5'-M54 | CGCCAGTCTGTATCCGTCCAT |
| 3'-M54 | ATCATCCGTTGCATCTCGTTG |

# ABBREVIATIONS

| | | | |
|---|---|---|---|
| aa | amino acid(s) | μg, μL | micrograms, microlitre |
| amp | ampicillin | mg, mL | milligrams, millilitre |
| BAC | bacterial artificial chromosome | mm | millimetre |
| Bla | beta-lactamase | mM | millimolar |
| bp | base pairs | MHV | murine herpesvirus |
| BSA | bovine serum albumin | min | minute(s) |
| °C | degree Celsius | MOI | multiplicity of infection |
| C- | carboxy terminal | mRNA | messenger RNA |
| cam | chloramphenicol | N- | amino terminal |
| cm | centimetre | NEC | nuclear egress complex |
| CMV | cytomegalovirus | ng | nanograms |
| CR(s) | conserved region(s) | NLS | nuclear localisation signal |
| Δ | deletion | nm | nanometre |
| DN | dominant negative | nt | nucleotide(s) |
| DNA | desoxyribonuleic acid | o/n | overnight |
| dNTP | desoxynucleotide triphosphate | $OD_x$ | optical density at the wavelength |
| dox | doxycycline | | of x nm |
| dpi | day(s) post-infection | ONM | outer nuclear membrane |
| *E. coli* | *Escherichia coli* | ORF | open reading frame |
| EBV | Epstein-Barr virus | PAA | phosphonoacetic acid |
| (E)GFP | (enhanced) green fluorescent protein | *pac* | packaging signal(s) |
| ER | endoplasmic reticulum | PBS | phosphate buffered saline |
| FCS | foetal calf serum | PCR | polymerase chain reaction |
| FRT | Flp recombination target | pfu | plaque forming units |
| g | grams | PIC | protease inhibitor cocktail |
| *g* | gravity acceleration | PrV | pseudorabies virus |
| GoI | gene of interest | r/t | room temperature |
| HCMV | human cytomegalovirus | RNA | ribonucleic acid |
| hpi | hours post-infection | RNP | ribonucleoprotein |
| hpt | hours post-transfection | rpm | rotations per minute |
| HSV | herpes simplex virus | SCP | smallest capsid protein |
| ICFA(R) | in-cell Flp-assisted (recombination) | SDS | sodium dodecyl sulfate |
| IE | immediate early | SEC | secondary envelopment complex |
| INM | inner nuclear membrane | s | second(s) |
| IP | immunoprecipitation | SV40 | simian virus 40 |
| IRES | internal ribosomal entry site | (T)EM | (transmission) electron microscopy |
| KAc | potassium acetate | tet | tetracycline |
| kan | kanamycin | TetR | tet repressor |
| kbp | kilo base pairs | TGN | *trans*-Golgi network |
| L | litre | Tn | transposon |
| LB | Luria-Bertani | TLB | total lysis buffer |
| LBR | lamin B receptor | U | unit |
| log | order of magnitude | UV | ultra violet |
| M | molar | VZV | varicella-zoster virus |
| MCMV | murine cytomegalovirus | w/v | weight per volume |
| MCP | major capsid protein | wt | wild type |
| MEF | mouse embryonic fibroblast(s) | zeo | zeocin |

# ACKNOWLEDGEMENT

# PUBLICATIONS AND PRESENTATIONS

This thesis describes work carried out at the Max von Pettenkofer-Institute in Munich between June 2008 and October 2012. Parts of this study were presented on conferences and published.

**Pogoda, M., J.B. Bosse, F.M. Wagner, M. Schauflinger, P. Walther, U.H. Koszinowski, and Z. Ruzsics.** 2012. Characterization of Conserved Region 2-Deficient Mutants of the Cytomegalovirus Egress Protein pM53. ***J Virol*** 86(23)**:**12512-12524.

**Pogoda, M., J.B. Bosse, K.K. Conzelmann, U.H. Koszinowski, and Z. Ruzsics.** A high-throughput screen for loss-of-function and dominant negative alleles of essential MCMV genes. *Submitted*.

**Related publications**

**Maninger, S., J.B. Bosse, F. Lemnitzer, M. Pogoda, C.A. Mohr, J. von Einem, P. Walther, U.H. Koszinowski, and Z. Ruzsics.** 2011. M94 is essential for the secondary envelopment of murine cytomegalovirus. ***J Virol*** 85(18):9254-9267.

# POSTERS AND PRESENTATIONS

**2012   4ᵗʰ Interact Symposium Munich**

Oral presentation: Characterisation of conserved region 2 (CR2) deficient mutants of the cytomegalovirus egress protein pM53

**2012    Annual Meeting of the German Society of Virology (GfV) in Essen**

<u>Poster presentation:</u> Characterisation of CR2 deficient mutants of the MCMV egress protein M53


**2011    International Herpesvirus Workshop in Gdansk (Poland)**

<u>Poster presentation:</u> Delineation of the C-terminal functional unit of the MCMV egress protein M53 by genetic analysis of its conserved region 2


**2011    13th International CMV/Betaherpesvirus Workshop in Nuremberg**

<u>Oral presentation:</u> Homotypic interaction of M53 is crucial for nuclear maturation of MCMV capsids


**2011    Annual GfV Meeting in Freiburg**

<u>Poster presentation:</u> Homotypic interaction of M53 is crucial for nuclear maturation of MCMV capsids


**2010    European Society of Virology Como (Italy)**

<u>Poster presentation:</u> A high-throughput approach for functional testing of mutants of essential herpesvirus genes


**2009    Annual GfV Meeting in Leipzig**

<u>Poster presentation:</u> Construction of dominant negative mutants of essential herpesvirus genes